ProQuest LLC.
789 East Eisenhower Parkway
P.O. Box 1346
Ann Arbor, MI 48106 - 1346

Errata

Page 8; Section (2.2); Note: The number of repeating units N can be very large, up to 10^5 in a polymer molecule, and much larger for a D.N.A. molecule which is also a polymer.

Page 15; Section (2.2.3); Sentence should read: This represents the change in energy when two unlike components in the **solution** come into contact.

Page 21; Section (2.3.1); Equation (2.17) should include an additional random noise term on the right hand side to produce diffusive Brownian motion.

Page 49; Section (3.3.3); Equation (3.12) should read $A=(4D_c t)^{-1/2}$.

Page 111; Section (6.3); Sentence should read: Equations (6.7) and (6.8) are used to calculate the new values of r_e and τ corresponding to the new state of the system.

UniS
University of Surrey

Monte Carlo Modelling of Case I and Case II Solvent Diffusion in Polymers

S. D. Parker

A thesis submitted to the School of Physical Sciences of the University of Surrey for the degree of Doctor of Philosophy

September 1999

Department of Physics
University of Surrey
Guildford, Surrey
GU2 5XH

Abstract

The development of two original Monte Carlo models of solvent diffusion into a polymer is described. Employing a coarse grained model of a polymer solution on a regular lattice, the dynamic properties of both the solvent and polymer molecules can be observed. The "Simple" Monte Carlo model reliably reproduces Case I dynamics, but no departure from this is seen for any reasonable model parameters. This "Simple" Monte Carlo model is unable to reproduce Case II diffusion dynamics. One reason for this is that in this Monte Carlo model the processes of solvent diffusion and polymer relaxation are entirely independent processes. In this thesis it is suggested that a simple Monte Carlo model of this type will always produce Case I diffusion dynamics. The dynamic algorithm described in this work relies on simple instantaneous molecular motions between neighbouring lattice sites. It is shown that a diffusion process based on these motions is purely concentration dependent, relying only on the current state of the system.

To use the Monte Carlo method to simulate Case II diffusion dynamics, the diffusion process is made time dependent by incorporating a history dependent model of diffusion first proposed by Crank (CRANK 1953). In this "History Dependent" Monte Carlo model the motions of both the solvent and the polymer are no longer instantaneous, but occur at a rate that approaches equilibrium by a first order process governed by a relaxation time characteristic of the viscoelastic relaxation of the polymer. This "History Dependent" Monte Carlo model successfully simulates most of the features of Case II diffusion and also demonstrates a return to Case I diffusion in the limit of long times. Unlike many models of Case II diffusion, this Monte Carlo model is able to simultaneously model the microscopic motions of both the solvent and the polymer molecules. This novel feature demonstrates the formation of a discontinuous moving boundary between the rubbery polymer and the glassy polymer that is typical of Case II diffusion dynamics.

For my family: past, present and future.

"Nothing is more repellent to normal human beings than the clinical succession of definitions, axioms, and theorems generated by the labours of pure mathematicians."

- John Ziman.

"If my hypothesis is not the truth, it is at least as naked; for I have not with some of our learned moderns disguis'd my nonsense in Greek, cloth'd it in algebra or adorned it with fluxions."

- Benjamin Franklin.

Preface

The work presented in this Ph.D. thesis represents three years of research carried out at the University of Surrey. The subject of this thesis is the computational modelling of solvent diffusion in polymers, in particular studying the usefulness of Monte Carlo modelling in two limiting cases of solvent diffusion known as Case I and Case II. Interest in polymer research has grown rapidly over the past fifty years due to the unique properties of polymers and the wide range of industrial applications in which they are employed. It is particularly important to understand how these polymer materials react in different environs and in the presence of solvents, as this determines their usefulness in many applications. At the University of Surrey, research into polymers has been carried out with the use of Magnetic Resonance Imaging (MRI), a non-invasive experimental technique that provides spatial information on the diffusion dynamics occurring within a polymer solution. I undertook the task of developing a computational model of solvent diffusion into polymers with the aim of gaining new information on these diffusion processes, information that may not be available through experimental studies. The findings of this study are presented within this thesis, which is arranged as detailed below. Prior to this work, my only experience of polymers was of those found in everyday life. Therefore, this thesis also represents the knowledge I have gained in this interesting field of physics.

In Chapter 1 an overview of experimental and theoretical techniques employed in the field of polymer research is given before clearly defining the aims of this study. It is hoped that this will provide justification for the study undertaken here and of the methods used. In Chapter 2 a description is given of the fundamental properties of polymers, polymer solutions, and their diffusion dynamics. The aim of this chapter is to provide a fundamental understanding of the concepts used later in this study. Chapter 3 provides a description of the ways in which polymer dynamics can be modelled using the Monte Carlo method. The Monte Carlo model developed for this study is then described, which simulates the ingress of solvent into a polymer. Results are given to demonstrate the

operation of this model. Chapter 4 describes an MRI experiment carried out to gain experimental data to compare with the results of the Monte Carlo model. A description of MRI theory is also given to provide a complete understanding of the experiment. In Chapter 5 the limitations of the Monte Carlo model are discussed with the aim of simulating both limiting cases of solvent diffusion in polymers. Current limitations of this and other models of solvent diffusion are critically examined. In Chapter 6 a novel Monte Carlo model is described that may overcome these current limitations and simulate both limiting cases of solvent diffusion in polymers. Finally, Chapter 7 provides a summary of the work presented in this thesis and suggestions for future work using the Monte Carlo model developed here.

In this thesis I have attempted to explain all of the ideas carefully so that a graduate student of physics may read this work and gain some understanding of the research undertaken. I have sought to refer to mathematical descriptions only where necessary and where they will augment the text. The two quotations prior to this preface are from two famous physicists separated by many generations, yet both convey views regarding the use of mathematical descriptions of physics with which I have to agree. Mathematics is a vital tool to the physicist, yet I believe that the physical description of a system is often neglected in favour of a purely mathematical description. I have found this during many years of education and believe that this dependence on mathematics can lead to unimaginative teaching and a poor understanding of the physical reality of a system. In dealing with the abstract ideas and the particular methods contained in this work I have had to think carefully about the physical reality of the systems in question and the ways in which they can be modelled without relying on mathematics. Only then have I turned to mathematics in order to study the system further. I hope that this will be apparent in my writing and I hope that this may encourage other students to understand the physical system before understanding the mathematical description of that system.

Stuart Parker.
Guildford, Summer 1999.

Acknowledgements

I wish to acknowledge the following people:

Dr. David Faux for his many years of helpful support and good humour.

Dr. Peter McDonald for his relentless enthusiasm and very useful ideas.

Members of the Physics department for useful discussions: Dr. Joe Keddie,
Dr. Richard Sear, Dr. Ute Görke, Dr. James Downes, Robert Sackin,
Juan Salamanca, Elizabetta Ciampi.

Mum and Dad for a lifetime of moral support and for helping me to achieve so much.

Clare for insults and abuse, and for being a tolerable and tolerant sister.

Veryan for making me sandwiches, and for being very kind, caring and supportive.

Thank you to everyone who has helped me during the past three years,
however great or small your contribution.

To all those I leave behind at Surrey yet to complete their Doctorates, good luck.

Funding from the Engineering and Physical Sciences Research Council (EPSRC)
is gratefully acknowledged.

Contents

Chapter 1

Introduction

1.1 Overview

Polymers, which may be natural or synthetic, have become widely used in everyday life and are relied upon in many important applications. Plastics, rubbers, synthetic fibres and fabrics are all examples of polymers that pervade modern life. In fact, the volume of polymers produced already exceeds that of metals, even though polymers have been in production for only half a century. Polymers can be used to produce solid materials, flexible materials, adhesives or coatings, all having diverse properties that can be engineered to suit a particular application. These applications have become widespread, from the carrier bag to artificial valves implanted in the human heart. It is this diverse range of applications that has required a detailed understanding of the properties of polymers and of their physical and chemical stability. Of particular interest is the ingress of solvent into a polymer. This solvent ingress may cause swelling and softening of the polymer and ultimately lead to dissolution. This may be desirable in some applications, but often it is necessary to control this ingress, or at least be able to understand the extent of the ingress and predict its effect on the polymer. Particularly with biomedical implants, any material placed inside the human body must be resistant to the hostile chemical environment it encounters or, in the case of drug release implants, must degrade in a controlled manner as water ingresses. However, the action of a solvent does not produce a permanent chemical change in a polymer. The study of these different polymer systems can proceed in three main ways: experimental observation, analytic theory, or computer simulation.

Experimental observation can provide information on known polymer systems and on the macroscopic properties that they exhibit. However, many measurements do not directly probe the microscopic motion of the polymer molecules. Theoretical models can provide analytic theories for the observed behaviour and aim to relate the microscopic properties of the polymer to the macroscopic properties measured experimentally. However, most problems in statistical physics are too complicated to allow exact solutions and due to the need for approximations the accuracy of the results is often uncertain. Computer models offer an important bridge between experiment and analytic theory. Computer simulations can provide results for problems in statistical physics that could otherwise be solved only by approximate methods. They provide a direct route from the microscopic detail of the system to the macroscopic properties of experimental interest. Furthermore, computer simulations can provide a test of existing theories and a comparison with experimental results. Eventually, a successful computer simulation can assist in the interpretation of experimental observations. Thus, computer modelling has an important role in the study of polymeric systems. However, it has not been until the relatively recent growth in personal computers that this type of research has become widely accessible. Computer modelling, particularly in the field of polymer research, is a relatively new and rapidly growing discipline, and one that has attracted much interest (FRENKEL 1996).

Computer models of molecular problems in statistical physics follow one of two main approaches. These two very different methods of molecular simulation are Molecular Dynamics simulation or Monte Carlo modelling (ALLEN 1989, BINDER 1995). Molecular Dynamics simulation aims to model a molecular system by explicitly defining the classical Newtonian equations of motion for every molecule in the system and solving these equations exactly for a many body system of interacting molecules. Thus, Molecular Dynamics is a deterministic method that relies on the ability to describe the molecular system in full chemical detail. This is obviously a computationally intensive process and limits the size of the system in question to hundreds of particles and limits the time scale of the simulation to nanoseconds (COLBOURN 1994). Molecular Dynamics simulations were first accomplished for a system of hard spheres by Alder and Wainwright (ALDER 1957,

1959) and have since successfully been used to examine the microscopic properties of polymer molecules.

Monte Carlo modelling is an entirely different technique that aims to give a probabilistic description of the molecular system from the outset, relying on the use of random numbers to simulate a random sample of the system. Thus, Monte Carlo modelling is a stochastic method that does not require the system to be described in full chemical detail. Simplifications can be made to the model which allow larger systems to be simulated. With the ability to model tens of thousands of particles over macroscopic times, the Monte Carlo method clearly offers an advantage, particularly when the aim is to model macroscopic systems and to make comparisons with experimental observations. The Monte Carlo method was first developed by Neumann, Ulam and Metropolis at the end of the Second World War to study the diffusion of neutrons into fissionable material. The method's name was chosen because of the extensive use of random numbers in the calculation and hence the connection with the famous gambling casinos (METROPOLIS 1949, 1953).

The study of the dynamics of polymer solutions can be divided into two broad areas. The first area of investigation is the diffusion dynamics of polymer molecules within a solution. Experimentally, this has been studied by a number of methods. In 1952, Beuche et al. (BUECHE 1952) used radioisotopes to label polymer chains and to observe their motion through an unlabelled polymer. Since then, many methods have been employed to probe the motion of the polymer molecules; these include neutron scattering experiments (RICHTER 1989, 1993), infrared microdensitometry (KLEIN 1978), Rayleigh scattering (ANTONIETTI 1986), and forward recoil spectrometry (BARTELS 1984). Many theories have been presented during the past fifty years to explain the polymer dynamics that have been observed. In 1953, Rouse (ROUSE 1953) developed a famous model of the dynamics of a single polymer chain in a dilute polymer solution. Zimm (ZIMM 1956) continued this work in 1956 including a hydrodynamic interaction in the theory. It was not until 1971 that De Gennes (DE GENNES 1971) proposed a similar theory of polymer dynamics in a dense polymer solution. This work was later continued by Doi and Edwards (EDWARDS 1973, DOI 1978).

Both Monte Carlo and Molecular Dynamics modelling techniques have been employed to investigate these theories. They have given consistent results in the study of polymers, particularly in the semidilute region where the dynamics can change from those of the Rouse model to those of the Reptation model. Molecular Dynamics has only proved to be a worthwhile method in relatively recent years due to the computational requirements of the technique. Pierleoni and Ryckaert (PIERLEONI 1992), and Dunweg and Kremer (DUNWEG 1993) explored the dynamics of a single polymer chain in a dilute polymer solution, whose results indicate that the Zimm model is valid. For dense systems Kremer and Grest (KREMER 1990) have shown that Molecular Dynamics simulations can confirm the behaviour of the Reptation model. Verdier and Stockmayer (VERDIER 1962, 1966) carried out one of the earliest Monte Carlo studies of polymer dynamics. They simulated the dynamic behaviour of linear polymer molecules in a dilute polymer solution and confirmed the behaviour predicted by Rouse. Evans and Edwards (EVANS 1981) have used a similar model to Verdier and Stockmayer to model a polymer chain in a dense network of obstacles. They conclude that at high densities the Reptation model and its predictions are confirmed. Kovac and co-workers (GURLER 1983, CRABB 1985, DIAL 1985) have also developed Monte Carlo models based on the model of Verdier and Stockmayer to investigate the dynamics of polymer solutions but include the important constraint that two or more polymer molecules cannot simultaneously occupy the same region in space. Naghizadeh and Kovac included this excluded volume interaction in a Monte Carlo model that considered the simultaneous motion of the polymer molecule and the obstacles (NAGHIZADEH 1986).

The second broad area of investigation is the diffusion of solvent molecules into a polymer. The fundamental theory of diffusion was given by Fick in 1855 (FICK 1855) and has since provided an excellent description of solvent diffusion in many cases. However, studies of solvent diffusion into polymers have demonstrated diffusional behaviour distinct from Fickian dynamics. One of the first observations of this anomalous behaviour was by Hartley (HARTLEY 1949) and later by Crank (CRANK 1953). Based on this and other experimental evidence, Alfrey et al. (ALFREY 1966) classified two limiting cases of solvent diffusion into polymers.

Fickian diffusion was termed Case I diffusion and the non-Fickian diffusion was termed Case II diffusion. Many theories have been proposed to explain Case II diffusion and the departure from Fickian dynamics; for example those by Thomas and Windle (THOMAS 1980, 1981, 1982). Experimentally, Magnetic Resonance Imaging (MRI) has proved to be a very powerful technique in the study of this problem. The application of this method was established by Blackband and Mansfield (BLACKBAND 1986, MANSFIELD 1992). This and other MRI studies have demonstrated Case I diffusion in a range of polymer systems (WEBB 1990a/b, 1991, HALSE 1994, 1996). However, there is now a wide range of experimental evidence to demonstrate Case II diffusion (WEISENBERGER 1990a/b, ERCKEN 1996, LANE 1997).

Molecular Dynamics simulations have increasingly been used to model the ingress of solvent into polymers. The ingress of small penetrant molecules has been studied by several groups (TAKEUCHI 1990a/b, MULLER-PLATHE 1993), who have demonstrated the simulation of diffusion processes that deviate from Case I dynamics. These studies have explicitly defined the solvent component of the polymer solution. However, previous Monte Carlo studies of polymer solutions have not explicitly considered the motion of the solvent molecules. Therefore, Monte Carlo modelling has been underused in this field and has not previously been employed to study the ingress of solvent into a polymer in the limit of Case II diffusion.

1.2 Aims

The aim of the work presented in this thesis is to develop a computational model to simulate the diffusion of solvent into a polymer. This model will be developed using the Monte Carlo method, which has been chosen as the most suitable and interesting method to study this problem. This method has been widely used in the study of problems in statistical physics, but has been underused in the study of solvent diffusion dynamics. Yet, the Monte Carlo method is particularly well suited to the study of random processes, such as the diffusion of a penetrant into

a polymer. It will also be necessary to understand the applications and limitations of the Monte Carlo method in the study of solvent ingress into polymers.

In particular, the aim of this study is to examine the usefulness of the Monte Carlo method in simulating the ingress of solvent into polymer and to determine the extent to which this method can simulate the two important limiting cases of solvent diffusion. Case I and Case II diffusion (ALFREY 1966) define the two extremes of solvent dynamics observed in experiments of diffusion in polymers. A desirable feature of the model developed here would be the ability to simulate both limiting cases of solvent diffusion through the same model. It would also be of interest to observe whether any transition occurs between these two limiting cases. However, the ability of the Monte Carlo method to simulate solvent diffusion into polymers is yet to be determined.

Chapter 2

Polymers and Polymer Solutions

2.1 Introduction

The study of polymers has grown dramatically, particularly over the last fifty years, and has become an independent field of research. Early work on the synthesis of polymers was carried out by Staudinger (STAUDINGER 1920) in the 1920s who recognised that polymers consisted of large molecules, but who thought that these molecules were quite rigid. It was Kuhn (KUHN 1930, KUHN 1934) who, a decade later, discovered that the majority of polymer molecules are actually very flexible. It is this flexibility that leads to the diverse range of properties mentioned previously. It was not until the 1940s that Flory (FLORY 1942) and Huggins (HUGGINS 1942) independently proposed a thermodynamic theory for the static properties of a polymer solution. In 1953 Rouse (ROUSE 1953) proposed a theory for the dynamics of a flexible polymer molecule in a dilute polymer solution. This work was developed further by Zimm (ZIMM 1956) a few years later. It was not until the 1970s that de Gennes considered the dynamics of a polymer chain in a dense polymer solution and produced his model of Reptation (DE GENNES 1971). This work was later developed by Doi and Edwards (EDWARDS 1978). These theories and models have formed much of the modern understanding of polymers. The description of molecular motions in polymer solutions enables many non-equilibrium processes, such as diffusion, to be understood.

The aim of this chapter is to provide some understanding of the field of polymer science and the issues involved. Important definitions are made to

introduce the properties that are unique to polymers. Then a description is given of the most important models of polymer dynamics in a solution. Finally, fundamental theories of the diffusion of solvents in polymers are given to introduce the concepts used in later chapters of this work. It is hoped that this chapter will introduce the reader to this interesting field of science. Further reviews of static properties of polymers are given in Flory's book (FLORY 1953) and those concerning polymer dynamics in various reviews (FERRY 1970, GRAESSLEY 1974). An excellent review of the mathematics of diffusion is given by Crank (CRANK 1975).

2.2 Properties of Polymer Molecules

A polymer is a substance composed of molecules characterised by the multiple repetition of one or more species of atoms or groups of atoms (repeating units or monomers) (METANOMSKI 1991). These are linked to each other by covalent bonds in amounts sufficient to provide a set of properties that do not vary markedly with the addition of one or a few more of the repeating units. A specific example is Polyethylene where the repeating unit is $[CH_2]_N$. The number of repeating units N can be very large, up to 10^5 in a molecule, and this is called the degree of polymerisation. The average length of the polymer molecule N is related to an average molecular weight that can be defined in two ways. M_n denotes a number average molecular mass whilst M_w denotes a weight average molecular mass. The ratio of M_w to M_n represents the spread of molecular masses in the polymer and is known as polymer dispersity. If M_w is equal to M_n then the polymer is monodisperse. The word polymer originates from the Greek, meaning many - parts. Polymers may consist of only one type of repeating unit, homopolymers, or of two or more types of repeating units, copolymers. It is important to remember that polymer molecules are classified as macromolecules because of their very large size on a molecular scale.

The conformation of a polymer refers to the structure of the molecule defined by its sequence of bonds and torsion angles. The change in shape of a given molecule due to torsion about single bonds is referred to as a change of conformation. The molecular architecture of a polymer deals with the shape of a

polymer molecule. These may be classified as linear, branched, or ring polymers amongst others. The molecular architecture is important for many physical properties of polymers, such as strength and thermal stability (GEDDE 1995).

2.2.1 The Ideal Polymer Chain

A polymer molecule has many internal degrees of freedom and can take on many different conformations. Because of this high degree of flexibility a polymer chain can be considered as a very long piece of string, tangled up in a random, three - dimensional coil. This random conformation is illustrated in figure (2.1a). To simplify and study such a polymer molecule, the polymer chain is often restricted to following a simple regular lattice. In this lattice model the polymer's repeating units are called segments and lie only on the lattice sites, the rods connecting the segments are called bonds and are nearest - neighbour links on the lattice. This simplified polymer chain is also illustrated in figure (2.1b). It is assumed that there is no correlation between the directions that different bonds can take and that all directions have the same probability. The conformation of the polymer chain can then be described in the same way as a random walk on the lattice. This theoretical concept has been applied to many problems and provides a description of the dimensions produced by such a random path. It has been extensively reviewed by Chandrasekhar (CHANDRASEKHAR 1943).

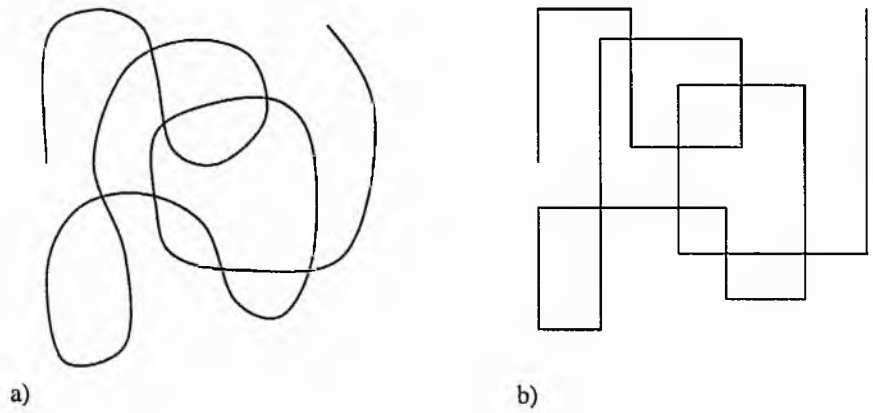

Figure (2.1): a) A two - dimensional representation of a linear polymer molecule as a randomly entangled coil; b) The corresponding polymer chain represented on a regular square lattice.

Two different measures are commonly used to describe a random polymer chain: the end - to - end distance and the radius of gyration. The end - to - end distance, r, is simply the distance between the two ends of the random coil. The radius of gyration, s, is defined as the average distance of the collection of segments in the chain from their common centre of gravity. However, meaningful chain dimensions can only be values averaged over the many chain conformations possible. Therefore, the two averages are defined as the mean square distance between the chain ends $\langle r^2 \rangle$, and the mean square radius of gyration $\langle s^2 \rangle$. For purely random polymer chains these two quantities are related by (GEDDE 1995);

$$\langle r^2 \rangle = 6 \langle s^2 \rangle \qquad (2.1)$$

Consider the end - to - end vector $\boldsymbol{r}$ connecting one end of the polymer chain to the other. If the polymer consists of N bonds each of length l, with $\boldsymbol{r}_n$ the vector of the n^{th} bond, then;

$$\boldsymbol{r} = \sum_{n=1}^{N} \boldsymbol{r}_n \qquad (2.2)$$

The average value of $\boldsymbol{r}$ is zero, since the probability of the end - to - end vector being $+\boldsymbol{r}$ is the same as it being $-\boldsymbol{r}$ so that the two contributions cancel. Therefore, the mean square end - to - end distance is calculated;

$$\langle r^2 \rangle = \sum_{n=1}^{N} \sum_{m=1}^{N} \langle \boldsymbol{r}_n . \boldsymbol{r}_m \rangle \qquad (2.3)$$

Since there is no correlation between the directions of different bond vectors, if $n \neq m$ then $\langle \mathbf{r}_n . \mathbf{r}_m \rangle = 0$, therefore;

$$\langle r^2 \rangle = \sum_{n=1}^{N} \langle r^2_n \rangle = Nl^2 \qquad (2.4)$$

where l is the length of each bond. So the end - to - end distance of an ideal polymer chain is proportional to $N^{1/2}$.

The probability density function of $\boldsymbol{r}$ can be shown to be a Gaussian distribution (DOI 1996) for very long polymer chains. The probability density function in this case is given by;

$$P(\boldsymbol{r}) = Q\exp(-3\boldsymbol{r}^2/2Nl^2) \qquad (2.5)$$

Here Q is a constant factor given by;

$$Q = (3/2\pi Nl^2)^{3/2} \qquad (2.6)$$

These Gaussian chains exhibit a random chain conformation as described above. These are termed "ideal" polymer chains, the reason for which will soon be clear. These ideal polymer chains are found in polymer melts and polymer glasses.

Polymers are found in many different states and can be classified into four phases depending on the kind and strength of interactions between the monomers. These phases are a semicrystalline state, a polymer glass, a rubbery polymer and a polymer melt. A perfect polymer crystal cannot easily be formed due to crystallisation occurring independently in different parts of the polymer. Crystalline regions in the polymer are usually separated by amorphous layers, forming a semicrystalline state. A polymer melt is a viscous liquid composed only of polymer molecules. The long polymer chains become highly entangled, but can move with respect to each other under thermal motion. If an external force is applied to the polymer melt it will begin to flow with an overall motion of the molecules. However, this can be rather slow due to the large number of entanglements. This is why polymeric liquids are usually highly viscous. If crosslinking occurs in the melt, where polymer molecules are joined together with covalent bonds to form a network, it becomes impossible for the polymer to flow. However, the mobility of the molecules between crosslinks will not be constrained by the crosslinks, they will be able to stretch from their original coiled state. This produces a rubbery state with

large elastic reversible deformations. If the temperature of the polymer melt is reduced the thermal motions become less and the motions of the polymer molecules become restricted. Eventually the temperature reaches a point where any thermal motion at any scale larger than the size of a monomer ceases to exist. Polymers in this frozen state are known as polymer glasses and are formed by a process known as a glass transition. The end - to - end distance of a chain in a polymer melt or a polymer glass scales as $N^{1/2}$ as shown for an ideal polymer chain.

The effect of short range interactions between monomers in the lattice model of the polymer must now be considered. Short range interactions are those that occur only between segments in close proximity along the polymer chain. If the orientation of each bond is random and completely independent of the previous bonds then the polymer chain is able to double back onto itself. This is a physical impossibility since two segments of the polymer chain cannot occupy the same region in space at the same time. The lattice model can be modified to disallow such doubling back of the polymer chain, however, this does not change the result that the mean square end - to - end distance is proportional to N for very long chains. If the interactions between the bonds extend only up to a finite distance along the chain, then in equation (2.3) the quantity $< \boldsymbol{r}_n.\boldsymbol{r}_m >$ will decay exponentially for long chains. For such systems the mean square end - to - end distance is always proportional to N for large N, and the distribution of $\boldsymbol{r}$ remains Gaussian. Such polymer chains are called ideal chains because this distribution of end - to - end distances is always maintained. These polymer chains incorporate short range interactions but exclude long range interactions.

Long range interactions are those that occur when two segments, widely separated along the chain, become spatially close to one another. An example of a long range interaction is the excluded volume interaction which prevents any two polymer segments from simultaneously occupying the same point on the lattice. Long range interactions cause a departure from the behaviour of an ideal chain.

2.2.2 Non – Ideal Polymer Chains

The ideal chain model described above only takes into account short range interactions along the polymer chain. This model allows a chain to fold over onto itself so that segments which are widely separated along the chain can occupy the same region in space at the same time. This is physically impossible since each segment has a finite volume. The excluded volume effect is therefore included by imposing the condition that two segments cannot simultaneously occupy the same lattice site. This effect was realised by Kuhn and Kuhn (KUHN 1943) in an attempt to make this model of a polymer chain more realistic. This excluded volume effect corresponds to the condition that the path of the chain cannot pass through any lattice sites that have been traversed previously. This corresponds to a self - avoiding random walk.

The average size of an excluded volume chain is larger than that of an ideal chain since the possibility of segments overlapping in an ideal chain is greater. The excluded volume polymer chain is therefore larger than the ideal chain of the same length. It can be shown (GROSBERG 1997) that for an excluded volume chain the root mean square end - to - end distance is proportional to $N^{3/5}$ and not $N^{1/2}$. The reason for this difference is that for the normal random walk of an ideal chain, each step is independent of all previous steps. In the case of the non - ideal chain the self - avoiding random walk is highly dependent on the previous steps of the walk. These polymer chains can be found in dilute solutions of polymers in a good solvent.

2.2.3 Polymer Solutions

A solution is any phase containing more than one component. Polymer solutions of primary interest are those in which a polymer interacts with one or more solvents. In a dilute polymer solution the polymer molecules are widely separated and hardly interact with each other at all. A polymer molecule in a dilute solution can be pictured as a coil, continuously changing its shape under the action of thermal motions. Thus a polymer molecule in a dilute solution can be characterised as a

random coil. As the concentration in a polymer solution is increased, the molecules start to overlap and begin to entangle with each other. This entanglement begins at a critical concentration called the overlap concentration c^* where the polymer molecules just begin to come into contact with one another. This situation is schematically illustrated in figure (2.2).

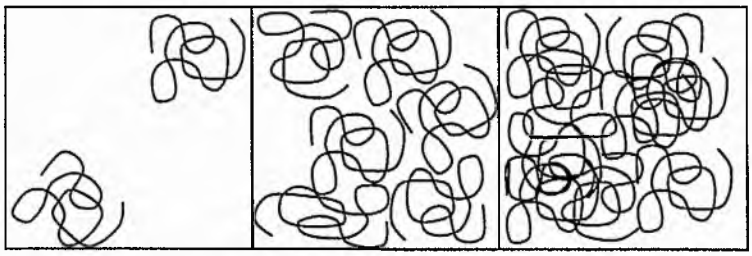

Figure (2.2): a) A dilute polymer solution with widely separated chains; b) A polymer solution at the overlap concentration where the chains are just in contact with one another; c) A dense polymer solution with highly entangled chains.

The overlap concentration c^* can be estimated by considering the volume occupied by a single random polymer coil; $V = (4/3)\pi R^3 \propto R^3 \propto l^3 N^{3/2}$. The average concentration of the segments in the coil is then;

$$c^* = N/V \sim N/(l^3 N^{3/2}) \sim l^{-3} N^{-1/2} \qquad (2.7)$$

This overlap concentration is dependent on the number of segments N in the polymer chain. The overlap concentration is lower if N is large, therefore long polymer chains are almost always in an entangled state even for very dilute solutions. At this concentration the polymer coils are entangled, yet there is still little polymer in the solution. This is known as a semi - dilute polymer solution. As the concentration of the polymer solution is increased further the polymer molecules become highly entangled and strongly interact with each other. This is a dense polymer solution. For convenience, the concentration c is often replaced by the volume fraction ϕ. This is the fraction of the whole volume occupied by the polymer segments.

The models described above do not explicitly include the presence of solvent molecules. However, the average size, or spread, of the polymer chain greatly depends on the type of solvent in which it is placed. If there is a high affinity with the solvent, a good solvent, and the polymer segments tend to repel each other, then the polymer is easily dissolved and the polymer configuration will be very widely spread. If the solvent is a poor solvent and the polymer segments tend to attract each other, then the polymer will not dissolve and the polymer configuration will be compact. The dependence of the polymer size on the type of solvent is due to the interactions between polymer and solvent molecules.

Assume each solvent molecule is the same size as a polymer segment and also occupies one site on the lattice. The interaction energies between neighbouring elements on the lattice are of three types: polymer - polymer, polymer - solvent, solvent - solvent. These energies, ε_{pp}, ε_{ps} and ε_{ss} respectively, are attractive and so are negative by convention. A quantity $\Delta\varepsilon$ can be defined to include the effects of the solvent interactions (FLORY 1953);

$$\Delta\varepsilon = \varepsilon_{ps} - \tfrac{1}{2}(\varepsilon_{pp} + \varepsilon_{ss}) \qquad (2.8)$$

This represents the change in energy when two unlike components in the solvent come into contact. If $\Delta\varepsilon<0$ the polymer and solvent tend to attract each other and the solvent is a good solvent. If $\Delta\varepsilon>0$ the polymer and solvent tend to repel each other and the solvent is a poor solvent.

The effects of these solvent interactions and the effects of the excluded volume can be expressed by a single parameter called the excluded volume parameter (FLORY 1953);

$$\nu = \nu_c(1-2\chi) \qquad (2.9)$$

where ν_c is the volume of one lattice site and χ is a dimensionless quantity called the χ parameter, which is defined as;

$$\chi = z\Delta\varepsilon / kT \qquad (2.10)$$

Here, z is the co-ordination number of the lattice, k is Boltzmann's constant and T is temperature.

In a good solvent, $\Delta\varepsilon$ is small and the excluded volume parameter v is positive. In a poor solvent, $\Delta\varepsilon$ is large, and as the temperature increases v will change sign from positive to negative at a certain temperature. The temperature at which the excluded volume parameter equals zero is called the Theta temperature. The Theta temperature is given by;

$$\theta = 2z\Delta\varepsilon / k \qquad (2.11)$$

At this temperature the repulsive excluded volume effect balances the attractive forces between the polymer segments and the polymer behaves as an ideal chain. The Theta state arises because of the cancellation of the effect of volume exclusion between segments, which tends to enlarge the molecule, and the effect of van der Waals attractions between segments, which contract the molecule. The polymer chain behaves as an unperturbed chain when in a solvent in the Theta state. Such solvents are called Theta solvents. All polymers dissolved in Theta solvents adapt to equation (2.4) for the mean square end - to - end distance. This is determined only by short range interactions. Long range interactions cause expansion of the coil that can be expressed by a swelling coefficient or linear expansion factor α;

$$\langle r^2 \rangle = \alpha^2 \langle r^2 \rangle_0 \qquad (2.12)$$

Here the subscript signifies the mean square end - to - end distance for the ideal unperturbed chain. The linear expansion factor measures the extent to which the linear molecule dimension is perturbed by the excluded volume effect and is also affected by temperature and type of solvent. At the Theta temperature the chain is unperturbed and α must equal unity. In a good solvent and for temperatures $T > \theta$, α

is greater than unity, and in a poor solvent and for temperatures $T < \theta$, α is less than unity. If the temperature decreases below the Theta temperature, attraction between the polymer segments prevails making the solvent poor and the size of the polymer becomes much smaller than that of an ideal chain. At temperatures above the Theta temperature, repulsion between polymer segments prevails making the solvent good, the polymer swells and the dimensions of the polymer coil increase.

2.2.4 Flory - Huggins Theory

Theoretical models of the static properties of solutions were proposed as early as 1910. In the 1930s the theory of a regular solution was independently introduced by Hildebrand and Wood (HILDEBRAND 1932) and Scatchard (SCATCHARD 1931). The regular solution theory is a useful description of mixtures of small molecule liquids. However, it is not valid for solutions containing polymers. The Flory - Huggins mean - field theory is a development of the regular solution theory with the inclusion of polymers. This was independently introduced by Flory (FLORY 1942) and Huggins (HUGGINS 1942) in the early 1940s using a lattice model of polymer solutions.

Simple molecule solutions often behave as ideal solutions for which many laws have been defined. However, solutions containing polymers exhibit large deviations from ideality. Ideal solution behaviour requires that the entropy of mixing the pure components must be given by;

$$\Delta S_M = -k\,(n_1 \ln N_1 + n_2 \ln N_2) \qquad (2.13)$$

where n_1 and n_2 are the numbers of molecules of the two components, N_1 and N_2 their mole fractions, and k is Boltzmann's constant. This entropy is the difference between the total entropy and the weighted average of the entropies of the pure polymer and pure solvent. Ideal solutions also require that the heat of mixing must be zero;

$$\Delta H_M = 0 \qquad (2.14)$$

Deviations from ideality may arise from failure of either of these conditions. However, these expressions rely on the assumptions that the two components are identical in size, spatial configuration, and external force field. This cannot possibly hold for polymer solutions in which the solute molecule may be a thousand times the size of the solvent molecule.

The Flory - Huggins model derives these two quantities for a polymer solution based on the lattice model in which the components of the solution are placed. The polymer chain is considered to consist of N chain segments, each of which is equal in size to a solvent molecule. A segment and a solvent molecule may replace one another in the lattice and it is assumed that the volume of the lattice is unchanged during mixing. Figure (2.3) shows the lattice model of a binary mixture of a polymer solute and a solvent. Each segment of the polymer occupies one site in the lattice as does each solvent molecule.

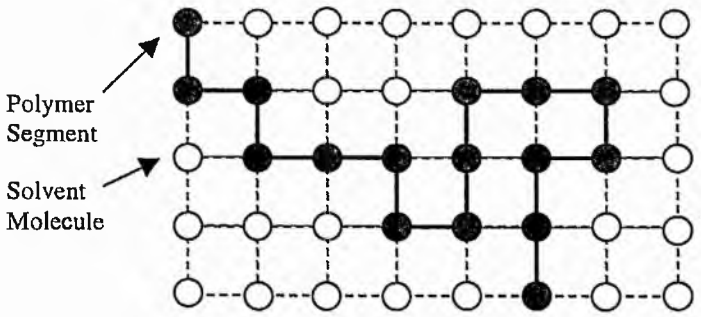

Figure (2.3): Lattice model of a binary polymer solution on a regular square lattice where the polymer segments are indicated in grey and the solvent molecules are indicated in white.

Flory calculated the total configurational entropy of the polymer solution arising from the variety of ways of arranging the polymer and solvent molecules on the lattice. This lead to the entropy of mixing of the polymer and solvent;

$$\Delta S_M = -k\,(n_1 \ln \phi_1 + n_2 \ln \phi_2) \qquad (2.15)$$

where ϕ_1 and ϕ_2 are the volume fractions of the polymer and solvent. Comparison of equations (2.13) and (2.15) reveals an analogy to the ideal entropy of mixing. Mole fractions occurring in the ideal expression are replaced with volume fractions in the formula for mixing molecules dissimilar in size. The ideal expression can be derived if the solvent and solute molecules are identical in size, in which case the mole and volume fractions are equal and the two expression are identical.

The heat of mixing is the difference between the total interaction energy in the solution as compared with that for the pure components. The absolute interaction energies are of no concern. Interaction energies are only considered between molecules or chain segments that are nearest - neighbours on the lattice. The heat of mixing, therefore, can be considered as originating in the replacement of the contacts between like species with contacts between unlike species in the solution. The formation of a solution may be likened to a chemical reaction in which the bonds between the solvent and polymer are formed at the expense of an equal number of the solvent - solvent and polymer - polymer bonds. Flory showed that the heat of mixing could be written as;

$$\Delta H_M = kT\chi n_1 \phi_2 \qquad (2.16)$$

where χ is the dimensionless interaction parameter which characterises the interaction energy per solvent molecule divided by kT, where T is the temperature. The quantity $kT\chi$ represents the difference in energy of a solvent molecule immersed in the pure polymer compared with one surrounded by molecules of pure solvent.

This simple lattice treatment of the mixing of polymers and solvents does have limitations. The most important of these is the assumption that a single lattice can describe both the polymer and the solvent. The lattice is merely a scheme to describe the positions of molecules and their nearest neighbours, but it does not account for the different spatial requirements of different species. Furthermore, this theory neglects correlations between segments of the polymer chain and hence is intrinsically associated with ideal chains. However, this remains the simplest approach to dealing with polymer solutions.

2.3 Molecular Motion of Polymers in Solution

Theoretical studies of polymer dynamics have developed over the past 50 years, but remain based on only a few important theories. Particular attention has been given to the dynamics in the crossover region from dilute polymer solutions to dense polymer systems. It has already been stated that the root mean square end - to - end distance scales differently in these two regions. In dilute polymer solutions this distance scales as $N^{3/5}$ due to the swollen polymer chains, but in dense polymer melts it scales as $N^{1/2}$ and the polymer chains behave as ideal chains. Dynamics in the dilute regime have been described by the Rouse model (ROUSE 1953) whilst dynamics in a dense polymer system have been described by the Reptation model (DE GENNES 1971). This change in dynamics can be described in terms of a hydrodynamic screening first introduced by Edwards (EDWARDS 1966). This can be considered (DE GENNES 1976a/b) in terms of a correlation length ξ dependent on the polymer concentration but independent of polymer chain length. This correlation length is inversely proportional to the number of entanglements between different chains in the entangled polymer and may be considered as the average distance between entanglement points. At distances greater than ξ, repulsive interactions between the monomers in a chain are screened out by the other chains in the system and the chain statistics are Gaussian. At distances less than ξ, each chain shows strong excluded volume effects. On increasing the polymer concentration, the range of the correlations decreases more and more, and the dynamics cross over from Rouse behaviour to Reptation behaviour. Understanding the molecular motions of polymers in solution allows many non - equilibrium phenomena, such as diffusion, to be explained.

2.3.1 Brownian Motion

Brownian motion was discovered in 1827 by the English botanist Robert Brown who observed the random motion of pollen particles suspended in water. The particles undergo chaotic thermal motion due to collisions with other molecules. In any polymer system the molecules undergo thermal motions of varying degrees. An

understanding of Brownian motion provides the initial foundation for theories of polymer dynamics and a description of their diffusive properties.

Consider the Brownian motion of a particle suspended in a solvent. If the particle moves through the solvent with a velocity V it experiences a frictional force $-\lambda V$ opposing its motion. Here λ is the coefficient of friction, which is also proportional to the viscosity of the solvent. The equation of motion for this particle can be written as;

$$mdV/dt = -\lambda V \qquad (2.17)$$

From this it can be seen that the velocity decays exponentially with a characteristic relaxation time $\tau=m/\lambda$. The mean square displacement of this motion $\langle x^2 \rangle$ can be related to a quantity known as the diffusion coefficient by;

$$D = \langle x^2 \rangle /2t \qquad (2.18)$$

Here D is the characteristic diffusion coefficient and it can be seen that the mean square displacement is proportional to the time for which the particle has been diffusing. Evidently, the greater the coefficient of friction, the lower the diffusion coefficient. The exact form of this relationship is given by the Stokes - Einstein relation;

$$D = kT/\lambda \qquad (2.19)$$

Here, D is again the diffusion coefficient, k is Boltzmann's constant, T is temperature, and λ is the coefficient of friction. This relation states that D increases with temperature, the particle undergoes greater thermal motions thus producing a greater mean square displacement. Polymer molecules are frequently modelled as a collection of interacting Brownian particles. However, before studying these models of polymer dynamics, it is first necessary to define the diffusion coefficient D more explicitly.

The diffusion coefficient D is a measure of the rate at which a particle diffuses through a system on some random trajectory. However, a number of different diffusion coefficients can be specified. The chemical diffusion coefficient D_c describes the random motion of indistinguishable particles diffusing along a potential gradient. The tracer diffusion coefficient D_t describes the random motion of distinguishable particles for a system in equilibrium where no potential gradient exists. These two diffusion coefficients become equal in the limit of zero concentration of solvent where the diffusion coefficient of the particle is called the intrinsic diffusion coefficient D_0. In equations (2.18) and (2.19) the diffusion coefficient in question is the tracer diffusion coefficient for a distinguishable tracer particle in a system where no potential gradient exists. With these elements in place, various models of polymer dynamics will now be described.

2.3.2 The Rouse Model

Rouse (ROUSE 1953) considered the Brownian motion of a single polymer molecule in a dilute polymer solution and studied its viscoelastic properties. The viscous and elastic properties of such systems arise from three factors: the length of the polymer molecule, the flexibility of the polymer chain, and the interactions of the polymer molecule with itself and other polymer molecules. For such a linear molecule to move through a viscous liquid it must co-ordinate the thermal motions of relatively short segments of the chain. Three types of force act on each segment of the polymer chain: a frictional force proportional to the relative velocity of the polymer segment with respect to the surrounding medium, a force from the adjacent polymer segments of the chain, and a random force due to Brownian motion. The Rouse model describes the effect of these forces on the flow dynamics.

The physical basis of Rouse's theory is that a velocity gradient in a solution of a linear polymer continuously alters the distribution of configurations of the polymer molecules. The co-ordinated thermal motions of the segments of the polymer molecules cause the configurations to drift continuously toward their most probable distribution. Direct contacts of a chain segment with other molecules or

with other segments of the same molecule are considered as contributing to the viscous forces that oppose the thermal motions.

The Rouse model consists of a polymer chain of N freely jointed segments or beads, each connected by a series of ideal springs. This bead - spring model is illustrated in figure (2.4). Each spring represents a series of monomers which is just long enough to obey Gaussian statistics. The motion of the surrounding liquid is modelled by a shearing stress applied to the liquid by a plane surface. This surface executes simple harmonic motion to produce a velocity gradient that varies rapidly with distance from the surface. The velocity gradient produces motions of the polymer molecule which can be resolved into two contributions; a motion at a junction between two segments with a velocity equal to that of the surrounding liquid, and the co-ordinated Brownian motion of the segments of each polymer molecule. The justification of this relies on the flexibility of the polymer chain. For each part of the polymer molecule to move with the velocity of the surrounding liquid the configuration of the molecule must be able to change as rapidly as required by the gradient of velocity of the liquid. Thus, the primary effect of the velocity gradient is to carry each segment of the polymer molecule along with the liquid.

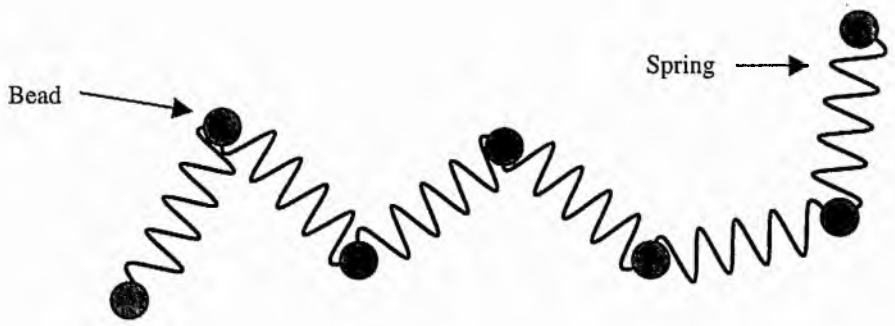

Figure (2.4): The bead – spring model of a polymer chain. Each chain segment is modelled by a bead connected to the next by an ideal spring.

Rouse gave a linear equation describing the relaxation of a polymer chain to an equilibrium state and resolved the co-ordination of the motions of the chain into a series of eigenmodes. Each mode has a characteristic relaxation time, the time taken

for the system to relax to its equilibrium state. Rouse found that the fundamental, or longest, relaxation time increased with the square of the chain length, $\tau \propto N^2$. Furthermore, it was found that longest relaxation time accounted for the solution's viscosity. This model also predicts the dependence on the chain length N of the viscosity, $\eta \propto N$, and the tracer diffusion coefficient, $D_t \propto N^{-1}$.

Limitations of the model arise because long range interactions between polymer segments were not included and the excluded volume interaction was neglected. The Rouse model may seem a natural way to describe the Brownian motion of a polymer chain, but its conclusions do not agree with experiment (BINDER 1995). The main reason for this is that Rouse assumed the average velocity of a particular segment is determined only by the external forces acting on it and is independent of the motion of other segments. In reality the motion of one segment is influenced by the motion of the surrounding segments through the medium of the solvent. However, Rouse's work remains the basis of many descriptions of polymer dynamics.

2.3.3 The Zimm Model

Zimm (ZIMM 1956) continued the work of Rouse and considered the motion of a polymer molecule diffusing through a viscous medium under the simultaneous influence of an external force field and of Brownian motion. In a viscoelastic fluid the external force on the polymer chain is supplied by the flowing medium as described above. However, Rouse neglected one important aspect. If one polymer molecule moves, the solvent surrounding it will also move and as a result other polymer molecules will be dragged along. This effect is termed a hydrodynamic interaction and was first modelled by Zimm. This hydrodynamic interaction amounts to long range correlations in the displacements of the chain segments, mediated by the flow of solvent. The effect of this interaction is illustrated in figure (2.5).

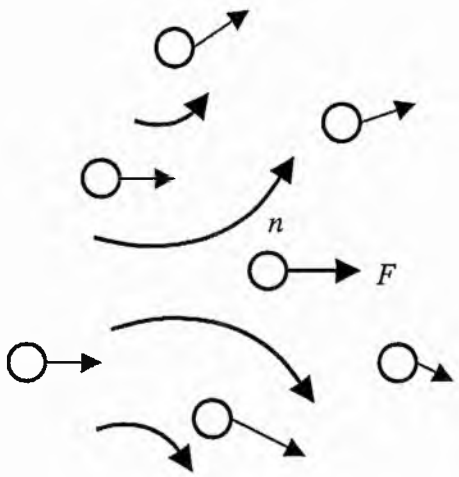

Figure (2.5): The hydrodynamic interaction; if particle *n* moves under the action of a force *F* a flow is created in the surrounding fluid which causes the other particles to move.

Zimm also used a bead - spring model consisting of a chain of N freely jointed segments connected to each other by ideal springs. The polymer chain is suspended in a viscous liquid with which it is supposed to interact only through the polymer segments, or beads. This interaction consists of a force exerted on the segments by the liquid. The force is assumed to be proportional to the velocity of the segment through the liquid. The connecting springs also exert a force on the segments. In addition to these mechanical forces, there is an effective force resulting from the Brownian motion of the chain. Zimm described a complicated equation of motion that included these three contributions, based on the Rouse model, that also included the hydrodynamic interaction.

Zimm found that the relaxation time τ of the polymer chain increases as $N^{3/2}$, which provides better agreement with experiment. The inclusion of the hydrodynamic interaction modified the relationship between relaxation time and polymer chain length. Rouse found that relaxation time increased with N^2, while Zimm has modified this dependency by considering a more detailed model.

2.3.4 The Reptation Model

In a dense polymer system, such as a polymer melt or a concentrated polymer solution where chains are highly entangled, polymers can flow like a highly viscous liquid or can behave elastically like a rubber. This viscoelastic behaviour has been understood for a long time (GREEN 1946, LODGE 1956). Depending on the frequency of an applied external force, polymeric fluids can behave either as viscous liquids or elastic solids. Generally, viscoelastic bodies tend to show a viscous response to slowly changing forces and an elastic response to ones that vary quickly. These two regions are separated by a relaxation time τ that strongly depends on the polymer chain length. The Reptation model (DE GENNES 1971) argues that every polymer chain is confined within an effective tube formed by the entangled neighbouring chains. This idea of a tube was proposed later by Edwards (EDWARDS 1973) in 1973. The chain cannot move through the walls of the tube, as it cannot intersect other polymer molecules. The chain thus moves inside this tube with a snake-like motion known as reptation, from the Latin reptare, "to crawl". At small times $t < \tau$, the crosslinks between the entangled chains do not have time to break and the polymer behaves as an elastic body. At large times $t > \tau$, the crosslinks decay by Brownian motion; the chains can slide past one another and are no longer confined to tubes, resulting in a behaviour similar to a liquid. This transient network is due to the finite lifetime of crosslinks between polymer chains. The time τ is called the longest relaxation time, when the polymer's type of response to stress changes. It is the time taken for a reptating polymer chain to leave its original tube. The Reptation model has since been augmented by Doi and Edwards (DOI 1978).

De Gennes originally considered a system simpler than an entangled polymer melt, where a single ideal polymer chain is trapped within a three - dimensional network. This network is illustrated in figure (2.6) and is described by fixed obstacles. The polymer chain consists of N freely jointed segments of length l. The chain is not allowed to cross any of the obstacles, but may move freely in a snake -

like fashion between them. This motion corresponds to the migration of certain defects along the chain, similar to the motion of unravelling a knotted rope.

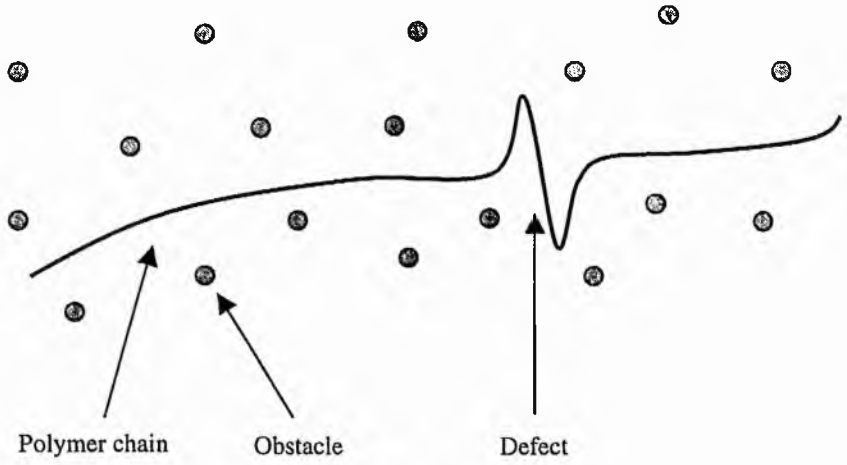

Figure (2.6): The Reptation model of a free polymer chain. The polymer chains forming the tube are modelled by fixed obstacles between which the polymer chain reptates through the propogation of a defect.

The notion of a tube in which the polymer chain is trapped is illustrated in figure (2.7). Within this tube the chain progresses by reptation, eventually leaving some parts of the tube and creating new parts.

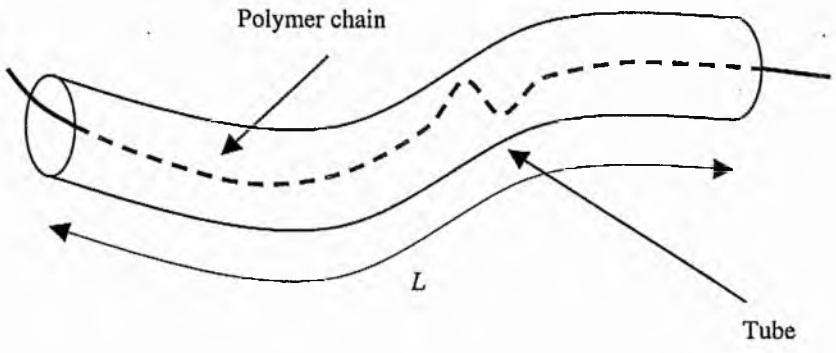

Figure (2.7): The tube model of a reptating polymer chain trapped within an effective tube of length L from which it diffuses into new tubes.

The longest relaxation time, or terminal relaxation time τ_t, is the time required for complete renewal of the tube. Within the tube the polymer chain has a certain mobility μ which is inversely proportional to the length of the polymer chain N. Similarly the diffusion coefficient within the tube D_t is also inversely proportional to the length of the polymer chain N. To completely renew the tube, the polymer chain must progress by tube diffusion over a distance equal to the length of the tube L. The corresponding time is;

$$\tau_t \sim L^2/D_t \qquad (2.20)$$

Since L is linear in N, the relaxation time is expected to scale as;

$$\tau_t \propto N^3 \qquad (2.21)$$

This is the time to completely disengage the chain from the tube confining it. This relationship has been shown to be very close to the experimentally observed result of $\tau \propto N^{3.3}$ (Kramer 1974, Kramer 1975). This relaxation time is very long, of the order of macroscopic times. Thus the reptation concept does give a plausible explanation of viscoelastic behaviour of polymers. In this time the polymer chain diffuses a distance in space smaller than L due to the contorted nature of the tube. The translational diffusion coefficient of the reptating chain can be shown to scale as $D \propto N^{-2}$ and viscosity as $\eta \propto N^3$. This work neglected the back flow effects studied by Zimm and the excluded volume interaction, but in a dense polymer system these effects are screened out and make no contribution.

2.4 Theory of Solvent Diffusion

The diffusive nature of a polymer solution poses many problems regarding the dynamics of the motion of the polymer chains. However, it is also important to be able to describe the diffusion of the solvent molecules within this system. Research in this area has been very active in the past few decades. It has been observed that solvent diffusion in a polymer rubber generally agrees with the

predictions of Fick's law (FICK 1855). However, solvent diffusion in a polymer glass often deviates from Fickian diffusion, leading to anomalous or non - Fickian diffusion. It was Alfrey et al. (ALFREY 1966) who recognised the two limiting cases of diffusional behaviour. Fickian diffusion was termed Case I diffusion and non - Fickian diffusion was termed Case II diffusion.

2.4.1 Case I or Fickian Diffusion

Diffusion is the process by which matter is transported from one part of a system to another as a result of random molecular motions (CRANK 1975). This can be demonstrated when a vessel is carefully filled with iodine solution and water so that no convection currents occur. Initially a clearly defined boundary is seen between the coloured iodine and clear water, but after a time the iodine diffuses into the water until the whole solution appears uniform in colour. A transfer of iodine molecules has occurred between the two regions of liquid. The motion of each iodine molecule is a random one with no preferred direction due to the constant collisions with solvent molecules. A net transfer of matter is seen from a region of higher concentration to a region of lower concentration because, on average, equal fractions of molecules will cross an arbitrary plane in the solution as a result of random molecular motions. If one side of this plane contains a higher concentration of iodine molecules than the other there will be a net transfer of iodine molecules to the region of lower concentration. Thus, diffusion is a purely random process that occurs to equilibrate any concentration gradient within the solution.

In 1855 Fick (FICK 1855) put diffusion on a quantitative basis by adapting the mathematical equation of heat conduction derived by Fourier in 1822. The transfer of heat is also due to random molecular motions and is analogous to a diffusion process. The theory of diffusion in isotropic substances is based on the hypothesis that the rate of transfer of diffusing substance through a unit area of a section is proportional to the concentration gradient measured normal to the section;

$$F = - D_c \, \partial c / \partial x \qquad (2.22)$$

This fundamental equation is known as Fick's First Law. Here, F is the flux, or rate of transfer per unit area of cross section, c is the concentration of the diffusing substance, x is the distance measured normal to the section and D_c is the chemical diffusion coefficient. In some systems, such as dilute solutions, the diffusion coefficient can be taken as constant, while in other systems, such as polymers, diffusion is highly dependent on concentration. The negative sign in this equation indicates that diffusion occurs in the opposite direction to the increasing concentration gradient.

The fundamental differential equation of diffusion in an isotropic medium can be derived from equation (2.22). If the concentration gradient exists only along the x axis then diffusion is in one dimension and this can be written simply as;

$$\partial c / \partial t = D_c \, \partial^2 c / \partial x^2 \qquad (2.23)$$

This equation is usually referred to as Fick's Second Law and is the fundamental differential equation of many diffusion processes where the diffusion coefficient is a constant. In many systems the diffusion coefficient depends on the concentration of the diffusing substance. In this case D_c may be a function of x and c, thus equation (2.23) becomes;

$$\partial c / \partial t = \partial / \partial x \, (D_c(c) \, \partial c / \partial x) \qquad (2.24)$$

Solutions of Fick's diffusion equations can be found for many different systems to provide a numerical solution of the diffusion process. General solutions of Fick's Second Law can be obtained for a variety of initial and boundary conditions provided the diffusion coefficient is constant. Such solutions will usually take the form of a series of error functions or related integrals, or the form of a trigonometrical series.

Several general characteristic features of Fickian diffusion remain dominant for all solutions of these equations. Firstly, solutions of the diffusion equation will be in the form of smoothly varying functions. If the solvent profile is plotted as

solvent concentration against distance for a particular time, then the solvent concentration will be a smoothly varying function of distance. Secondly, the distance that these solvent fronts progress through the system will be proportional to the square root of time. Thus, the distance of penetration of any given concentration will be proportional to the square root of time. Thirdly, the time required for any point to reach a given concentration is proportional to the square of its distance from the surface and varies inversely with the diffusion coefficient. Also, the amount of diffusing substance entering the medium through a unit area of its surface varies as the square root of time. These fundamental properties define the Fickian diffusion process and are illustrated in figure (2.8).

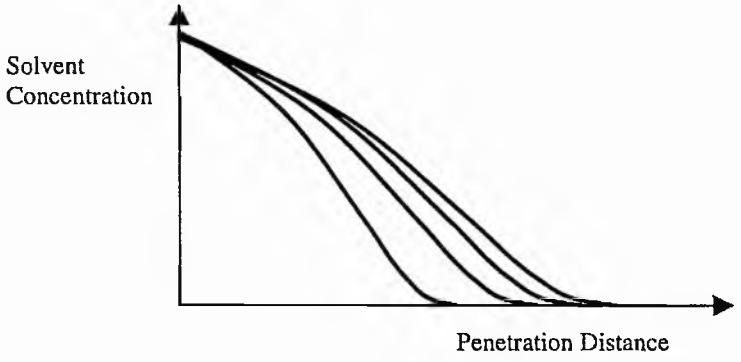

Figure (2.8): An illustration of the characteristics of Fickian diffusion showing solvent concentration against penetration distance for four solvent profiles at four equal time intervals. In this example, the solvent concentration at $x=0$ is held constant.

2.4.2 Case II or Non - Fickian Diffusion

Non - Fickian diffusion was first classified by Alfrey et al. in 1966 (ALFREY 1966) and was termed Case II diffusion. This second limiting case of diffusion has been observed for solvent diffusion into a polymer glass, especially where the penetrant causes extensive swelling of the polymer. Case II diffusion exhibits characteristic features distinct from those for Fickian diffusion. Firstly, the solvent profile for Case II diffusion shows a sharp vertical front which marks the innermost limit of penetration of the solvent and is the boundary between the unswollen polymer glass and the swollen rubbery polymer. The solvent concentration behind this front remains constant in the swollen polymer. Ahead of the front a region of

low solvent concentration is seen entering the polymer glass with Fickian characteristics. This Fickian precursor was first described by Peterlin (PETERLIN 1965) and is the result of Fickian diffusion into the polymer glass. Secondly, the solvent front advances through the polymer linearly with time. Thus, the distance of penetration of any given concentration will be proportional to time. If this distance d is described by the following equation at a time t;

$$d = k\,t^n \qquad (2.25)$$

where k and n are constants, then for Case I diffusion n=½ and for Case II diffusion n=1. Thirdly, the amount of diffusing substance entering the medium through a unit area of its surface varies linearly with time. These features of Case II diffusion are illustrated in figure (2.9). Anomalous diffusion occurs between the limits of Case I and Case II diffusion where $1>n>½$. Extensive reviews are available of the experimentally observed diffusion anomalies in various polymer systems (ROGERS 1965, PARK 1968, PETROPOULOS 1970).

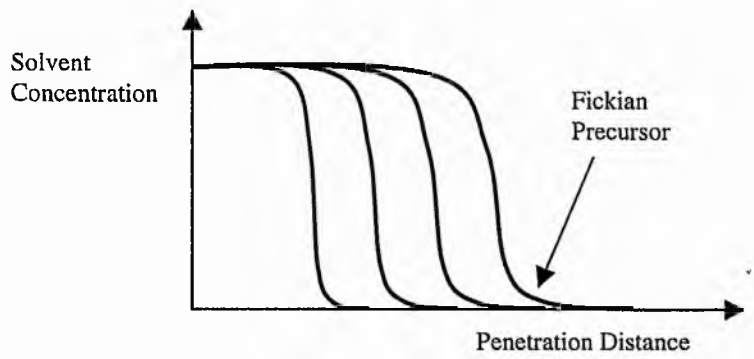

Figure (2.9): An illustration of the characteristics of Case II diffusion showing solvent concentration against penetration distance for four solvent profiles at four equal time intervals. In this example, the solvent concentration at $x=0$ is held constant.

2.5 Conclusions

This chapter has provided an introduction to all of the aspects of polymer physics that will be used in subsequent parts of this work and has given an overview of this interesting area of science. The current understanding of the properties of polymers, their dynamics, and the diffusive behaviour of the solvent is by no means complete. Many theoretical models have been presented to explain aspects of these different problems and some models have been very successful. However, these models rely on approximations and idealisations and may still need further development in the light of new advances in this field. There is still the opportunity for new models to be developed that will supersede current models if they provide a better explanation of experimental findings and a better understanding of the underlying physics.

The most important points that the reader should carry forward from this chapter regard the random nature of the polymer systems considered here. The ideal polymer chain can be considered as a random coil whose statistics are analogous to a random walk. The models of polymer dynamics presented here rely on the idea of a collection of interacting particles undergoing random Brownian motion. Finally, the diffusion of solvent in a polymer is also a random process that equilibrates any concentration gradient in the solvent. These properties will be utilised in the modelling of solvent diffusion in a polymer.

Chapter 3

Monte Carlo Modelling of Solvent Ingress into Polymer

3.1 Introduction

Polymer science has profited from the development of computer simulations in many ways. They have been used to study complex macromolecular systems in detail and provide insights that may not have otherwise been gained. Since the invention of the Monte Carlo algorithm (METROPOLIS 1953) more than 40 years ago, Monte Carlo modelling has become a widely used tool for problems of statistical mechanics (BINDER 1979) and also for polymers (BINDER 1995). There have been a number of studies of polymer systems using the Monte Carlo method to investigate the static and dynamic properties of polymer molecules in melts (NAGHIZADEH 1986, TEN BRINKE 1988, BASCHNAGEL 1995) and solutions (WALL 1957, 1959, VERDIER 1963, 1966, 1973, GEROFF 1993, SHENG 1995). However, this method has not previously been used to explicitly study the ingress of solvent into a polymer.

In this chapter a Monte Carlo method is described to model the ingress of solvent into a polymer. A brief discussion is given of the considerations necessary in choosing a suitable model and the simplifications that must be made to make the model computationally viable and efficient. The Monte Carlo method is also reviewed briefly. The details of the methods used and the algorithm developed for this "Simple" Monte Carlo model are then described. Results are given to show the

model's dependence on a number of interesting model parameters. This chapter should provide an understanding of the development, and application, of a Monte Carlo model of solvent ingress into polymers.

3.2 Monte Carlo Modelling of Polymers

Monte Carlo modelling can be a very powerful tool in the study of a wide range of numerical systems. However, as with all numerical modelling techniques, assumptions and simplifications must be made to reduce the physical problem to a computationally viable and efficient model. Numerical simulations of polymers pose particular challenges due to the enormous spread of length scales and time scales involved. Length scales may vary from the dimensions of the chemical bond (~ 1Å) to the dimensions of the radius of gyration (~ 100Å). Since a valid computer simulation must choose a system size with linear dimensions larger than the characteristic lengths of the problem, one finds that for many problems of interest it would be necessary to simulate systems containing of the order of at least 10^6 atoms (BINDER 1995). Simultaneously, time scales may range from bond vibration times (~ 10^{-13} sec) to macroscopic times (~ 10^3 sec). For these reasons one must abandon the idea of simulating polymeric systems in full atomistic detail. One method that achieves this is to introduce a coarse - grained model.

3.2.1 Coarse - Grained Models

There are many ways to construct coarse - grained models that abandon chemical detail to simplify the polymer system of interest. The choice of model depends on the physical problems that one may wish to address, and also on the desire to construct computationally efficient algorithms. Generally though, a coarse - grained model of a polymer chain replaces several monomers by one effective segment. These segments are connected together by bonds thus producing an equivalent chain of N segments and $(N-1)$ bonds. Coarse - grained models may be free to take on arbitrary angles between successive segments of the chain or alternatively may be restricted to a regular lattice.

For an off - lattice, coarse - grained model each polymer chain is modelled by a succession of rigid bonds jointed together at arbitrary angles as illustrated in figure (3.1). The relaxation of polymer chains to an equilibrium state in this model is achieved by the random rotation of bonds around the axis connecting the nearest - neighbour segments along the chain to some other arbitrary angle. The most popular (KREMER 1986, 1990, 1993) and efficient off - lattice model is the bead - spring type used by Rouse (ROUSE 1953). In this model the rigid bonds are replaced by bonds with a simple harmonic potential, giving the polymer chain a certain extensibility. The segments in this model are known as beads because they represent solid spheres.

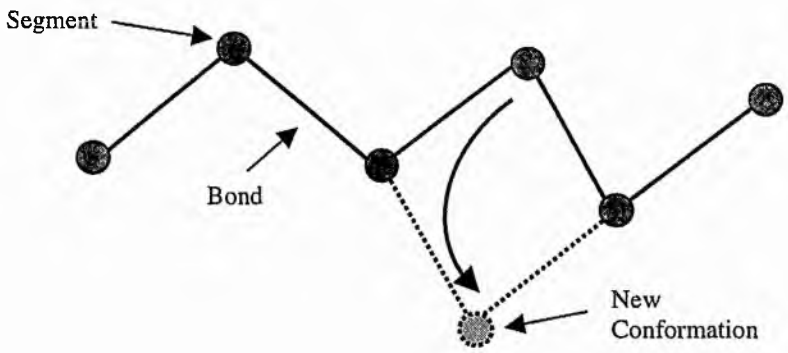

Figure (3.1): Off – lattice model of a freely jointed polymer chain showing how a new conformation may be achieved (dashed lines) by the random rotation of bonds.

Lattice models simplify the problem further by representing the polymer chain as a self - avoiding walk (ROSENBLUTH 1955) on a regular lattice. This approach is very old and has been used to study the static properties of polymers in solutions (FLORY 1941, HUGGINS 1941) and polymer melts. The simplest model consists of a regular lattice where each segment of the polymer chain occupies only a single lattice site, and the bond connecting two segments is simply a nearest - neighbour link on the lattice. This is illustrated in figure (3.2). Since each lattice site can at most be occupied by one segment of the polymer chain, the chain cannot intersect itself and thus an excluded volume interaction is inherent in the model. A simple cubic lattice also imposes rigid bond angles of 90^{o} and 180^{o} and is thus a further idealisation. The main advantages of this method are that integer arithmetic

can be used, and that the excluded volume interaction is implicitly included through the occupancy of lattice sites.

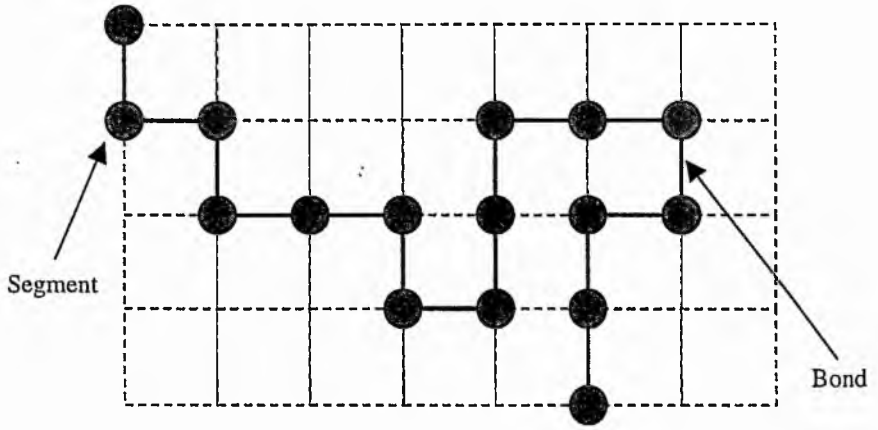

Figure (3.2): Lattice model of a polymer chain on a square lattice where each segment is represented by a dark circle connected by a series of rigid bonds.

Various dynamic algorithms can be applied to the lattice model to allow the polymer chains to relax to an equilibrium state. These elementary moves were first proposed by Verdier and Stockmayer (VERDIER 1962) whose original algorithm used only two types of motion: end rotations and bend moves. This resulted in a slow algorithm (VERDIER 1966) which neglected to include the excluded volume interaction. The bend move is simply an exchange of two neighbouring bond vectors that are mutually perpendicular. Therefore, new bond vectors are only created by the random rotation of bonds at the chain ends and must slowly diffuse into the interior of the chain to equilibrate its configuration (VERDIER 1970). These two types of motion form the minimum useful set, but additional moves can be included. In the generalised Verdier - Stockmayer algorithm the crankshaft rotation is also included. This type of motion is the rotation of two locally parallel bond vectors to a new orientation. These three motions, illustrated in figure (3.3), will have a low acceptance rate at high volume fractions ϕ of occupied sites, since the vacant sites needed for an acceptable move are then very rare. Due to the need for sufficient vacancies this algorithm has only been used for volume fractions $\phi \leq 0.8$ (SARIBAN 1988). Another problem with this algorithm is that it can be proven to be non-

ergodic (MADRAS 1988). Locally compact chain configurations can be found that cannot relax by the simple motions shown.

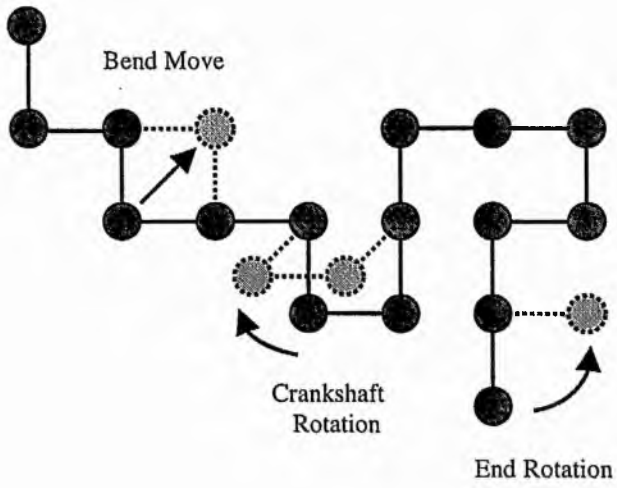

Figure (3.3): The generalised Verdier - Stockmayer algorithm on a simple cubic lattice showing three types of motions: end rotations, bend moves, and crankshaft rotations as described in the text.

Alternatively, the "slithering snake" algorithm (WALL 1975), illustrated in figure (3.4), needs only one vacant lattice site near to a chain end for a move to be accepted and can be used for significantly denser systems $\phi \leq 0.976$ (BAUMGARTEN 1984). In this algorithm an end bond of the polymer chain is removed and added to the opposite end of the chain with a random orientation. However, this algorithm is not strictly ergodic and has no counterpart in the dynamics of real chains. The advantage of this algorithm is that it relaxes faster than the Verdier - Stockmayer algorithm as new chain conformations are generated more quickly due to the need for fewer vacancies. However, the generalised Verdier - Stockmayer algorithm must be used if one is interested in dynamical chain properties.

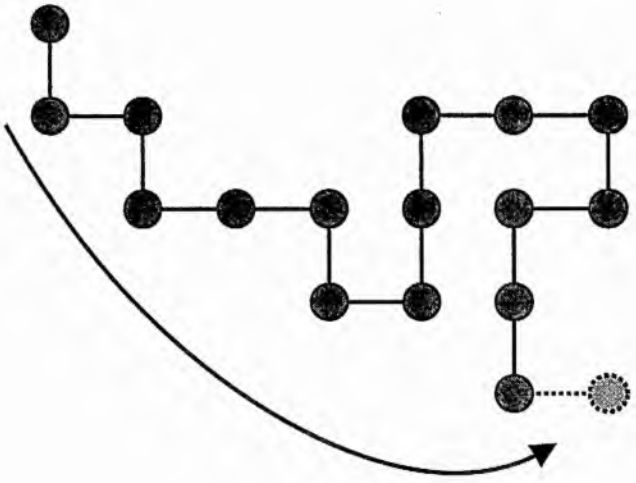

Figure (3.4): The "Slithering Snake" algorithm; an end bond is removed from one end of the chain and replaced at the other.

For most static properties of single polymer chains the pivot algorithm is used (MADRAS 1988). A bond in the chain is chosen at random and rotated, together with the rest of the chain, to a randomly chosen new orientation on the lattice as shown in figure (3.5). The advantage of this algorithm is that new chain configurations are generated very rapidly which are not correlated with their predecessors. However, this algorithm cannot be used to study the dynamic properties of the chains and is also not useful for dense polymer systems due to the need for a large number of vacant lattice sites for an acceptable move to be made.

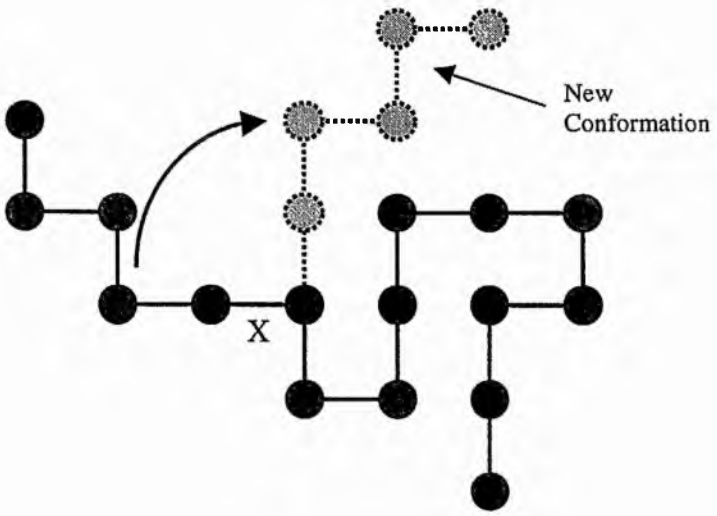

Figure (3.5): The Pivot algorithm; a bond (X) is randomly chosen and rotated , together with the preceding section of chain, to a new orientation.

To represent a linear polymer chain as a self - avoiding walk on a lattice appears to be a very crude model. Real linear polymer molecules live in continuous space, usually have tetrahedral bond angles (*109.47°*) and have a complicated monomer - monomer interaction potential. The self - avoiding walk however, lives on a discrete lattice, has non - tetrahedral bond angles (*90°* and *180°* for a simple cubic lattice), and has a repulsive hard - core monomer - monomer potential due to the excluded volume interaction. However, this method of simplification has been shown to be very effective and a very good model of real polymers (SARIBAN 1988, BINDER 1995).

3.2.2 The Monte Carlo Method

The Monte Carlo method is based on the use of random numbers. It was in 1953 that Metropolis et al. (METROPOLIS 1953) first described how random numbers could be used to investigate many - body problems. In this method, random numbers generated by a computer can be used to simulate any process where an event occurs on the basis of some probability. Monte Carlo methods can be classified as static or dynamic. Static methods are those that generate a random sequence of statistically independent samples from a given probability distribution of possible states. Dynamic methods are those that generate a random sequence of correlated samples from some stochastic process.

Static Monte Carlo is the simplest method for generating a random sample of polymer chain configurations. A lattice site is chosen at random as the chain's starting point. From here the polymer chain is formed by randomly selecting one of the nearest - neighbour lattice sites and extending the chain by one segment length l in that direction. This is repeated until the desired chain length N is achieved. If the chosen site is already occupied by a chain segment the chain cannot be extended in this direction without violating the excluded volume principle. In this case the entire chain conformation is discarded and the process repeated from the beginning. In this way many uncorrelated chain conformations are generated, each with equal probability.

The dynamic Monte Carlo method generates new polymer chain conformations from existing chain conformations through a stochastic process where each event occurs with some probability (LOWRY 1970). The time evolution of this stochastic process is then simulated, starting from an arbitrary initial configuration of chain conformations. In physical terms, a stochastic time evolution is invented for the given system to allow its dynamic properties to be studied. However, this time evolution need not apply to any real physical dynamics, the process is simply the numerical dynamic algorithm chosen for its computational efficiency. In practice the stochastic process is always taken to be a Markov process, where successive events form a Markov chain. This has the property that, given all previous values of the process, the n^{th} step ω_n depends only on the preceding step ω_{n-1}. In this way the Markov chain will gradually forget its initial state as new polymer chain conformations are generated.

A dynamic Monte Carlo algorithm is specified by the state space S and the transition probability matrix $P=\{p(\omega_n \rightarrow \omega_{n+1})\}$ for a change of conformation from configuration ω_n to ω_{n+1}. Here S specifies the model, while P specifies the numerical algorithm by which the model is studied. To define P, one must specify the set of allowed elementary moves, i.e. the transitions $\omega_n \rightarrow \omega_{n+1}$ for which $p(\omega_n \rightarrow \omega_{n+1})>0$, and their probabilities $p(\omega_n \rightarrow \omega_{n+1})$. Each self – avoiding walk has equal probability, therefore the transition probability must satisfy the detailed balance principle. This requires that the probability of making a transition $\omega_n \rightarrow \omega_{n+1}$ must be equal to the probability of making the reverse transition $\omega_{n+1} \rightarrow \omega_n$. For each transition from state ω_n to ω_{n+1}, the chosen algorithm should also be ergodic; such that each state can eventually be reached from any other state by some finite sequence of allowed moves.

In practice a segment of a polymer chain is chosen at random from the initial configuration of the system and an attempted move is made using one of the elementary moves discussed in section (3.2.1). This elementary move will produce a new random - walk that is not guaranteed to be self - avoiding. Therefore, if the walk is self - avoiding, the attempted move is accepted. However, if the attempted move would violate the excluded volume principle, the attempted move is rejected.

This procedure can be understood as the Metropolis criterion for the energy function $E(\omega)$: $E(\omega)=0$ if ω is self-avoiding and $E(\omega)=+\infty$ otherwise. The energy required to make the move is zero if the new random - walk is self - avoiding, but an infinite positive repulsive energy exists if the move is not self - avoiding. This procedure can be modified further to include the energy difference ΔE between states ω_n and ω_{n+1}, where;

$$\Delta E = E(\omega_{n+1}) - E(\omega_n) \qquad (3.1)$$

If the new walk is self - avoiding and the difference in energy is negative, then the attempted move will happen with certainty, $p(\omega_n \rightarrow \omega_{n+1})=1$. This follows the convention that a favourable interaction has a negative change in energy. If the new walk is self - avoiding and the difference in energy is positive, then the move will happen with a transition probability;

$$p(\omega_n \rightarrow \omega_{n+1}) = \exp(-\Delta E/kT) \qquad (3.2)$$

where k is Boltzmann's constant and T is the temperature of the system. Practically, these moves are realised according to their transition probability by selecting a random number from a uniform distribution in the interval $[0,1]$. If the transition probability is greater than the random number, the attempted move is executed. Otherwise, the attempted move is abandoned and the existing chain configuration is taken once again. By repeating this procedure over many cycles a dynamic algorithm is created. After every cycle the elapsed time for the system is incremented by one time period. In this case, the time period will be equal to the time between attempted moves and is a constant.

The Monte Carlo algorithm has since been developed further in the study of Molecular Beam Epitaxy (MAKSYM 1988) and electron transport. Instead of a polymer segment being chosen randomly at each cycle and a dynamic move being attempted, a transition rate r is now defined. If r_n is the rate at which a segment at lattice site n can attempt to move by a particular process, then the total transition rate R of the system is given by;

$$R = \sum_{n=1}^{N} r_n \qquad (3.3)$$

Here, N is the total number of occupied lattice sites. A random number is then chosen between *1* and R, corresponding to a particular attempted move. The advantage of this method is that only segments of the polymer chain that are able to make an attempted move can be chosen. A linear series of segments of the chain are unable to move and consequently would be assigned a rate $r=0$. These segments would not be chosen in this scheme and hence this quasi - random sampling is a more efficient algorithm. In this method, the time period by which the elapsed time is incremented is not constant, but depends on these rates to allow for different processes occurring on different time scales. The relative probability of a particular process occurring will be the ratio of the rate r of that process to the total rate R of the system. The time between attempted moves τ must be distributed according to a Poisson distribution (WALPOLE 1978), where;

$$P(\tau) = R \exp(-R\,\tau) \qquad (3.4)$$

If $P(u)$ is the distribution of a uniformly distributed random number between *0* and *1*, i.e. $P(u)=1$ where $(0 < u \leq 1)$, then the following identity can be used;

$$P(\tau)\, d\tau = P(u)\, du \qquad (3.5)$$

which, comparing these two equations, yields;

$$du/d\tau = R \exp(-R\,\tau) \qquad (3.6)$$

Thus, the time increment of the system may be evaluated by generating a uniformly distributed random number u and substituting it into the integrated form of equation (3.6);

$$\tau = -(1/R) \ln u \qquad (3.7)$$

The time elapsed for the system is therefore not proportional to the number of Monte Carlo cycles but increases in random increments scaled by the total transition rate. The importance of this method is that it allows a number of different processes to take place in the system, each on different time scales, and is necessary if the number of particles in the system able to attempt to move is not constant with time.

3.3 A Monte Carlo Model of Solvent Ingress

The methods discussed above are now applied to a Monte Carlo model of solvent ingress into a polymer. Recent Monte Carlo studies of polymer solutions have not explicitly included the solvent component (GERROFF 1993, MILCHEV 1993). These models have used a reduced polymer density to represent the volume fraction of the polymer in a solution. In this model the solvent component is explicitly included to study the diffusive properties of the solvent in the polymer. The diffusion of the solvent is also a random process and is incorporated into the dynamic Monte Carlo method previously described. The computer code developed for this problem was written in FORTRAN 77 and its operation is illustrated in the appendix, figure (A.1).

3.3.1 The "Simple" Model

The physical system to be studied by this model is that of a bulk polymer that comes into contact with a solvent reservoir at a time $t=0$. The system then evolves with time as the solvent diffuses into the polymer. It is assumed that only one face of the bulk polymer at $x=0$ is in contact with the solvent and that an infinite supply of solvent at this surface maintains a constant surface concentration. Furthermore, the bulk polymer is semi - infinite, in that, the dimensions of the bulk polymer extend to infinity so that the solvent molecules never reach these boundaries and introduce surface effects other than those described at $x=0$.

The Monte Carlo computer model of this system employs a semi - infinite three - dimensional cubic lattice which defines an array of locations at which the solvent molecules or polymer segments may be placed. Both the solvent molecules and polymer segments are modelled as hard spheres. It is assumed that the solvent molecule has the same dimensions as the polymer segment and that each occupies only one lattice site. Thus, the excluded volume interaction is automatically included. Periodic boundary conditions are used in the y and z directions to simulate the semi - infinite bulk polymer. In the x direction the lattice extends to infinity, or at least to a distance well beyond the maximum penetration distance of the solvent. This configuration is illustrated in figure (3.5).

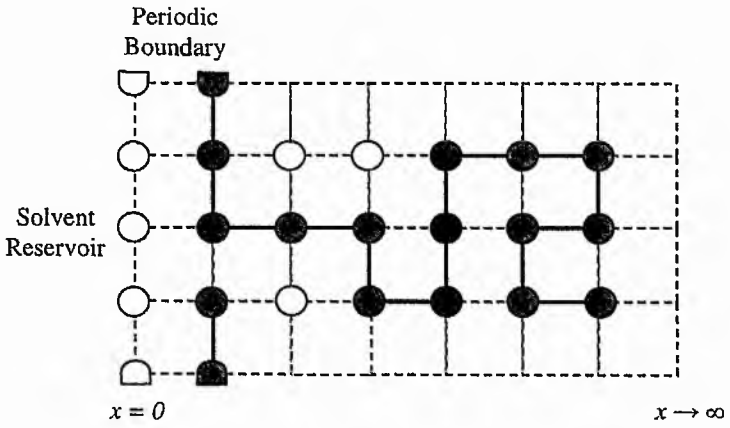

Figure (3.5): A two - dimensional illustration of the model configuration showing the placement of solvent molecules (white circles) and polymer molecules (grey) on the semi - infinite lattice. Periodic boundaries are also indicated

Solvent molecules are placed at random in the initial surface plane $x=0$ by selecting a target site at random and placing a solvent molecule there only if that site is unoccupied. This is repeated until the required volume fraction of lattice sites occupied by the solvent ϕ_s is achieved in that plane. Polymer chains are placed within this lattice using the static Monte Carlo method described previously. An initial lattice site is chosen at random for the start of each polymer chain. A target site is then chosen at random from the six nearest - neighbours and, if unoccupied, the polymer chain is extended by one segment length l in that direction. This is repeated until the required chain length N is achieved. The volume fraction of lattice sites occupied by the polymer chains ϕ_p placed in the lattice is equal to the volume

fraction of solvent molecules ϕ_s placed in the initial plane to conserve density across this boundary. The conformation of each polymer chain placed is then tested to decide which of the three Verdier - Stockmayer (VERDIER 1962) moves each chain segment would be able to perform. Each of these three types of move constitutes a distinct process, as does the motion of a solvent molecule. Therefore, within this system there are four possible processes that may occur with each cycle. For each particle successfully placed in the system the computer program uses linked arrays to store a unique numeric label for the particle, its location within the lattice, and the type of process associated with that particle. In addition, a further array is used to count the number of particles corresponding to each process.

The main body of the program now implements the Metropolis (METROPOLIS 1953) dynamic Monte Carlo method to study the dynamics of this system. A rate r is defined for each of the four processes described above: r_s, r_e, r_b, r_c for solvent, end, bend, and crankshaft moves respectively. The transition rate for each process is then this process rate multiplied by the total number of particles corresponding to that process, $R_s=N_s r_s$, $R_e=N_e r_e$, $R_b=N_b r_b$, $R_c=N_c r_c$. The total rate R for the system is the sum of these four transition rates. For each cycle of the program, an attempted move is chosen at random by selecting a random number between 0 and R. If this total rate is considered in terms of a rate line along which a random position is selected, then this method can be illustrated by figure (3.6).

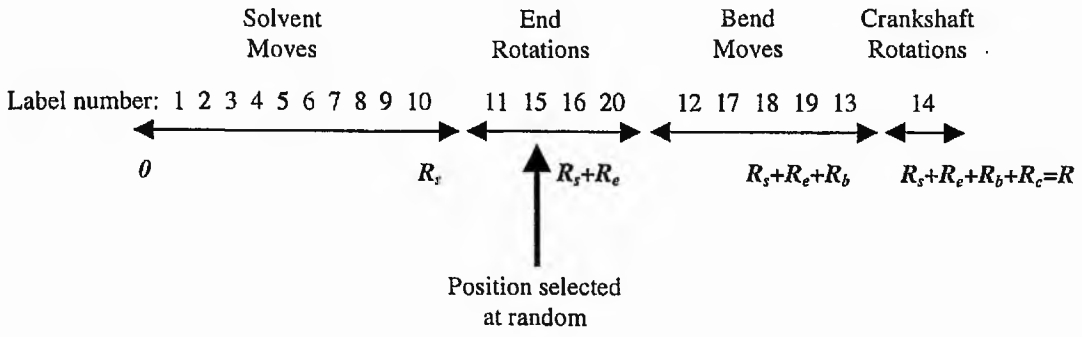

Figure (3.6): An illustration of the selection method for an attempted move from a transition rate line. In this example, position 12 is chosen at random along the total rate line. This corresponds to particle number 15 which is able to attempt an end rotation.

From the random number selected, the computer program uses a simple search algorithm to find the corresponding particle, its location, and the type of move it is able to attempt. If a polymer segment has been chosen then one of the three Verdier - Stockmayer moves is carried out as described in section (3.2.1). If a solvent molecule is chosen from the initial plane then it will move in a randomly chosen direction to a nearest - neighbour site, but a constant volume fraction is always maintained in the initial plane. If a solvent molecule is removed from the initial plane it is immediately replaced to maintain this constant volume fraction. Similarly, if a solvent molecule enters the initial plane then it is absorbed into the solvent reservoir. The probability of an attempted move being successful is calculated according to the Metropolis Monte Carlo algorithm described in section (3.2.2). Each move is assumed to occur instantaneously and, following a successful move, each of the linked arrays must be updated to account for any change in the state of the system. Following every attempted move the elapsed time of the system is incremented according to the method also described previously. In this way a Monte Carlo algorithm is specified to study the ingress of solvent into a polymer.

3.3.2 Solution of the Diffusion Equation

For the physical system described above there is an analytic solution of the differential diffusion equation, equation (2.23), assuming that the chemical diffusion coefficient D_c is constant with increasing solvent volume fraction. The net flow of solvent molecules is in the positive x direction along the concentration gradient, thus only a one - dimensional solution is required. This is described in detail by Crank (CRANK 1975 p.20). Here, the solution for the semi - inifinite medium is reviewed briefly. The boundary at $x=0$ is kept at a constant surface volume fraction ϕ_0 and the initial volume fraction, at time $t=0$, is zero throughout the medium $x>0$. A solution of the diffusion equation is required that satisfies the following boundary conditions;

$$\phi = \phi_0, \qquad x = 0, \qquad t > 0$$
$$\phi = 0, \qquad x > 0, \qquad t = 0$$

This can be solved by using the Laplace transform to remove the time variable, leaving an ordinary differential equation the solution of which yields the transform of the volume fraction as a function of the space variable. An expression for the volume fraction in terms of the time and space variables can then be found that satisfies the boundary conditions. Following this method, the solution of the diffusion equation is given by;

$$\phi = \phi_0 \, erfc \, [x/2\sqrt{(D_c t)}] \qquad (3.8)$$

Here, *erfc* is known as the error function complement. This is related to a standard mathematical function, the error function, usually written as *erf*, by;

$$erfc(z) = 1 - erf(z) \qquad (3.9)$$

where;

$$erf\,(z) = (2/\sqrt{\pi}) \int_0^z \exp(-x^2)\, dx \qquad (3.10)$$

Expression (3.8) shows that the solution of the problem of diffusion into a semi - infinite medium with a constant surface volume fraction involves only a single dimensionless parameter;

$$x/2\sqrt{(D_c t)}$$

From this the characteristic features of Fickian diffusion can be inferred that were described in section (2.2.1). The most important of these is that the distance of penetration of any given volume fraction will be proportional to the square root of time. Therefore, the analytical solution of the diffusion equation for this system predicts Fickian diffusion.

3.3.3 Measuring the Solvent Diffusion Coefficient

To study the diffusion of solvent through the polymer, one of the most important parameters that must be measured is the diffusion coefficient of the solvent molecules. In this work three different methods have been used to find this chemical diffusion coefficient for the diffusion of solvent molecules along the concentration gradient.

Firstly, the analytic solution given by equation (3.8) can be used to fit a solution to the solvent profile generated by the computer simulation. By fitting a function of the form;

$$\phi = \phi_0 \, erfc\,(Ax) \qquad (3.11)$$

to the solvent profile at a particular time t, a graphics software package (XVGR) will give the value of A, where;

$$A = (4D_c t)^{-1} \qquad (3.12)$$

Hence, D_c can be easily deduced assuming that D_c remains constant with increasing solvent volume fraction. For cases where the diffusion coefficient is not a constant another method must be used.

A second method reverts to Fick's original hypothesis given in equation (2.22) which stated that the rate of transfer of diffusing substance through a unit area of a section is proportional to the concentration gradient measured normal to the section. By defining a plane in the lattice that is perpendicular to the net flow of solvent molecules, the number of solvent molecules moving through this plane can be counted to give a measure of the flux. The concentration gradient can also be deduced from the simulation, hence only the diffusion coefficient D_c remains to be calculated.

The third method used required the development of a second computer simulation using finite difference methods to generate the solvent profiles independently of the Monte Carlo simulation. The advantage of this numerical simulation is that the functional form of the chemical diffusion coefficient must first be specified. Therefore, data from this model can be fitted to the Monte Carlo model to determine the best functional form for the diffusion coefficient. This method is also reviewed by Crank (CRANK 1975 p.139).

3.4 Results of the "Simple" Monte Carlo Model

The aim of the following simulations is to study the operation of this computer model with different model parameters and to see which types of diffusion the model can reproduce. In each set of results that follow a three - dimensional cubic lattice is used of *100x50x50* lattice sites with a lattice spacing of $1x10^{-8}$ *m*. The size of this lattice was chosen to be large enough to reduce any statistical errors in the results whilst remaining small enough to be computationally viable. The elementary period of time was chosen to be $1x10^{-9}$ *s*. These dimensions were chosen arbitrarily, but can be scaled to a particular system of interest. In each simulation the volume fraction of solvent in the initial plane of the lattice is always maintained at *0.5*. Unless stated otherwise, the volume fraction of polymer in the lattice is also *0.5*, with a molecular weight $N=200$, and the rates of the solvent and polymer, r_s, r_e, r_b, r_c, are unity. Also, the system can be considered as athermal where $\chi = 0$ and temperature has no effect on the polymer structure. This is the case for a good solvent (DE GENNES 1979).

3.4.1 Polymer Concentration Dependence

The results shown in figure (3.7) show the effect of the polymer volume fraction ϕ_p on the solvent diffusion for four different polymer volume fractions. In the first case, figure (3.7a), there is no polymer present in the lattice $\phi_p=0$. The solvent is free to diffuse into an empty lattice. Figure (3.7a) shows the solvent volume fraction ϕ_s against the distance d through the lattice for five solvent profiles at five consecutive times: $t=1x10^{-5}s$, $5x10^{-5}s$, $1x10^{-4}s$, $5x10^{-4}s$, $1x10^{-3}s$. For each

profile three different curves are shown: the bold black line is the result of the Monte Carlo model; the solid black line is the fit of the analytic solution of the diffusion equation; the dashed black line is the fit of the finite difference simulation. In this case both the analytic solution and the finite difference solution can be seen to fit almost exactly to the Monte Carlo data. This confirms that the Monte Carlo model is working as would be expected for this system, producing solvent profiles in the form of error functions that are identical to the analytic solution for a semi - infinite media with a constant diffusion coefficient. The finite difference simulation confirms this where a constant diffusion coefficient has been assumed.

Figure (3.7b) shows the same simulation but with a polymer volume fraction of $\phi_p=0.25$. Therefore, in this figure the five additional curves represent the volume fraction of polymer in the lattice and are shown by a solid thin line for each consecutive time. In this case the solvent profiles do not appear to be significantly different, but closer inspection shows that their distance of penetration is less. This is expected since the volume fraction of polymer restricts the number of available lattice sites to the solvent; the probability of a successful solvent move is then less. Most importantly though, the analytic solution of the diffusion equation is now no longer a good fit to the Monte Carlo data and shows significant differences. The finite difference simulation is therefore used to find the best fit to the Monte Carlo data. It was found that by specifying a functional form for the chemical diffusion coefficient's dependence on solvent volume fraction, a good fit could be achieved. The form of this function is given by;

$$D_c(\phi_s) = D_0 \exp(-p\,\phi_s) \qquad (3.12)$$

where D_0, the intrinsic diffusion coefficient, and p are constants. Equation (3.12) was found to give the best fit to the Monte Carlo simulation although fits were attempted with other exponential and linear functions. The form of this function is discussed further in Chapter 5. It can be stated that the chemical diffusion coefficient is no longer a constant in the presence of polymer but instead has some dependence on the volume fraction of solvent in the lattice. However, this dependence may not be on the volume fraction of solvent but rather on the number-

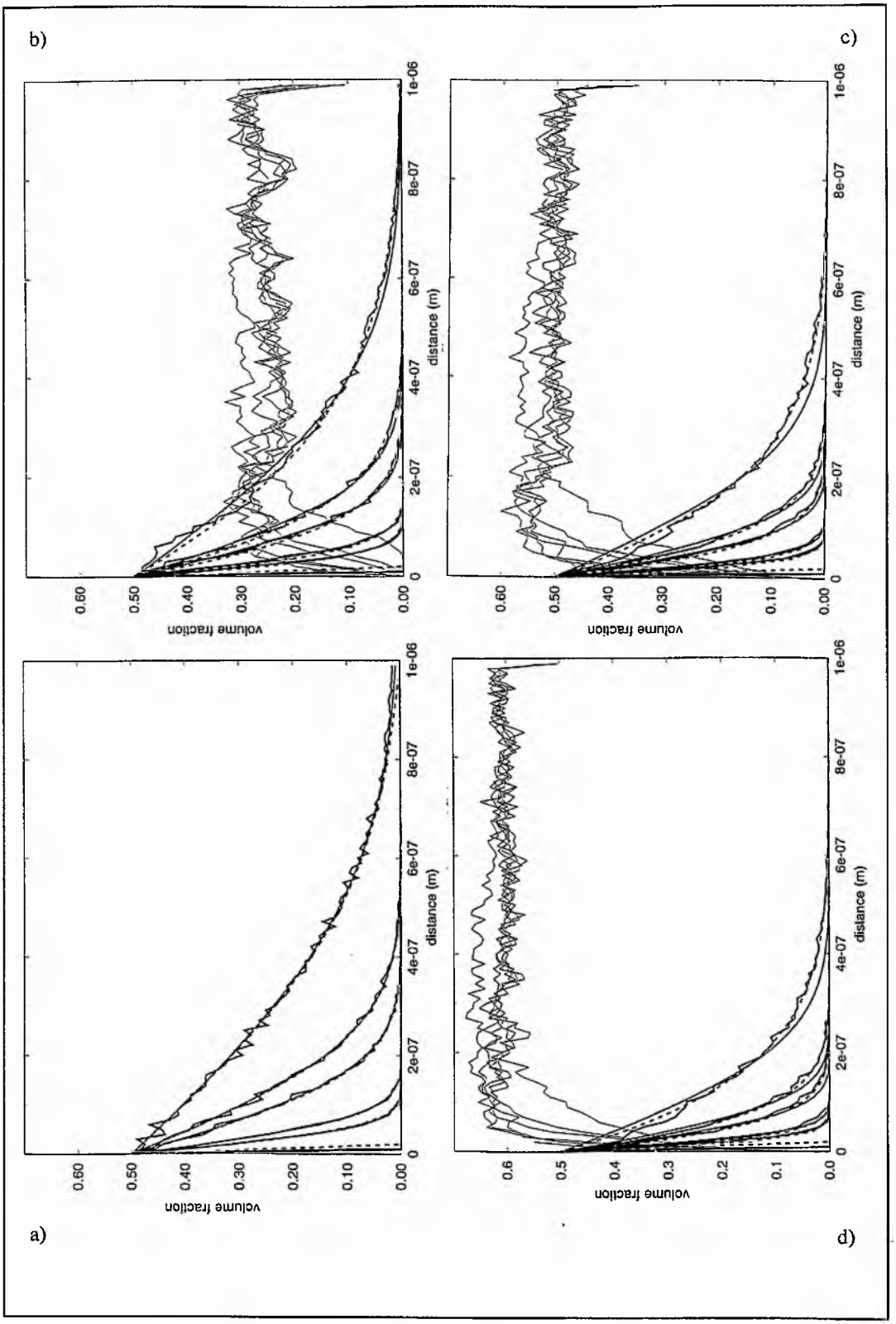

Figure (3.7): Volume fraction against solvent penetration distance showing solvent profiles obtained from the Monte Carlo simulation (bold), analytic solution (solid), and finite difference solution (dashed) for five consecutive times at four different polymer volume fractions: a) ϕ_p=*0.0*, b) ϕ_p=*0.25*, *c)* ϕ_p=*0.5*, *d)* ϕ_p=*0.75*. The corresponding polymer profiles (solid) are shown for each time.

of free lattice sites available, which itself is a function of the solvent volume fraction within the system given that the total number of lattice sites occupied by polymer molecules remains constant.

Figures (3.7c) and (3.7d) show the same simulation for polymer volume fractions of $\phi_p=0.5$ and $\phi_p=0.75$ respectively. The difference between the Monte Carlo data and the analytic solution appears to increase with increasing polymer volume fraction due to the further reduction of free lattice sites. The finite difference simulation confirms this where fits were obtained for an increasing value of p with the polymer volume fraction, showing an increasing dependence on ϕ_s. At the same time D_0 decreases with increasing polymer volume fraction as would be expected for a system with fewer free lattice sites restricting the diffusion of solvent molecules. This is shown explicitly in figure (3.8), which shows the chemical diffusion coefficient against time for each of the four polymer volume fractions. With no polymer present D_c is constant with time, but with polymer present this figure shows an initial fall in D_c before a constant value is reached. This suggests that at extremely short times the diffusion coefficient would essentially be independent of solvent volume fraction and that the volume fraction dependence described above becomes significant after a short time.

Finally, figure (3.9) shows the progression with time of the solvent fronts shown in figure (3.7). If the penetration distance of the solvent front is related to the elapsed time by equation (2.25), then by plotting a double logarithmic plot of distance against time, the coefficient n can be immediately measured from the gradient of that plot. It is found, unsurprisingly, that the solvent fronts' progression with time in this simulation is characterised by $n=0.50 \pm 0.06$. This is characteristic of Fickian diffusion and shows that the penetration distance of solvent is proportional to the square root of time.

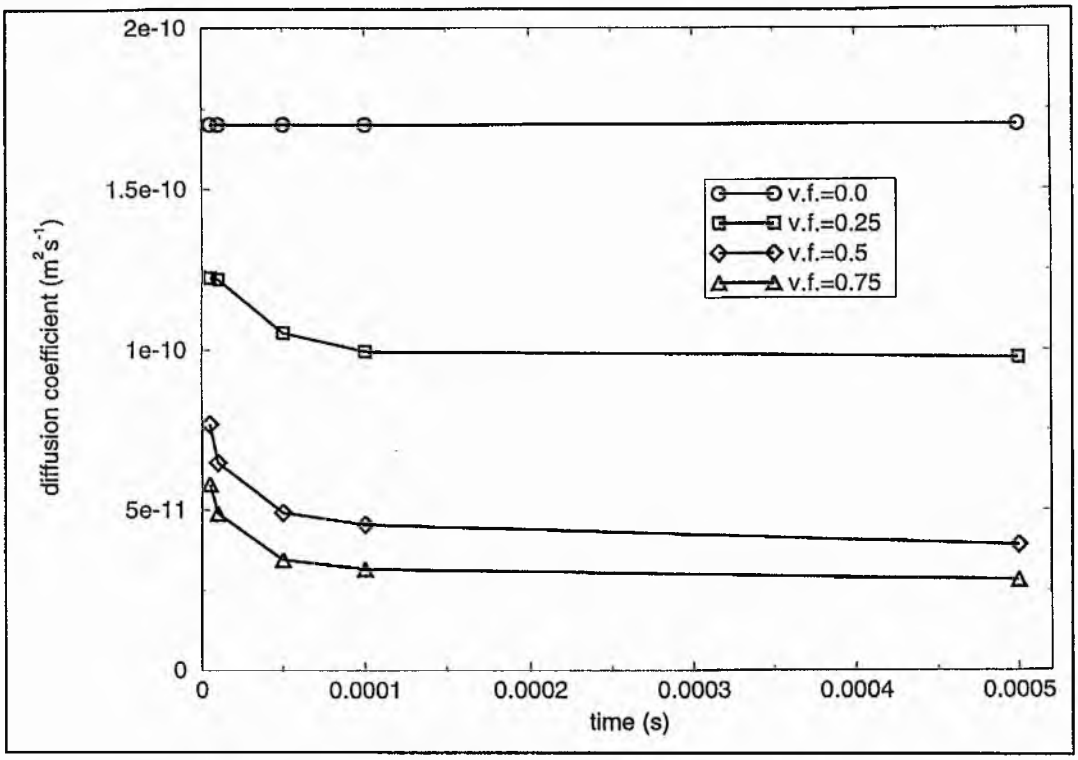

Figure (3.8): Solvent chemical diffusion coefficient against time for the Monte Carlo data shown in figure (3.7) for each of the for four polymer volume fractions *v.f.*

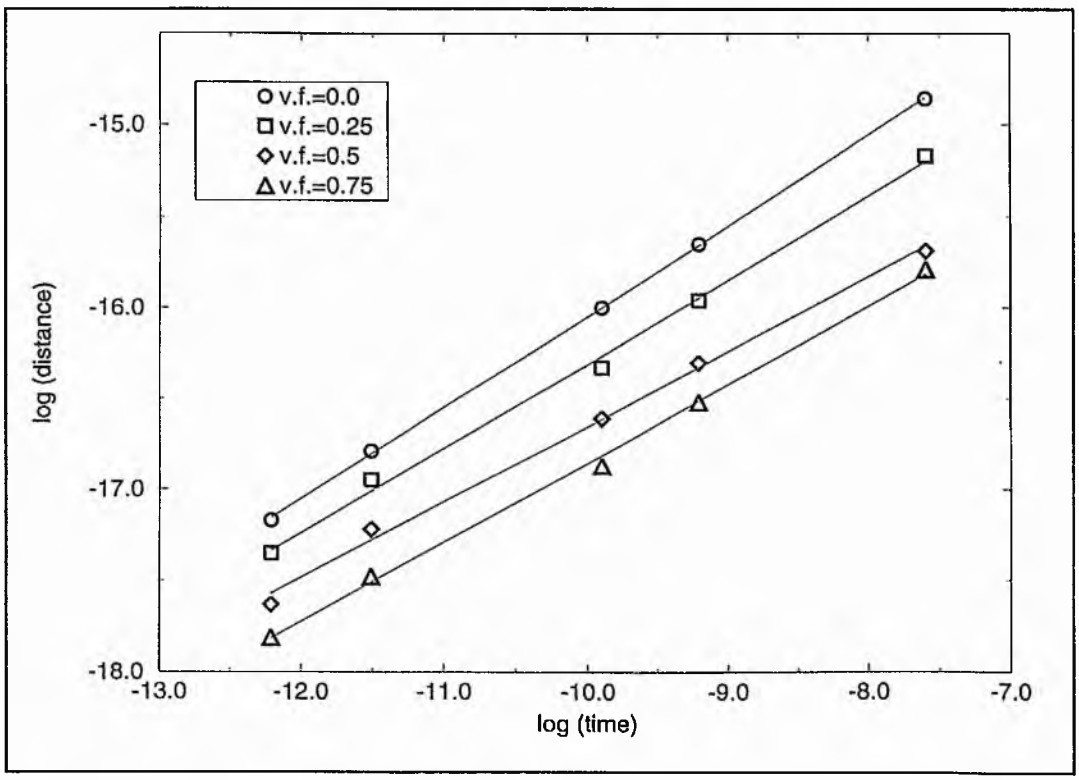

Figure (3.9): Double logarithmic plot of solvent penetration distance against time for four polymer volume fractions showing progression of the solvent front with time.

3.4.2 Molecular Weight Dependence

The effect of molecular weight, or polymer chain length N, is now studied. Figure (3.10) shows the solvent profiles as described previously, but for four different molecular weights. In figure (3.10a), the solvent front is shown for a system with a polymer volume fraction of $\phi_p=0.5$ and a chain length of $N=10$. Again, it can be seen that solvent profile is not quite an error function and that the analytic solution of the diffusion equation is a poor fit. However, the finite difference simulation again provides a good fit to the Monte Carlo data using the functional form for the chemical diffusion coefficient given by equation (3.12). Figures (3.10b), (3.10c) and (3.10d), show the solvent profiles for molecular weights of $N=50$, 100 and 200 respectively. With increasing chain length, there are few differences between these four sets of data. The volume fraction of polymer is identical in each, the only difference being the increased length of the chains. This behaviour is confirmed by the finite difference simulation where a small decrease in D_0 is observed with increasing polymer chain length. However, the value of p remains constant, showing no change in the diffusion coefficient's dependence on the solvent volume fraction with increasing chain length. This is acceptable since the number of free lattice sites available to the solvent molecules remains constant in these simulations despite varying the length of the polymer chains. The variation in the solvent's chemical diffusion coefficient with time for each of the four molecular weights is shown in figure (3.11). These show the same trend with time described previously and a decrease in diffusion coefficient with increasing molecular weight. This change is due entirely to the connectivity of the polymer chains since the volume fraction of occupied sites is unaltered. This can be related to Rouse's model (ROUSE 1953) since he predicted that the viscosity of the polymer chains would be proportional to the molecular weight. With higher molecular weights, the polymer chains would be more viscous due to the greater number of entanglements and would move more slowly. Therefore, the vacancies in the bulk polymer would become available to the solvent molecules more slowly, inhibiting their diffusion. The progression of the solvent front with time is again Fickian in each case, with the coefficient n measured as previously where $n=0.50 \pm 0.04$.

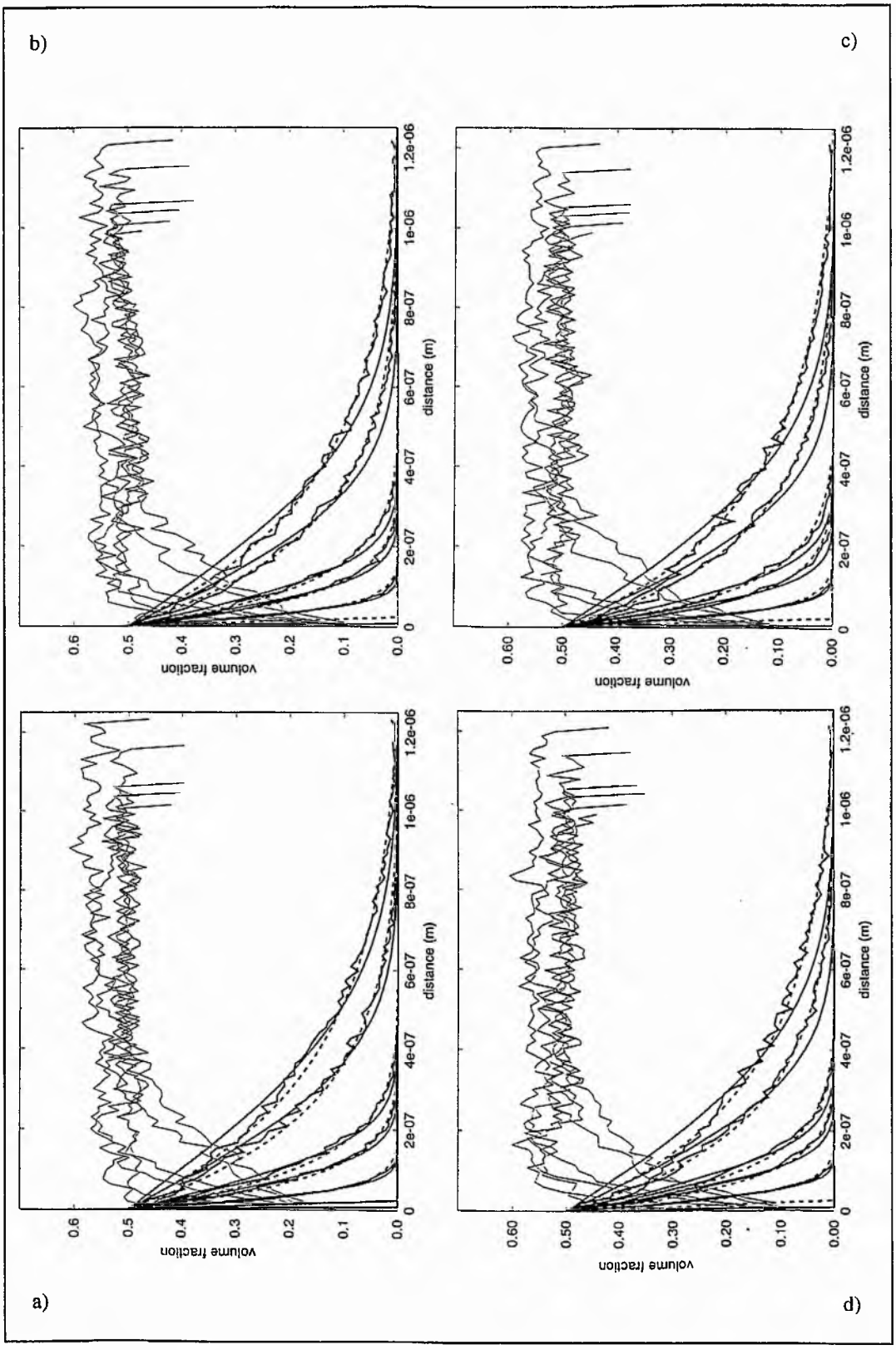

Figure (3.10): Volume fraction against penetration distance showing solvent profiles obtained from the Monte Carlo simulation (bold), analytic solution (solid), and finite difference solution (dashed) for five consecutive times at four molecular weights: a) *N=10*, b) *N=50*, c) *N=100*, d) *N=200*.

In this and the previous simulation, the graphs of volume fraction with distance show the polymer volume fraction moving slowly in response to the solvent molecules entering the system. On average, it is more probable that a polymer segment will move away from the initial solvent plane and the ingressing solvent molecules than move towards this region with fewer vacancies in the lattice. This is indeed seen in figures (3.7) and (3.10). However, this creates a localised increase in the polymer volume fraction at a distance away from the initial solvent plane. This simulation has therefore been modified to allow a localised swelling of the polymer to occur in response to this. If the volume fraction of occupied sites in a particular plane in the lattice changes from its initial average value, the distance between this lattice plane and the next will change by a distance proportional to this change in volume fraction. In this way the density of every plane in the system remains constant and a swelling of the polymer is simulated. This is evident in figure (3.10) where the polymer volume fraction for the longest elapsed time extends beyond the initial length of the lattice. This swelling scales with time as $n=0.5 \pm 0.05$ as expected for Fickian diffusion.

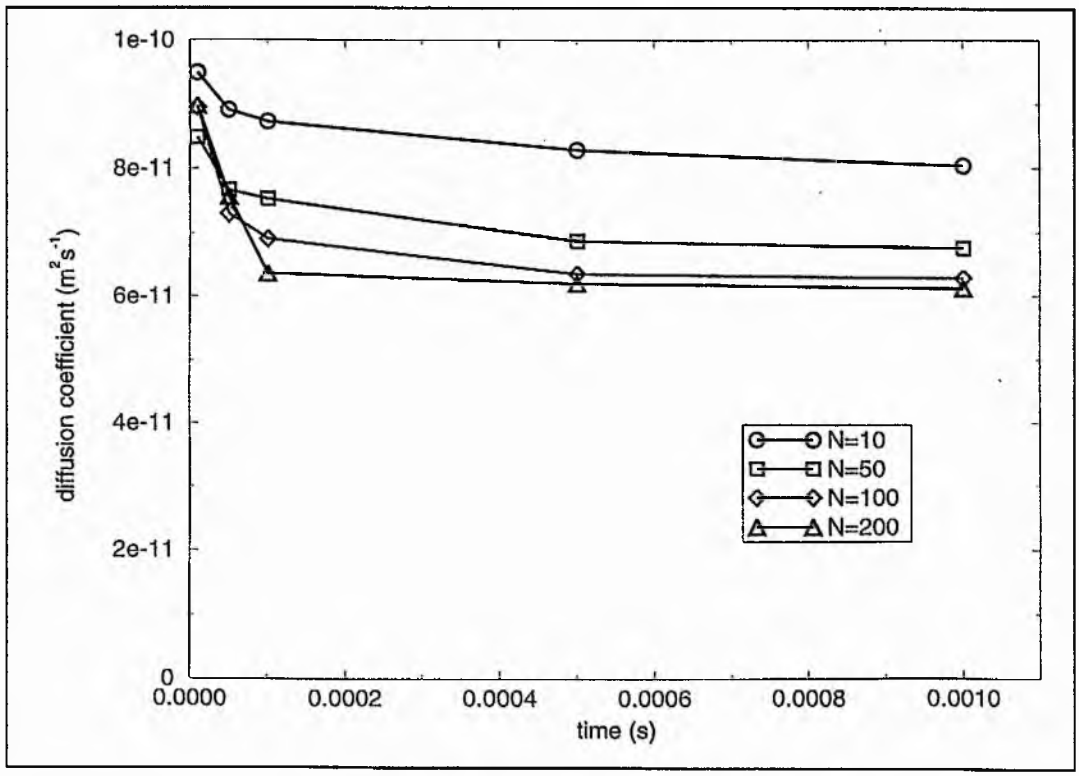

Figure (3.11): Solvent chemical diffusion coefficient against time for the Monte Carlo data shown in figure (3.10) for four molecular weights *N*.

3.4.3 Rate of Polymer Motion Dependence

The process rates described in this chapter are now put into use to study their effect on the simulation. Firstly, the rates of the polymer processes r_e, r_b, r_c, are varied whilst the solvent process rate is maintained at a constant $r_s=1.0$. These control the rate at which the polymer segments attempt to move. In this simulation these three rates have been assigned values $r_e=r_b=r_c=0.0$, 0.25, 0.5, 0.75, 1.0 consecutively. In figure (3.12) solvent profiles are shown for polymer process rates of 0.0 and 1.0 for comparison. In the first case, figure (3.12a), the polymer process rate is zero, simulating a polymer glass where polymer chain configurations are frozen and will not move. Here the solvent profiles indicate that the diffusion of solvent is inhibited by the polymer chains with a solvent profile that is clearly not an error function. The finite difference simulation produces only a reasonable fit to the Monte Carlo data. The solvent profiles in this case are due to diffusion through a porous media where the solvent molecules have to diffuse through vacancies between static polymer chain configurations. Consequently, there may be a large proportion of free lattice sites that the solvent is unable to reach. In comparison, figure (3.12b) shows the same simulation with a polymer process rate of unity. This illustrates the features previously described for a system in which the polymer molecules are free to move in response to the solvent ingress. Thus, this system can be thought of as a rubbery polymer and demonstrates the features of Fickian diffusion expected for such a polymer. In fact, for all five polymer process rates the progression of the solvent front with time remains Fickian and the coefficient n is found to be $n=0.48 \pm 0.04$.

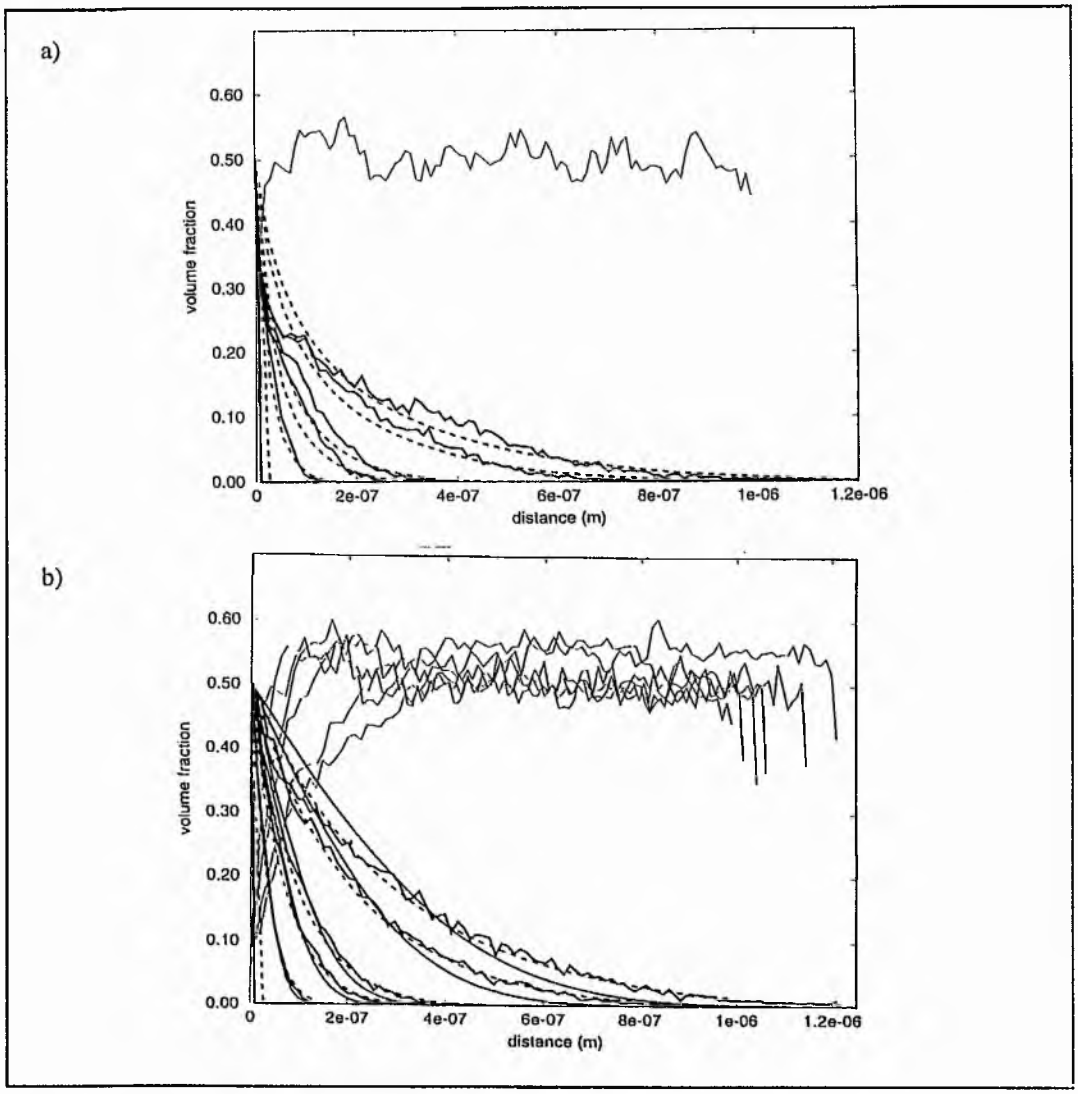

Figure (3.12): Volume fraction against penetration distance showing solvent profiles for two different polymer process rates: a) polymer glass, *r=0.0*, b) polymer rubber, *r=1.0*.

The variation of the solvent's chemical diffusion coefficient with time is shown in figure (3.13) for each of the five polymer process rates. This figure illustrates how the average value of the diffusion coefficient decreases with the polymer process rate. This is to be expected in this model since the diffusion of solvent molecules in this polymer glass is inhibited by the frozen chains, whereas diffusion in the rubbery polymer is aided by the co-operative motion of the polymer chains.

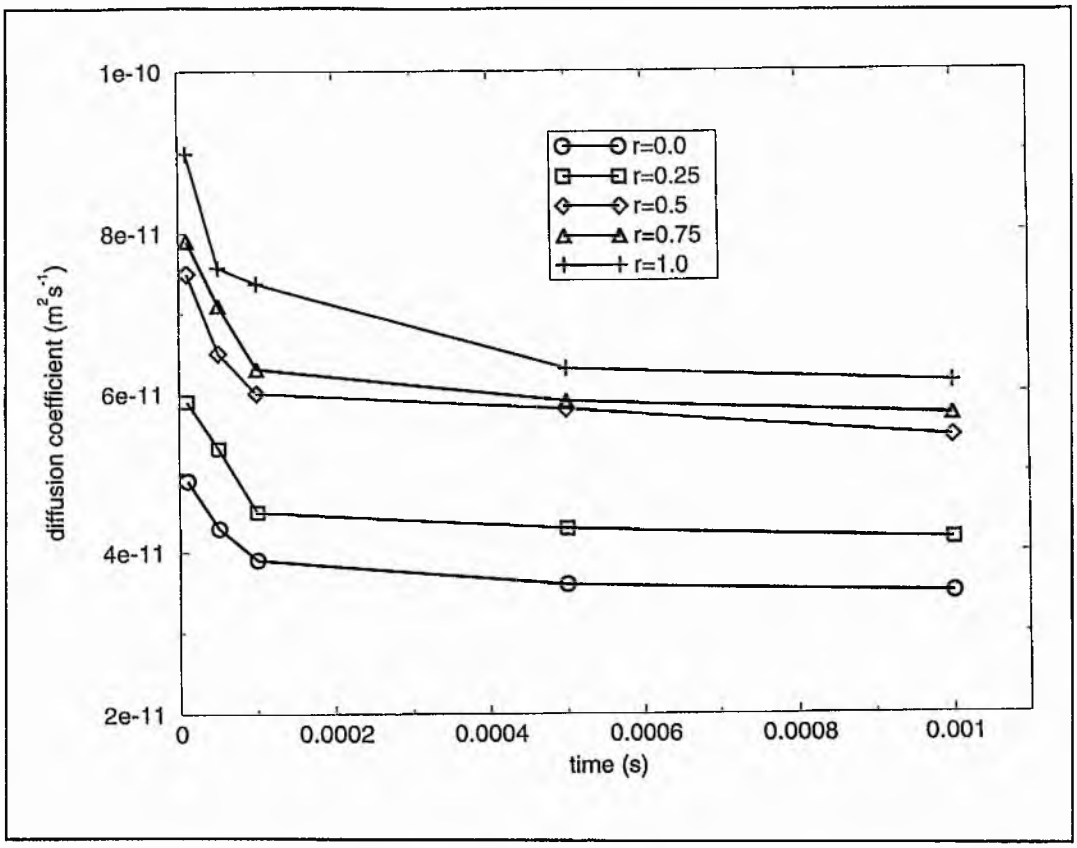

Figure (3.13): Solvent chemical diffusion coefficient against time for five polymer process rates *r*.

3.4.4 Rate of Solvent Motion Dependence

Next, the rate of the solvent process is studied in the same way as above whilst maintaining constant values of the polymer process rates $r_e=r_b=r_c=1.0$. The solvent rate r_s is assigned five different values $r_s=1.0$, *1.25*, *1.5*, *1.75*, *2.0*, and the solvent profiles with time are recorded for each. Figure (3.14) illustrates the solvent profiles for solvent process rates of *1.0* and *2.0* for comparison. Few differences are seen to the results previously described, other than an increase in the penetration distance of the solvent with increasing solvent process rate. This simply confirms the operation of the model. If the solvent process rate is doubled then the probability that a solvent molecule will make an attempted move will also double given that all other process rates remain unchanged. Therefore, solvent diffusion becomes a faster process where the mean time between actual solvent moves decreases.

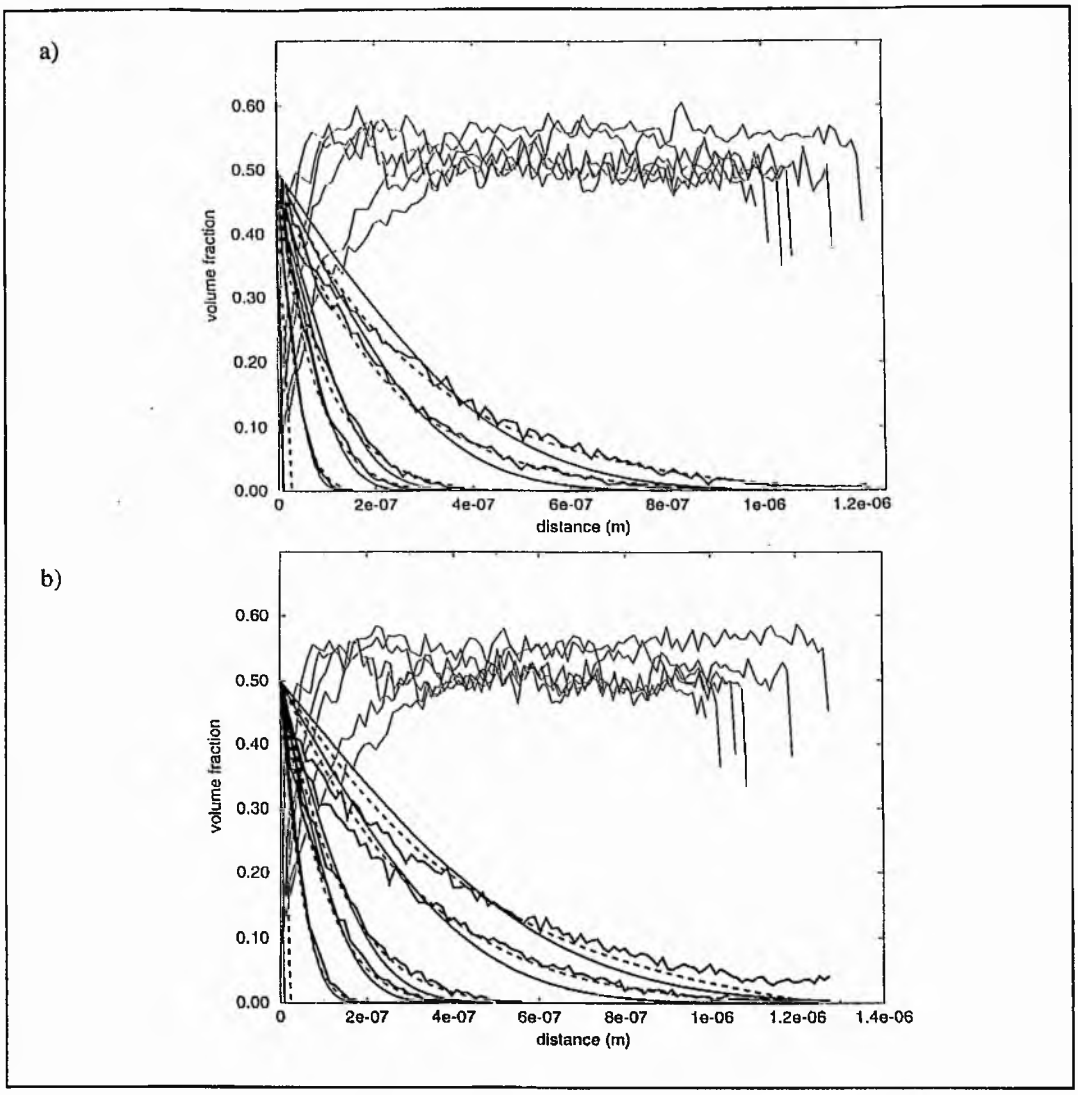

Figure (3.14): Volume fraction against penetration distance showing solvent profiles obtained from the Monte Carlo simulation (bold), analytic solution (solid), and finite difference solution (dashed) for five consecutive times at two different solvent process rates: a) $r=1.0$, b) $r=2.0$.

This behaviour is also illustrated by figure (3.15), which shows the solvent's chemical diffusion coefficient against time for each of the five solvent process rates. Again, a higher average value of the solvent diffusion coefficient is seen with an increasing solvent process rate. This diffusion coefficient increases approximately linearly with the solvent process rate and demonstrates that this simulation behaves as expected. For this simulation, both the solvent front's progression with time and the system's swelling with time demonstrate Fickian diffusion with a coefficient of $n=0.47 \pm 0.04$ and $n=0.51 \pm 0.06$ for each respectively.

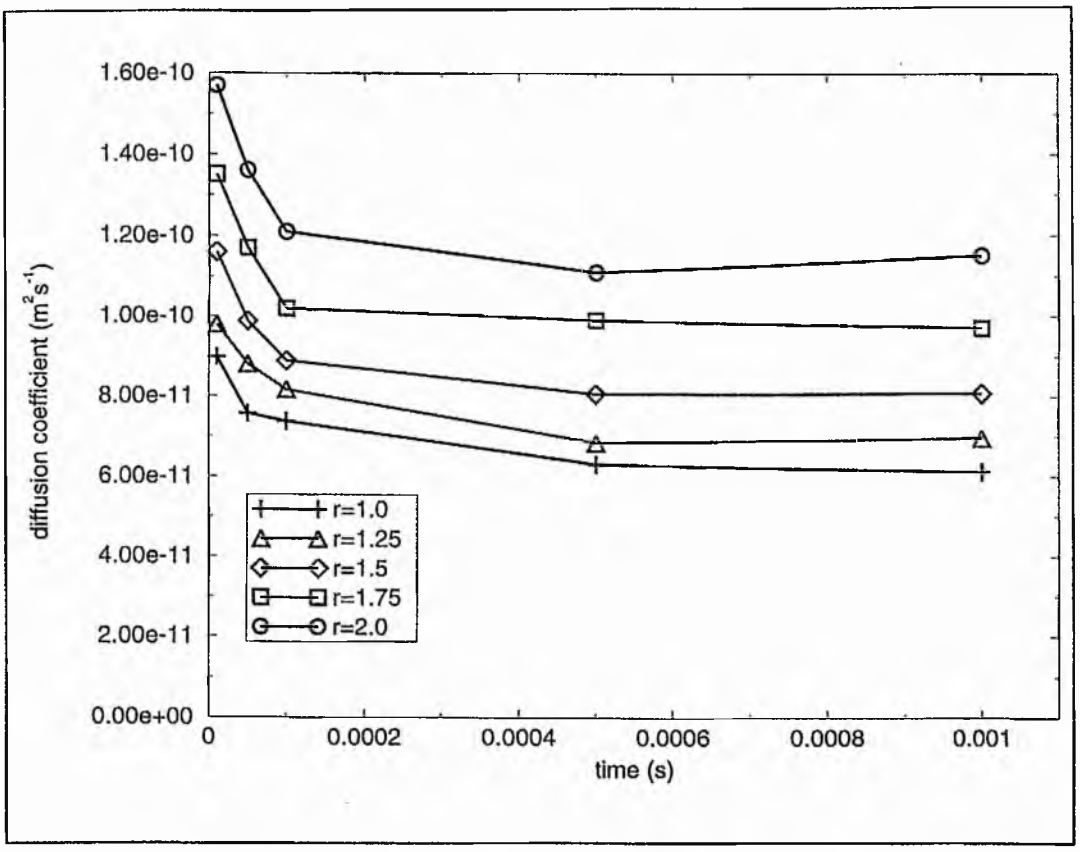

Figure (3.15): Solvent chemical diffusion coefficient against time for five solvent process rates *r*.

3.4.5 Interaction Energy Dependence

Interaction energies are now introduced into this system which has hitherto been athermal. In this model an interaction energy ε_{ps} is considered only between the polymer segments and solvent molecules and only between particles at nearest - neighbour lattice sites. A particle is more likely to move to a new lattice site if that site is surrounded by attractive nearest - neighbours. The change in energy ΔE associated with such a move would be negative and would lower the energy of the system. Hence, attractive interaction energies between the polymer and solvent are negative and repulsive energies are positive. This is realised in the computer program by summing the interaction energies for the particle's six nearest - neighbour sites at its initial location and at its proposed location following the move.

The change in energy ΔE is then the difference between these two values. The probability that the attempted move is successful is governed by the Metropolis algorithm as described in equations (3.1) and (3.2). In reality, the magnitude of the polymer - solvent interaction energy is of the order *0.1 eV* (GROSBERG 1997). It's effect on the system though is relative to the thermal energy of the system governed by kT, where k is Boltzmann's constant and T is temperature. At room temperature, kT is of the order *0.01 eV*.

In this simulation the interaction energy between the polymer and the solvent ε_{ps} is assigned five different values: ε_{ps}=*-2.0, -1.0, 0.0, +1.0, +2.0*. It was found that only a doubling of the interaction energy was sufficient to produce significant changes in the solvent profiles produced by the Monte Carlo simulation. The units of these energies are unimportant since the program deals only with values relative to kT, equation (3.2). Unless stated otherwise, the thermal energy is defined by kT=*1.0*. Results of this simulation for ε_{ps}=*-1.0* and ε_{ps}=*+1.0* are illustrated in figures (3.16a) and (3.16b) respectively.

For a negative interaction energy it is expected that the polymer and the solvent components will attract each other. This is illustrated in figure (3.16a) where the solvent profiles are steeper and penetrate further than would be expected if the system were athermal (figure (3.14a) for example). Furthermore, the solvent actually attracts the polymer towards the initial plane of solvent thereby causing a local increase in the polymer volume fraction in this region. If the interaction energy is positive then it is expected that the polymer and solvent components will repel each other. Again, figure (3.16b) demonstrates this, where the solvent profiles have suddenly become very steep and do not penetrate as far into the polymer. In this figure a separation can be seen developing between the polymer and the solvent. This causes a local increase in the volume fraction of the polymer near to the initial plane of solvent and consequently creates a barrier, impeding the diffusion of solvent molecules. No attempt has been made to fit a solution to either of these solvent fronts. It is clear that they are no longer error functions and the use of the finite difference simulation would require something more complex than a simple exponential function to generate these profiles. However, despite these extreme

changes in the profiles of the solvent fronts, this diffusion process remains Fickian as characterised by a coefficient $n=0.46 \pm 0.06$. The swelling of the system also scales with the square root of time where $n=0.50 \pm 0.05$.

The chemical diffusion coefficient for this simulation has been estimated from the flux of solvent molecules through a plane of the lattice as described in section (3.3.3). The results of this are shown in figure (3.17). For the positive repulsive energies a sudden decrease in the solvent diffusion coefficient is seen compared to the case for zero interaction energies. This is due to the separation of the polymer and solvent and the local increase in the polymer volume fraction creating a barrier to the diffusion of the solvent molecules. For the negative attractive energies the solvent diffusion coefficient initially rises with increasing interaction energy before falling to below its athermal value. What appears to happen is that the solvent attracts the polymer towards the initial plane to such an extent that the polymer volume fraction increases in this region and again impedes the solvent diffusion in the same way that the positive interaction energy did. The reality of this is questionable although the simulation is working in accordance with the program. The effects seen here may be extreme and may simply require more refined parameters to make the simulation more realistic.

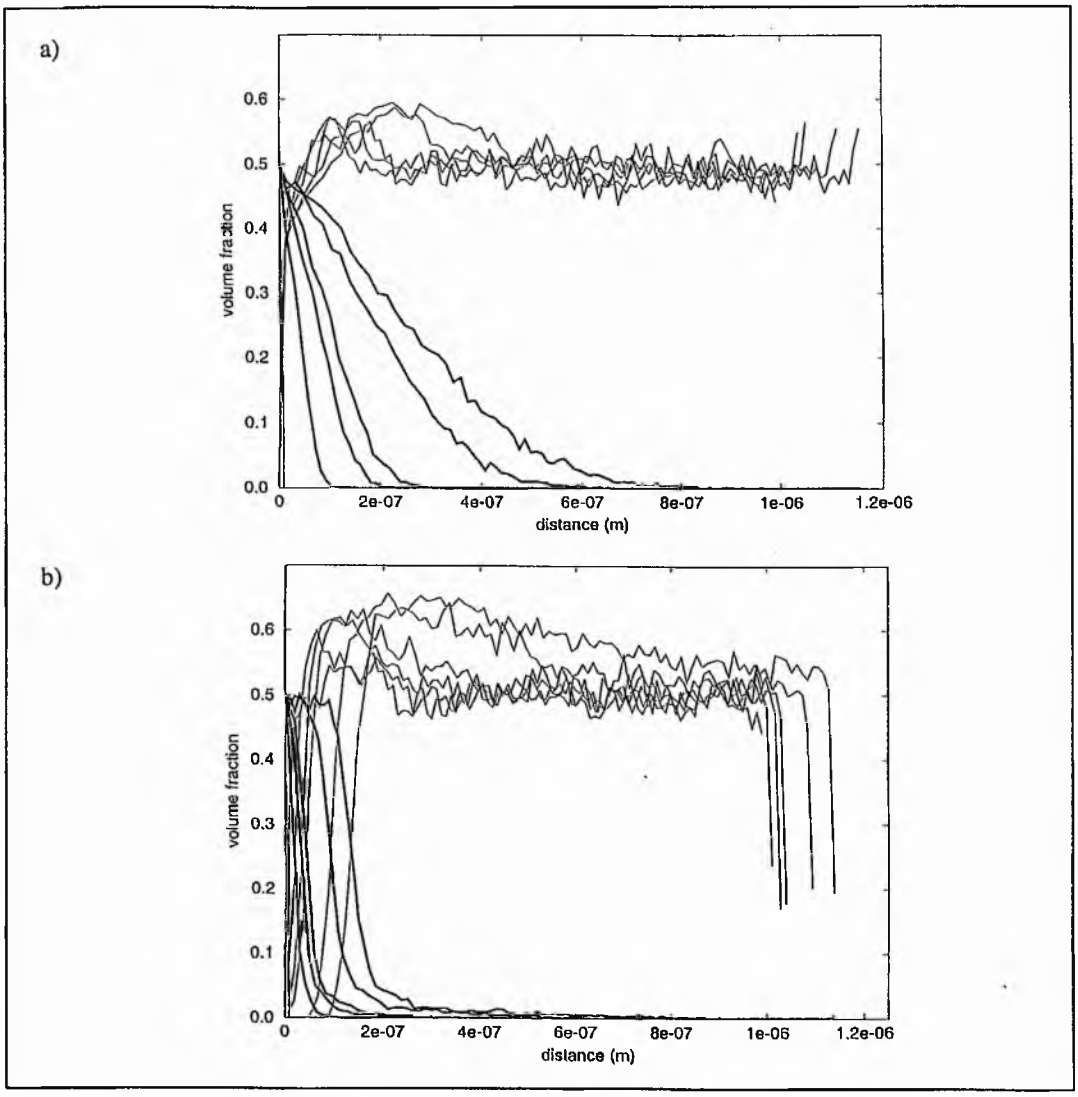

Figure (3.16): Volume fraction against penetration distance showing solvent profiles for two different interaction energies: a) E=*-1.0*, b) E=*+1.0*. Only the Monte Carlo data is shown.

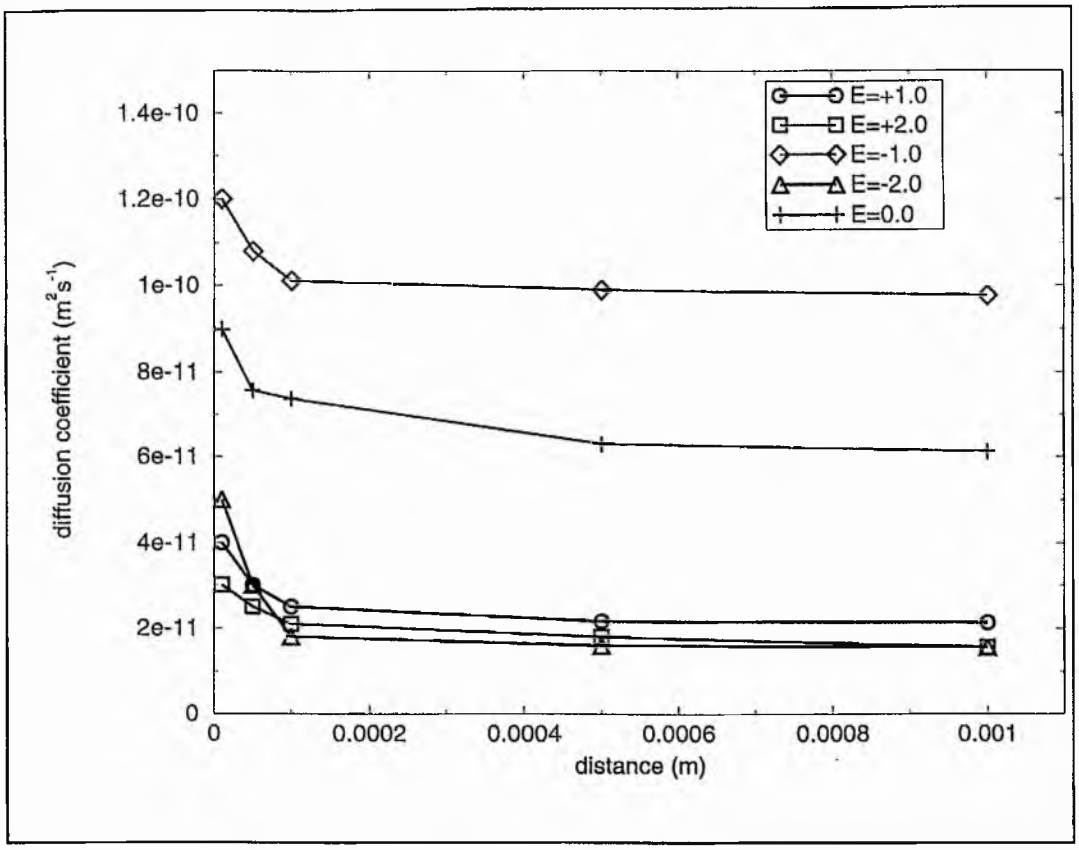

Figure (3.17): Solvent chemical diffusion coefficient against time obtained from the flux of solvent molecules measured in the Monte Carlo simulation for five interaction energies *E*.

3.4.6 Temperature Dependence

Finally, the effects of temperature are studied through the parameter kT and equation (3.2). In this simulation, temperature only affects the probability at which a particle will move against a repulsive force, governed by equation (3.2). The probability at which a particle moves in response to an attractive force is unity and remains unchanged. If the temperature of the system increases, the probability that a particle will make a successful move against a repulsive force increases. This can be understood physically, since particles in a system with greater thermal energy will be more thermally active and are more able to oppose any repulsive forces. This has a significant effect on the diffusion of solvent into the system.

This simulation was carried out for five values of kT between *0.1* and *2.0*, with a constant attractive interaction energy between the polymer and the solvent. For low temperatures very little diffusion is seen indicating that the probability of a successful move is greatly reduced. For higher temperatures the diffusion increases as the probability of a solvent molecule opposing a repulsive force increases. This is illustrated in figure (3.18), which shows the chemical diffusion coefficient of the solvent against time for each of the five temperatures. Furthermore, the progression of the solvent fronts with time also changes with temperature. For low temperatures the progression of the solvent front is severely restricted and the coefficient n is measured as $n=0.05 \pm 0.04$ due to the restricted diffusion of the solvent. As temperature increases, so the progression of solvent front increases until the coefficient n is $n=0.48 \pm 0.04$. This is shown in figure (3.19). Thus, Fickian diffusion is still dominant in this simulation and, more importantly, the progression of the solvent front never exceeds this dependence on the square root of time.

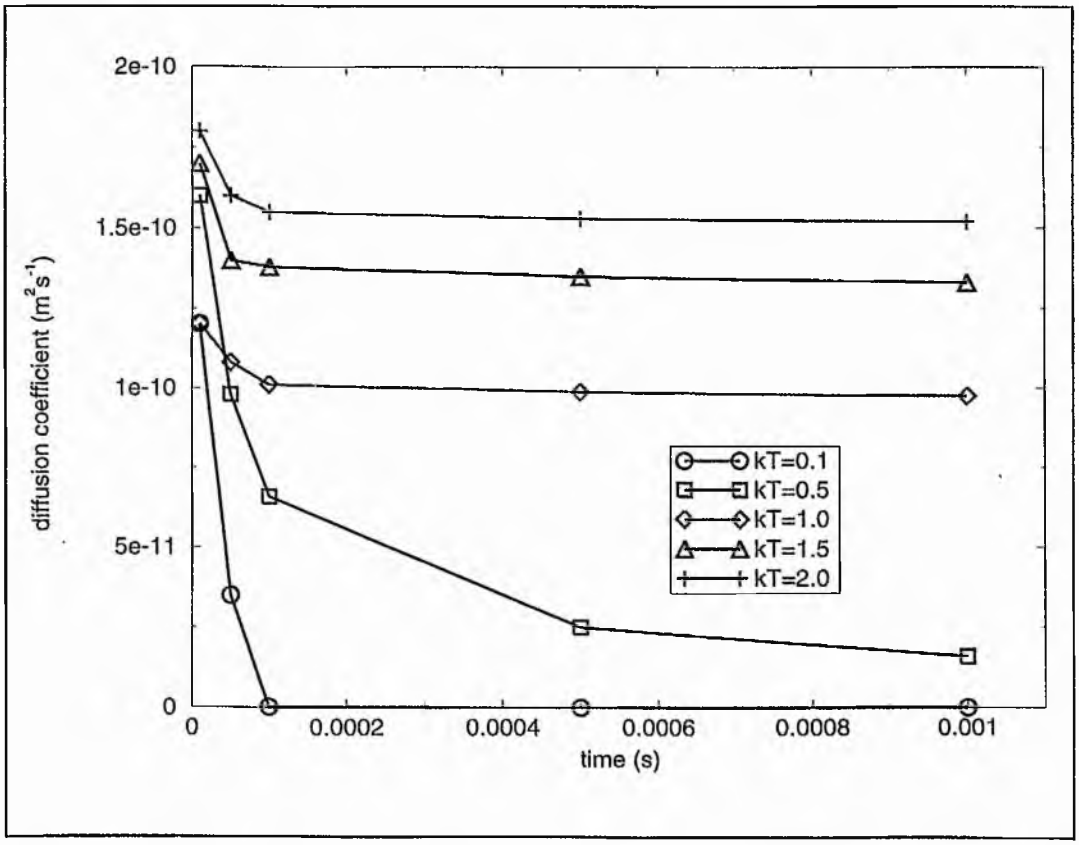

Figure (3.18): Solvent chemical diffusion coefficient against time obtained from the flux of solvent molecules measured in the Monte Carlo simulation for five temperatures kT.

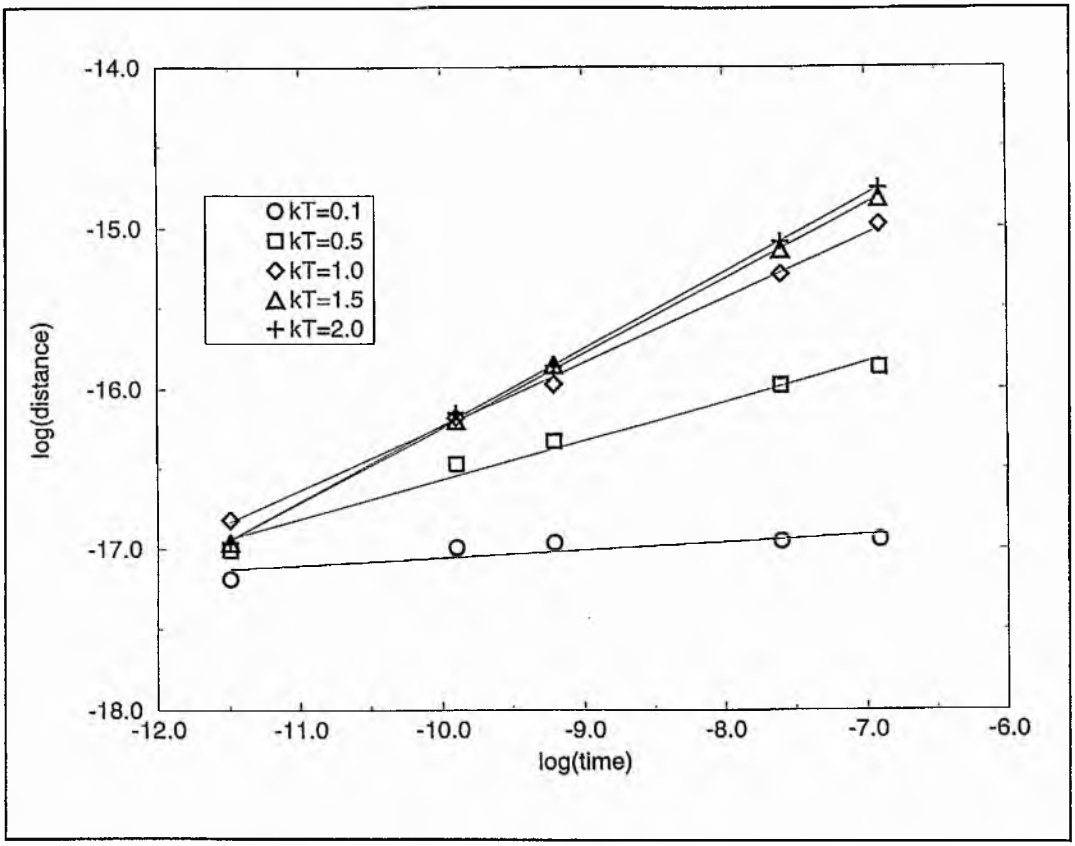

Figure (3.19): Double logarithmic plot of solvent penetration distance against time for five temperatures kT, showing progression of the solvent front with time.

3.5 Conclusions

The results presented in this chapter represent the preliminary findings of an original dynamic Monte Carlo model of solvent ingress into polymer. These results have been chosen to demonstrate the operation of the model and to illustrate the effects that the model parameters have on the solvent diffusion process. The behaviour of this "Simple" model is in accordance with the computer algorithm developed in that no unexpected behaviour is seen. Furthermore, the simulated behaviour of the system can be related to the dynamics of a real system to gain a better understanding of the processes taking place. Limitations of this model have not been discussed in detail here and will be examined in chapter (5). However, the most obvious limitation is that only Fickian diffusion is simulated with no departure from this behaviour for any reasonable parameters.

Chapter 4

Comparison With MRI Experiment

4.1 Introduction

Many experimental methods have been employed over the past fifty years to study polymers and polymer solutions, including optical, radiative and penetrant mass uptake methods (CRANK 1968). Amongst these, Nuclear Magnetic Resonance (NMR) has proved to be one of the most powerful and useful methods for studying the dynamic properties of polymers and their solutions non-invasively. This technique was established by two groups of physicists working independently in the 1940s (PURCELL 1946, BLOCH 1946). Nuclear magnetic resonance was first applied to the study of polymers in 1951 when Holroyd (HOLROYD 1951) and co-workers studied the mobility of polymers. More recently Kimmich and co-workers (KIMMICH 1993, WEBER 1993) have carried out extensive studies to correlate NMR data with theories of polymer dynamics.

Magnetic Resonance Imaging (MRI) relies on the principle of nuclear magnetic resonance and is increasingly being used to study the ingress of solvent into polymers. It is a non-invasive method that can provide spatially resolved information on the solvent concentration within the polymer as a function of time. Blackband and Mansfield (BLACKBAND 1986, MANSFIELD 1992) established the basic principles by which MRI is used to study solvent in polymer with a study of the ingress of water into solid blocks of nylon. Solvent diffusion processes have been studied in a wide range of systems from rubbers (WEBB 1990a/b, 1991, HALSE 1994) to biomedical polymers (BOWTELL 1994). These polymer systems

have predominantly displayed Fickian diffusion characteristics, but systems displaying Case II diffusion characteristics are increasingly being investigated. The ingress of methanol into polymethylmethacrylate (PMMA) has been extensively studied (WEISENBERGER 1990a/b, ERCKEN 1996, LANE 1997) and exhibits Case II diffusion.

The aim of this chapter is to describe an MRI experiment carried out to gain data to compare to the results of the "Simple" Monte Carlo model. Only by comparing the simulated data to real data can the validity of the model be ascertained. This chapter will first outline the principles of Magnetic Resonance Imaging required to gain an understanding of this experiment. Reviews of MRI and NMR theory are given in books by Callaghan (CALLAGHAN 1991) and Goldman (GOLDMAN 1993). The experimental procedure is then explained before comparing the results of this experiment to the results of the Monte Carlo model. It is hoped that this chapter will also provide a link to the extensive experimental field currently using MRI methods to study the properties of polymer systems.

4.2 Magnetic Resonance Imaging

Atomic nuclei within a polymer sample possess an electric charge and an angular momentum or spin. This rotating charge creates a magnetic dipole. In the absence of any external magnetic field, these magnetic dipoles are randomly oriented in all possible spatial directions throughout the sample. If a magnetic field B_0 is applied to the sample along the z direction, the magnetic dipoles attempt to align with the direction of the magnetic field and precess along a conical path around the field direction with a frequency ω_0. However, the spins of the atomic nuclei in the magnetic field are quantised and can achieve only two possible stable orientations relative to the magnetic field. These spins can align either parallel to the magnetic field or anti-parallel to the magnetic field. Hence, the magnetic dipole moment also aligns in just these two directions. An orientation parallel to the external magnetic field requires less energy than an anti-parallel orientation as energy is required to rotate the magnetic dipole against the magnetic field. Thus, two energy levels are created for a spin ½ system such as ^1H, known as Zeeman levels. The difference in

energy ΔE between these two levels is proportional to the field strength B_0. At room temperatures, more spins are aligned parallel to the magnetic field than anti-parallel due to the thermal energy of the system. This situation is illustrated in figure (4.1). Consequently, a macroscopic magnetisation M_z of the sample in the magnetic field exists which can be detected by a nuclear resonance experiment.

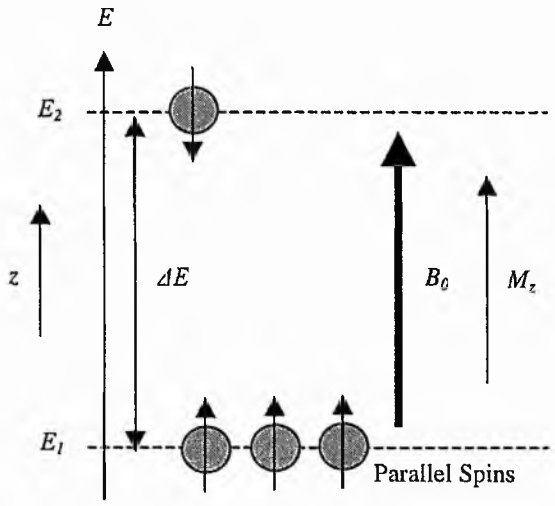

Figure (4.1): Illustration of energy level difference ΔE during spin alignment in an applied field B_0 resulting in a macroscopic magnetisation M_z within the sample.

4.2.1 Nuclear Magnetic Resonance

Transitions of nuclei between the two energy levels described above are produced by the absorption of electromagnetic radiation with a frequency ω_0 defined by the relationship;

$$\Delta E = \hbar\omega_0 \qquad (4.1)$$

where $\hbar = h/2\pi$ and h is Planck's constant. The transition of a spin from one energy level to another represents a change of its spin direction. However, as the probability of spontaneous emission or absorption is very low this is only possible if an additional electromagnetic field with frequency ω_0 is applied to the sample. This is the resonance condition where ω_0 is the resonant frequency;

$$\omega_0 = \gamma B_0 \qquad (4.2)$$

here γ is a constant called the gyromagnetic ratio, specific to the type of nuclei, and ω_0 is known as the Larmor frequency. For the hydrogen ^1H nucleus in a magnetic field of strength *1 Tesla* this resonant frequency is *42.58 MHz*. Such radio frequencies are easily produced inside the coil of a resonance circuit so that nuclear transitions can be excited by a radio frequency electromagnetic field.

If a short, intense radio frequency pulse of frequency ω_0 is applied to the sample perpendicular to the magnetic field B_0, an equilibrium in the distribution of nuclei between the two energy levels is produced. With equal numbers of parallel and anti-parallel spins the magnetisation M_z in the z direction is zero and the magnetisation is aligned in the x-y plane, i.e. $M_{x,y}$. A pulse which has turned the magnetisation through *90°* is called a *90°* pulse. Following this *90°* pulse, the magnetisation is aligned with the axis of the electromagnetic coil. This magnetisation can be pictured as the nuclear spins precessing in phase. The nuclear spins have a rotational frequency ω_0 and hence cause the magnetisation to oscillate with this same frequency. This oscillating magnetic field induces an alternating voltage in the electromagnetic coil also with frequency ω_0. Thus, it is possible to detect the magnetisation of the sample. The electromagnetic coil therefore acts as both a transmitter, to excite the nuclear resonance, and a receiver, for the detection of nuclear resonance signals. Following the application of the radio frequency pulse the nuclear resonance signal decays, resulting in the observed signal known as the Free Induction Decay. However, an important property of the nuclear resonance signal is that the signal intensity at a constant field strength is a measure of the density of a particular type of atomic nucleus within the sample.

4.2.2 Nuclear Magnetic Relaxation

The nuclear resonance signal decays with time and can also yield important information. Following the excitation, the sample returns to a state of equilibrium within a certain time. This means that the oscillating magnetisation in the x-y plane

$M_{x,y}$ no longer exists and is restored in the z direction M_z. This transition to the state of equilibrium after the disturbance by the pulse is termed the relaxation of the spin system. Two relaxation processes may be differentiated: spin - spin relaxation and spin - lattice relaxation (BLOEMBERGEN 1948). The decay of the transverse magnetisation $M_{x,y}$ is characterised by the spin - spin relaxation time T_2. The recovery of the longitudinal magnetisation M_z is characterised by the spin - lattice relaxation time T_1. The difference between these two relaxation times is illustrated below.

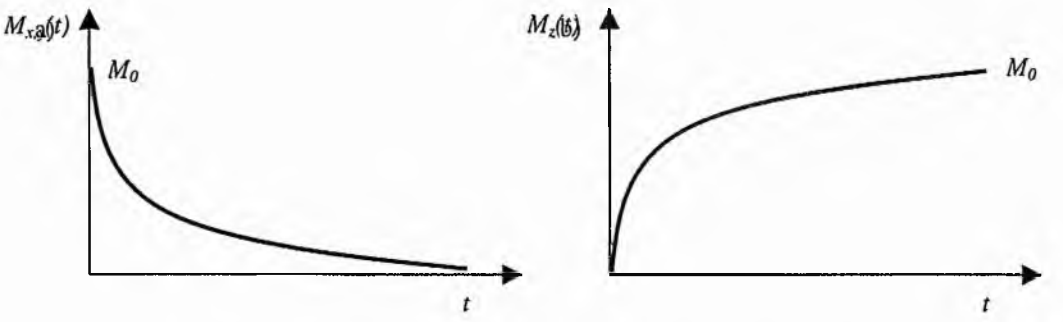

$$M_{x,y}(t) = M_0 \exp(-t/T_2) \quad (4.3) \qquad M_z(t) = M_0 [1-\exp(-t/T_1)] \quad (4.4)$$

Figure (4.2): Illustration of a) the spin - spin relaxation and b) the spin - lattice relaxation as characterised by equations (4.3) and (4.4) respectively where M_0 is the net magnetisation of the sample.

By applying different radio frequency pulse sequences to the sample, different magnetisations can be induced in the sample and hence T_1 or T_2 can be measured as required. The spin - echo sequence uses a $90°$ pulse to turn the magnetisation to the x-y plane and produce the transverse magnetisation $M_{x,y}$. Due to inhomogeneities in the applied magnetic field, individual spins possess slightly different resonant frequencies, some precessing faster and some slower (HAHN 1950). This de-phasing causes the nuclear resonance signal to decay in a time T_2^*. After a time τ_e, a $180°$ pulse is applied to invert all the spin directions and the de-phasing process is converted to one of re-phasing. After a further period τ_e has elapsed, the spins align in phase as they were after the initial 90° pulse. This re-phased signal is termed the spin - echo and τ_e is known as the echo time. Despite this rephasing, the amplitude of the spin - echo signal will still decay with a characteristic time T_2, the true spin - spin relaxation time. If a multiple sequence of

180° pulses is applied, the intensity of successive spin - echos decay with time. This method is used to determine the T_2 relaxation time of the sample (CARR 1954, MEIBOOM 1958).

4.2.3 Spatial Imaging

Magnetic resonance imaging can provide spatial information about the sample in question as well as temporal information (ERNST 1987). Spatial information can be obtained using the resonance frequency if the applied magnetic field changes linearly with distance through the sample (LAUTERBUR 1973). This magnetic field gradient increases linearly in a particular direction and hence the magnetic field strength and consequently also the resonance frequency increase linearly with distance. Nuclei at different spatial locations along the magnetic field gradient precess at different Larmor frequencies. Therefore, if the nuclear resonance signal is plotted as a function of frequency, a density profile of the nuclear spins with distance is obtained. However, the two directions perpendicular to the magnetic field gradient remain unresolved and only a one - dimensional profile of the sample is obtained. This situation is illustrated in figure (4.3). Three - dimensional profiles are possible by manipulation of three magnetic field gradients applied in orthogonal directions.

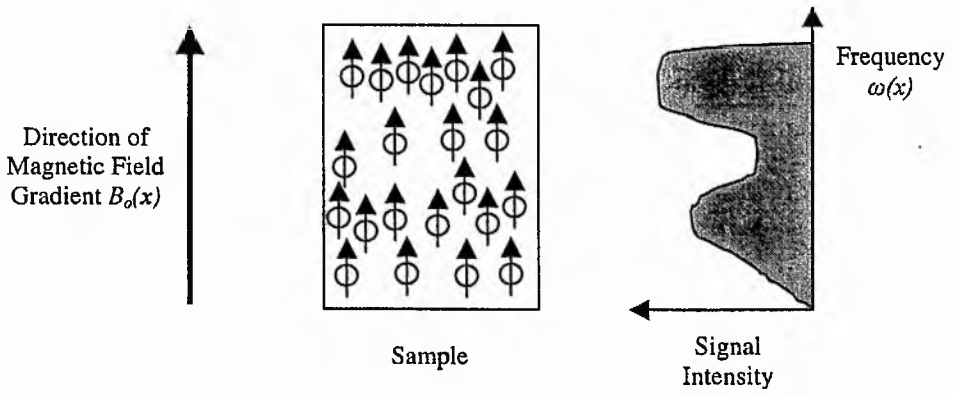

Figure (4.3): A schematic illustration of a magnetic field gradient applied along the length of a sample containing different densities of spins. A plot of the nuclear resonance signal intensity with frequency produces a profile of this changing spin density with distance.

4.3 Experimental Procedure

With the aim of comparing experimental MRI data to the results of the "Simple" Monte Carlo model, it is clear that a solvent/polymer system is required that displays Fickian dynamics. The diffusion of decane into lightly crosslinked natural rubber is such a system. Halse (HALSE 1994, 1996) has shown that this system can be studied by MRI and that it produces Fickian diffusion dynamics. The decane/rubber system is therefore chosen for this experiment, but it is also an important example of the softening of rubbers by organic solvents used in many industrial processes.

4.3.1 Sample Geometry and Preparation

The ingress of solvent into a polymer can cause significant swelling of the polymer. The volume of the swollen polymer is approximately equal to the sum of the volumes of the separate components. However, if the volume of absorbed solvent is very much less than the volume of dry rubber, the swelling can be neglected and known analytic solutions of the one - dimensional diffusion equation can be used. Polymer samples are prepared in the form of thin sheets of thickness $2L$ and are immersed in the decane for a period of time before being removed and imaged. A thin layer of solvent is absorbed onto each surface, which then diffuses towards the interior of the polymer sample. This is illustrated in figure (4.4). Halse (HALSE 1994) assumed that the thin layer of solvent absorbed onto each face of the sample approximated a delta function in concentration. Using this boundary condition and the condition that no solvent reached the centre of the sheet, a solution of the differential equation of diffusion was given for the solvent concentration as a function of time and distance through the polymer sheet for a constant diffusion coefficient. This solution was based on a derivation given by Parker (PARKER 1961). However, Halse recognised that this solution was only true if the exposure of the polymer to the solvent was infinitely short and that the finite exposure time used could be too long. While the polymer sample is immersed in the solvent , the surface of the polymer is exposed to a constant concentration of solvent for a finite time

before being imaged. This is closely related to the system modelled by the Monte Carlo method provided that the imaging process is carried out within a short period of time after the polymer sample is removed from the solvent.

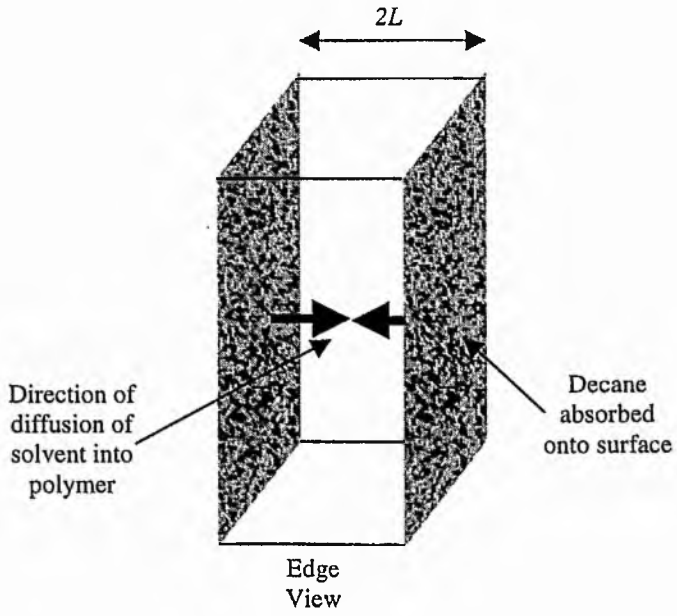

Figure (4.4): Sample geometry showing the direction of solvent diffusion into a rubber sheet of thickness $2L$ where decane is absorbed onto only two faces of the sample as indicated.

Samples of vulcanised, unfilled natural rubber sheets of thickness 2 *mm* were supplied by the Tun Abdul Razak Research Centre. Two different cure systems were used during production, each producing three different effective crosslink densities as specified in figure (4.5).

Sample Number	*Cure System*	*Crosslink Density (mol/m^3)*
1	*Dicumyl peroxide 1 phr*	*35*
2	*Dicumyl peroxide 2 phr*	*66*
3	*Dicumyl peroxide 3.5 phr*	*123*
4	*Sulphur/CBS 0.8/0.8 phr*	*28*
5	*Sulphur/CBS 1.6/1.6 phr*	*63*
6	*Sulphur/CBS 3/3 phr*	*118*

Figure (4.5): Samples of natural rubber showing the cure system and effective crosslink densities for each sample.

The solvent decane ($C_{10}H_{22}$) was supplied by Aldrich chemicals. Rubber samples of *50x10 mm* and thickness *2 mm* were cut from each rubber sheet. They were then immersed in the decane for a time *T* before being removed and dried on filter paper to remove any excess solvent. A section of polymer of *10x10 mm* was then cut from the sample and trimmed to approximately *8x8 mm* to eliminate edge effects before immediately imaging the sample. The remainder of the sample was returned to the solvent for a further time *T*. This was repeated for five consecutive *3 min* periods *T* so that the total immersion time of the fifth section was *15 min*. Once each section of each sample was prepared, it was mounted in a sample holder and placed into the magnetic resonance imager.

4.3.2 Imaging Procedure

The MRI system used for this study was a *0.47 T* (*20 MHz* for ^1H) bench - top system built by Maran Resonance Instruments. A temperature controller maintained the sample at a constant *20°C*. A spin - echo sequence consisting of a *90°* excitation pulse followed by a *180°* rephase pulse was used to induce the transverse echo magnetisation $M_{x,y}$ as described above. The signal amplitude was recorded at *256* points across the echo and Fourier transformed to produce a spin density profile. This was repeated for each section of the sample at successive solvent exposure times *T*. However, in this study it is important to be able to differentiate between the resonance signal arising from the solvent and the signal arising from the polymer. This is possible because of the large differences between the relaxation times of the solvent and polymer signals. The dry rubber has a T_2 relaxation time of approximately *1 ms* whilst the decane has a T_2 relaxation time of approximately *200 ms*. Similarly, the dry rubber has a T_1 relaxation time of approximately *50 ms* whilst the T_1 relaxation time of the swollen rubber is approximately *500 ms*. This relaxation contrast avoids the need to use a deuterated solvent. For rapidly repeated measurements the signal amplitude at position *r* is given by;

$$M_z(r) = \sum_{i=1}^{2} M_0^i(r)[1-\exp(-t_{RD}/T_1^i)]\exp(-\tau_e/T_2^i) \quad (4.5)$$

where i indicates each component of the polymer solution and $M_0^i(r)$ represents the local magnetisation intensity of component i. In equation (4.5) t_{RD} is the relaxation delay, the time between the 90° pulse and the start of the next average of the data acquired; τ_e is the echo time, the time between the 90° pulse and the 180° pulse. By choosing a suitable time for this relaxation delay, it is possible to selectively image either the dry rubber or the swollen rubber. If t_{RD} is much less than the T_1 of the solvent but longer than the T_1 of the rubber, the magnetisation signal from the rubber will be dominant since the longitudinal magnetisation of the solvent has not had sufficient time to recover. However, if t_{RD} is greater than the T_1 of the solvent as well, then the longitudinal magnetisation amplitude will consist of contributions from both the rubber and the solvent. By a minimum of three measurements at suitably chosen t_{RD} it is possible to extract M_z for the decane component only. In this experiment τ_e is defined as a constant $900\ \mu s$, which is short compared to the T_2 of the polymer and the solvent. Therefore, the second exponential term in equation (4.5) can safely be neglected.

For each sample imaged, three profiles are recorded at three relaxation delay times of *25 ms*, *50 ms* and *2000 ms*. The last of these times will produce a spin density profile comprising contributions from both the decane and the rubber. To eliminate the rubber contribution from this final profile, the signal amplitudes for the two shorter relaxation delay times are extrapolated at each point across the profile using equation (4.5) to give the expected amplitude A_3 of the magnetisation signal arising from the rubber after a relaxation delay of *2000 ms*. This amplitude profile can then be subtracted from the recorded profile to leave a profile consisting only of the magnetisation signal amplitude arising from the solvent. This is illustrated in figure (4.6).

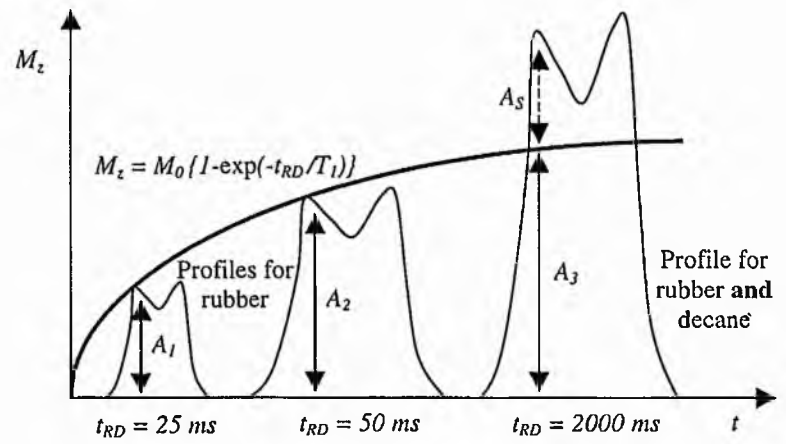

Figure (4.6): Illustration of the spin density profiles recorded at each of the three relaxation delay times t_{RD} showing the amplitude A_3 expected for a pure rubber sample at receiver delay time of t_{RD} = *2000 ms*. The corresponding amplitude arising from the decane is assigned A_S.

For each of the two rubber profiles (t_{RD}=*25 ms*, t_{RD}=*50 ms*), an equation can be written for the amplitude of each point of the profile using equation (4.5);

$$A_1 = M_0\{1\text{-exp}(-25/T_1)\} \qquad (4.6)$$

$$A_2 = M_0\{1\text{-exp}(-50/T_1)\} \qquad (4.7)$$

Solving these equations simultaneously gives the amplitude A_3 of the rubber component as t_{RD} approaches infinity and $A_3 \rightarrow M_0$.

$$A_3 = A_1^2/(2A_1 - A_2) \qquad (4.8)$$

Figure (4.7) shows these three profiles at each exposure time for sample *1* as an example of the typical spin density profiles recorded in this experiment. Also shown are profiles for the dry rubber (*t=0*) and profiles for the swollen rubber after an exposure time of *60 mins*. For this latter time the sample is saturated with decane, showing a constant signal amplitude across the sample. For the remaining five profiles a marked variation in signal amplitude can be seen across the sample.

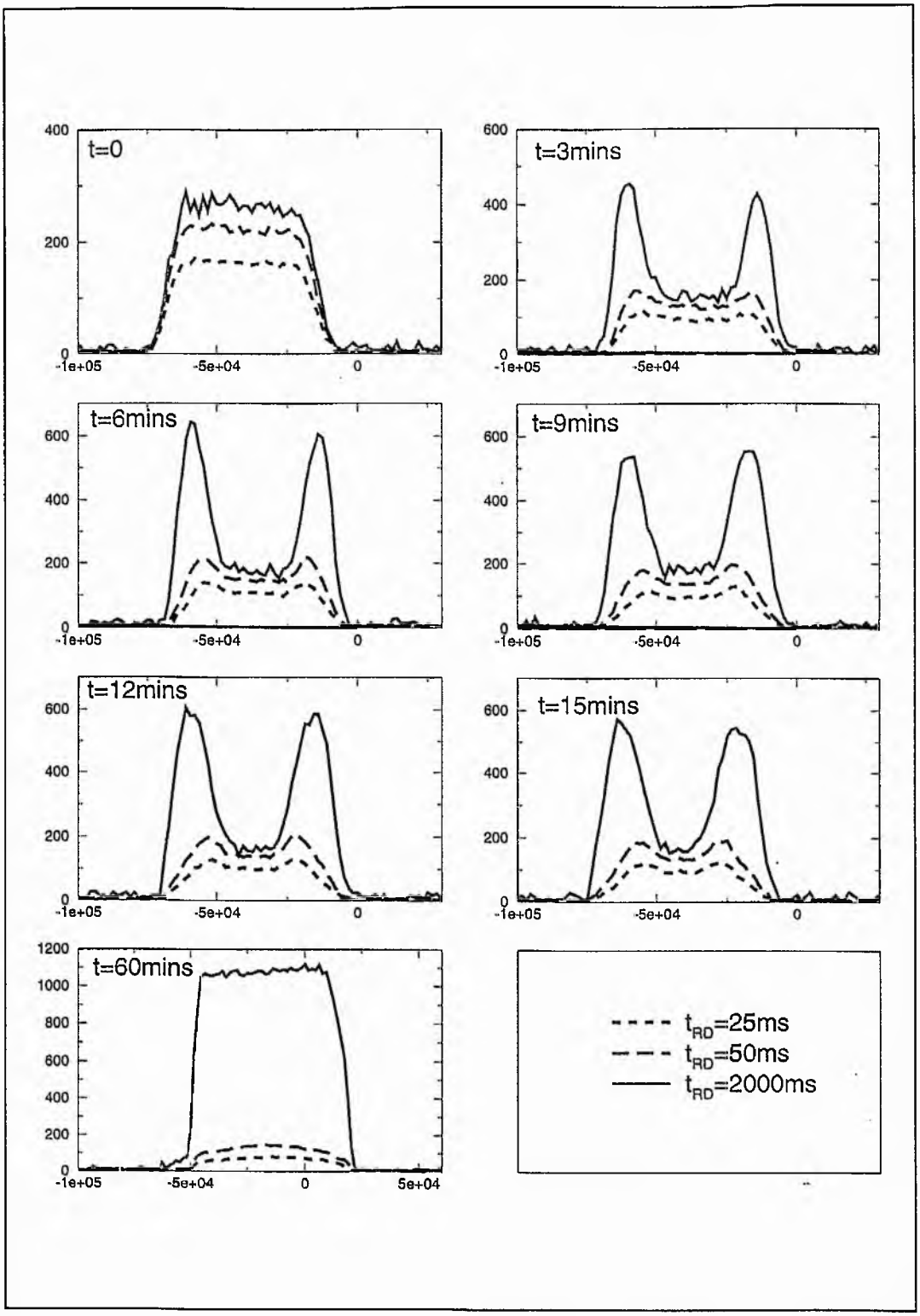

Figure (4.7): Spin density profiles for sample *1* showing magnetisation signal amplitude against recorded position for seven solvent exposure times. For each exposure time three profiles are shown for relaxation delay times of *25 ms*, *50 ms*, and *2000 ms* .

4.4 Comparison with the Monte Carlo Model

Figures (4.9) and (4.10) show the experimental data for samples *1*, *2*, *3* and *4*, *5*, *6* respectively. Each graph shows the experimental data plotted as points for each of the five solvent exposure times stated above. In deriving the experimental data points, the amplitude of each point has been calculated using the method outlined previously to eliminate the signal arising from the rubber. Thus a one - dimensional profile of solvent intensity against distance is obtained. In figures (4.9) and (4.10) this solvent intensity has been normalised to give a solvent volume fraction with distance through the sample.

Furthermore, the original MRI data showed solvent ingressing from two opposing faces towards the centre of a sample of width $2L$. Provided that the solvent does not reach the centre of the sample, this is equivalent to the solvent ingressing two semi - infinite media from opposite directions. Thus, these two effective sets of data are used to reduce statistical errors by reversing one of the data sets and taking an average of the two. Therefore, figures (4.9) and (4.10) show the decane ingressing only in one direction through a sample of width L.

In this study, the "Simple" Monte Carlo model has been used as described in the previous chapter to generate solvent profiles to compare to the experimental data. Solvent molecules and polymer chains were placed in the lattice with equal volume fractions of $\phi=0.5$ and a maximum polymer chain length of $N=200$ segments. Transition rates were uniformly set to unity and no interaction energies were included in the model as is the case for an athermal system of a polymer in a good solvent (DE GENNES 1979). A lattice spacing of $1x10^{-6}$ m was used, with equal time increments between successive profiles. This lattice spacing produces a very coarse - grained model compared to the scale of the solvent molecule. However, it was chosen in order to achieve a manageable computing time. The simulated data was fitted to the experimental data, primarily, by varying the transition rate of the polymer motion between successive sets to simulate the effect of the increasing crosslink density in the rubber and a reduction in the polymer's mobility.

The main difference between the experimental data shown here and the results of Monte Carlo model is that the sharp discontinuity expected at the edge of the profile has been rounded by the finite image resolution of the MRI method. To allow for this effect, the Monte Carlo data fitted to these experimental results was first convolved with a Gaussian point spread function of the form;

$$G(x) = \exp\{ -(x/\Delta x)^2 \} \qquad (4.9)$$

where Δx is an adjustable parameter equal to the standard deviation of Gaussian broadening function. An example of this convolution is shown in figure (4.8) for a typical set of simulated Fickian solvent profiles. The best fit for the Monte Carlo data was obtained with $\Delta x = 0.15$ *mm*.

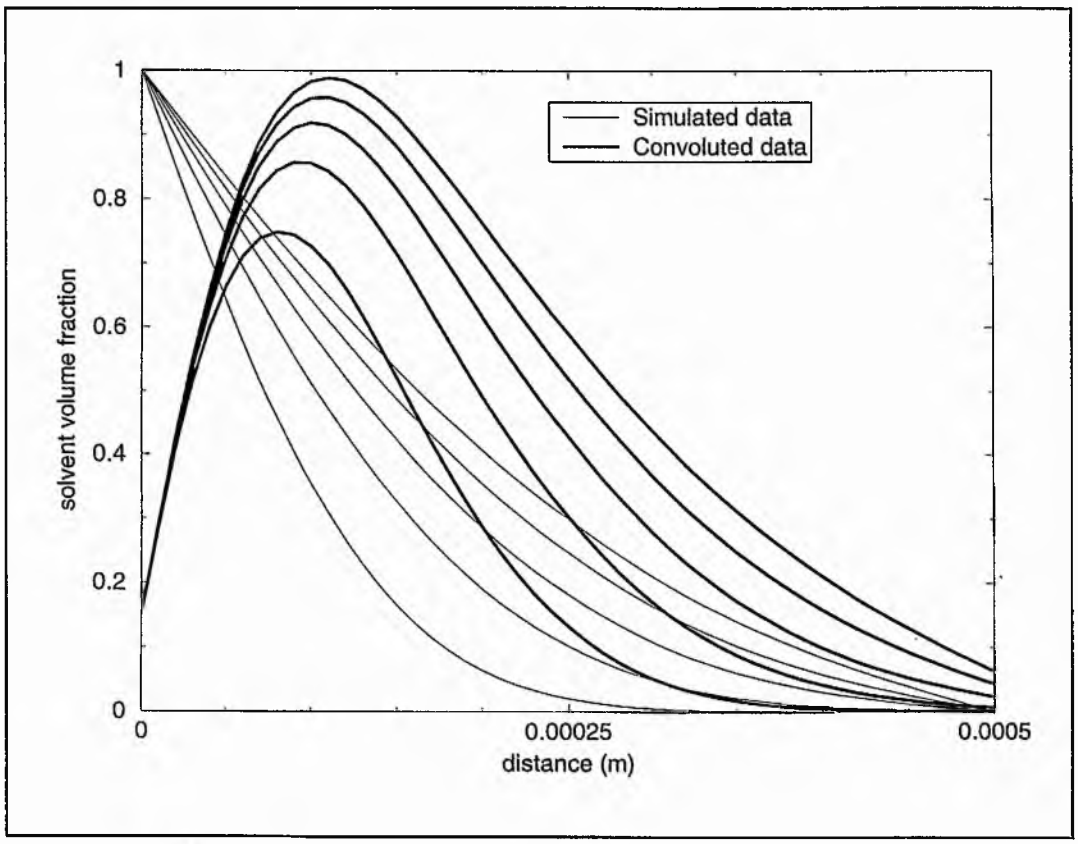

Figure (4.8): An example of the effects of convolution for a typical set of Fickian solvent profiles at five equal time intervals. The original simulated profiles are shown by thin lines, while the convoluted data is shown by the thick lines.

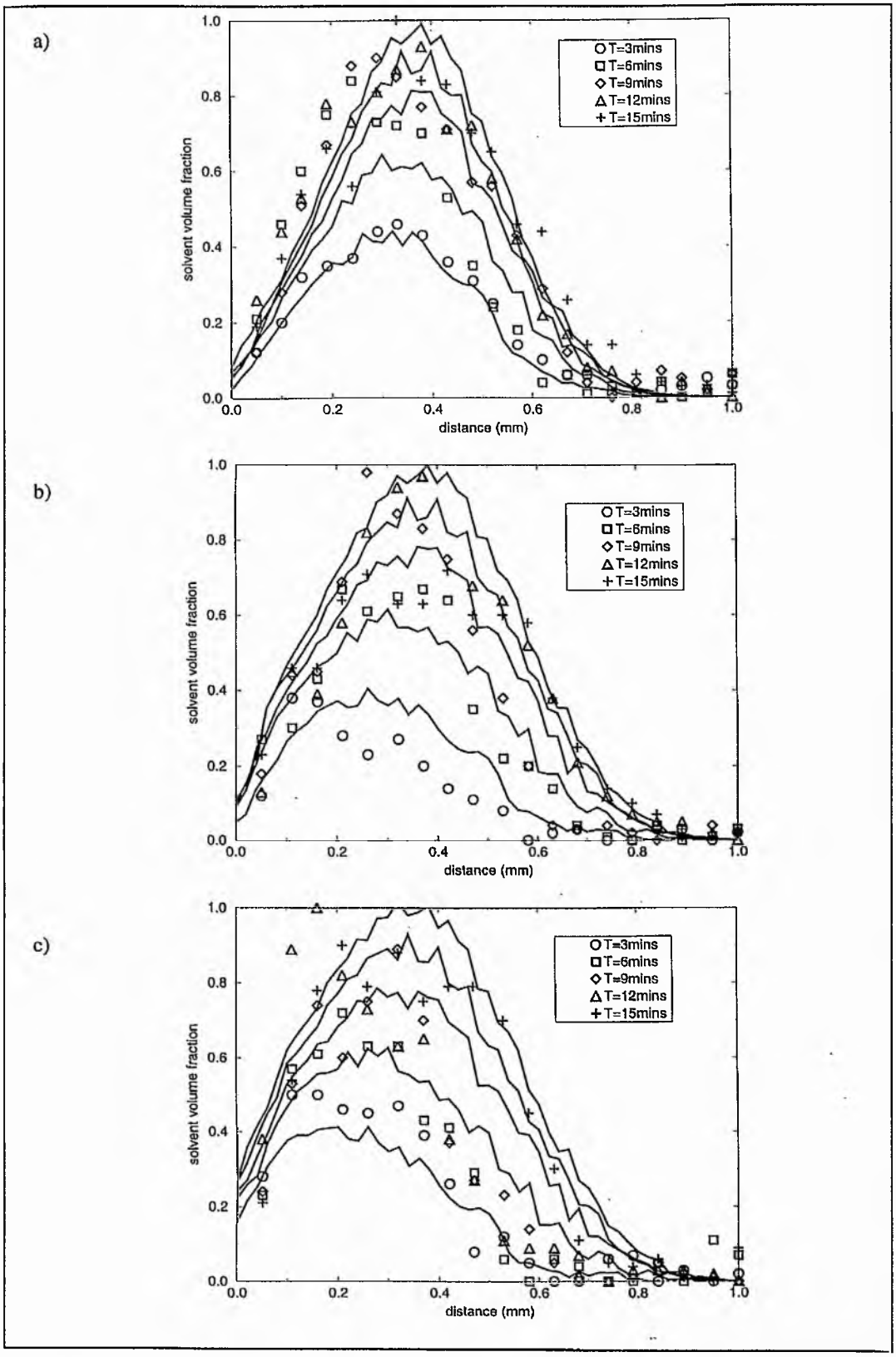

Figure (4.9): Averaged one - dimensional solvent profiles showing MRI experimental points together with fits from the Monte Carlo model (solid lines) for samples a) *1*, b) *2*, c) *3*.

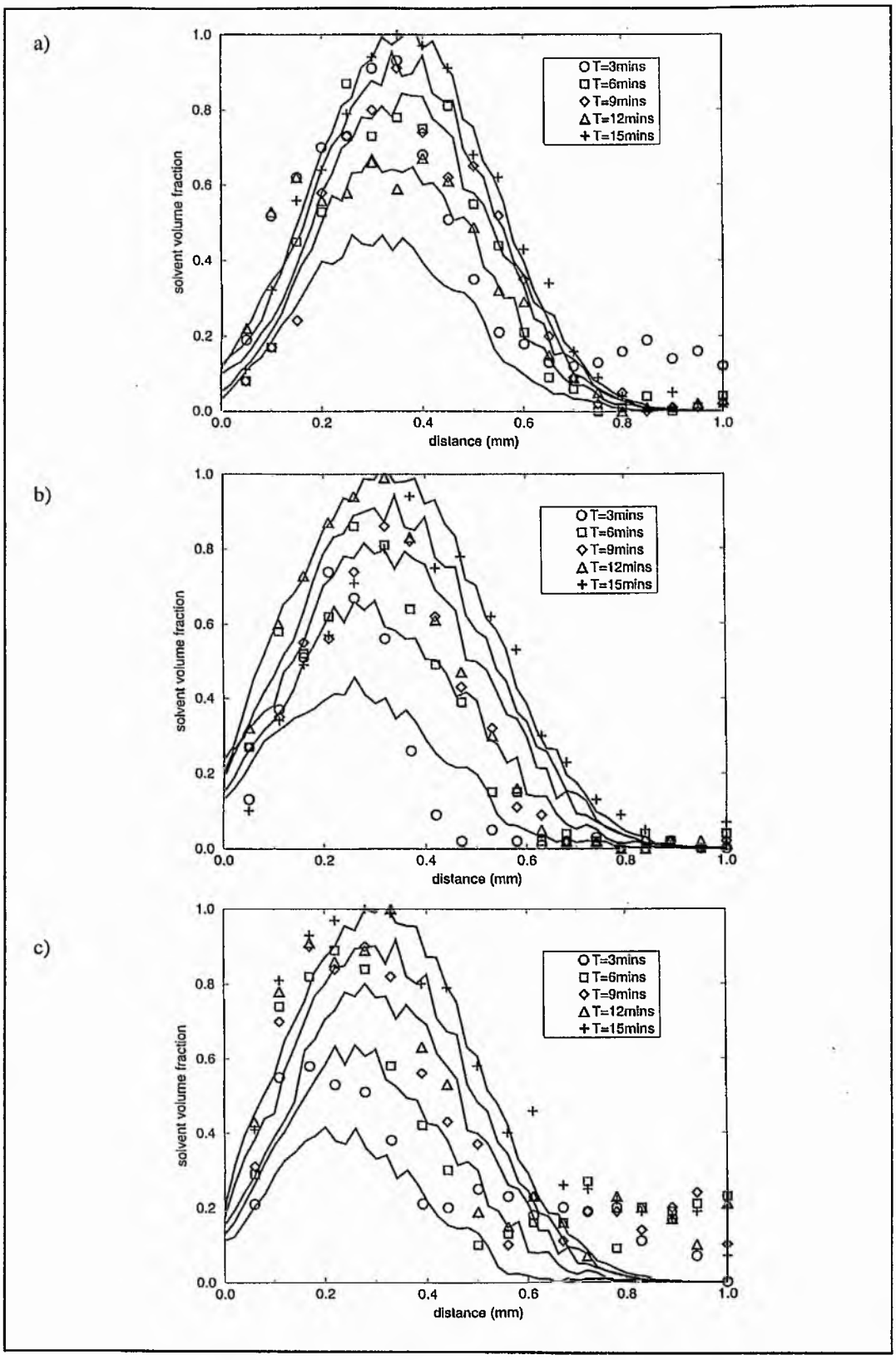

Figure (4.10): Averaged one - dimensional solvent profiles showing MRI experimental points together with fits from the Monte Carlo model (solid lines) for samples a) *4*, b) *5*, c) *6*.

The Monte Carlo results shown in figures (4.9) and (4.10) do not show a conclusive fit with the experimental data due to the errors in the experimental data arising from the manipulations it has undergone. In particular, errors arise from the use of equation (4.8) if the amplitude $A_1 << A_2/2$. It is unclear how this may be avoided using the current method. The accuracy of the Monte Carlo data is also questionable due to the large lattice spacing used here. This limitation of the model arises from the need to maintain a manageable computing time. An accurate fit of the Monte Carlo model to the experimental data would require careful specification of the model parameters to correlate with the dimensions of the system being studied. Therefore, the simulated data is only an approximation intended to show the general features of the diffusion process. However, it is clear that there is some correlation between the experimental data and the Monte Carlo data and that the two sets of data follow similar trends. It is possible to conclude that the "Simple" Monte Carlo model offers a reasonable comparison to the MRI data presented in this chapter.

4.5 Conclusions

Magnetic Resonance Imaging is an important experimental method in the study of the dynamic properties of polymers and polymer solutions. The results presented in this chapter demonstrate the type of information that can be extracted from such an experiment and the methods that are used. These results show the diffusion of the decane into the interior of the rubber. However, errors introduced during the analysis of the results mean that the extracted solvent profiles are relatively poor. It is possible to fit data from the "Simple" Monte Carlo model to this experimental data and show that the Monte Carlo method provides a comparison to the experimental data that reasonably reproduces its general features. It is therefore possible to conclude that the Monte Carlo model is able to reproduce the general features of solvent diffusion into polymer in the limit of Fickian diffusion. To improve the accuracy of these results would require improvements in the collection and analysis of the experimental data. The imaging system used for this experiment is a relatively basic "bench-top" system. Better MRI techniques and systems have been developed to study polymer systems in more detail. For example, Stray - Field

Magnetic Resonance Imaging (STRAFI) has been used extensively at the University of Surrey and will be discussed in Chapter 6. To improve the fit of the Monte Carlo model would require a detailed knowledge of the binding energies of the particular solvent/polymer system and of the solvent and polymer molecules. A finer lattice would also improve the situation, simulating more closely the scale of the solvent molecule. However, this would require a much greater computing time. Both are beyond the scope of this work.

Chapter 5

Limitations of Current Models of Solvent Diffusion

5.1 Introduction

It has so far been demonstrated that the Monte Carlo method may be used to model the ingress of solvent into a polymer. Case I, or Fickian, diffusion dynamics have been successfully modelled, but the limitations of this method have not been discussed in detail. However, it is the aim of this work to use the Monte Carlo method to also model Case II, or non - Fickian, dynamics. So far, this has not been achieved with the current "Simple" Monte Carlo model and must be the primary limitation of the model. This is a very important consideration and requires detailed examination. It is necessary to understand why Case II dynamics have not been achieved and what modifications are required to move away from Case I dynamics.

In this chapter the limitations of the Monte Carlo method, and specifically the limitations of the "Simple" Monte Carlo model, are critically discussed. The possibility of using the Monte Carlo method to model Case II diffusion in its current form is also considered. However, an important limit is proposed that restricts the use of the Monte Carlo method in its present configuration. Current theories of Case II diffusion and their limitations are then discussed. It is hoped that this chapter will provide a discussion of the limitations of these different models and provide an understanding of the motivation for adapting the Monte Carlo method to produce Case II dynamics.

5.2 Limitations of the Monte Carlo Method

In Chapter 2, the qualitative differences between Case I and Case II solvent diffusion dynamics were described. The most important of these is the time dependence of the progression of the solvent front characterised by t^n, where $n=0.5$ for Case I diffusion and $n=1$ for Case II diffusion. It is now necessary to examine the differences in the diffusion processes that give rise to these two types of behaviour. Case I diffusion is commonly associated with solvent diffusion in rubbery polymers (WEBB 1991, HALSE 1994). In this state, the polymer molecules respond rapidly to changes in their condition brought about by the ingress of solvent. Case II diffusion is generally associated with solvent diffusion in glassy polymers (WEISENBERGER 1990a/b, ERCKEN 1996). Unlike the rubbery polymer, the properties of the glassy polymer tend to be time dependent and show a slow response to changes in their condition (CRANK 1975). Therefore, Case I diffusion occurs when the polymer responds instantaneously to the ingress of solvent, the mobile polymer molecules moving rapidly to accommodate the ingressing solvent. Case II diffusion occurs when the polymer's response to the ingressing solvent is characterised by the relaxation of the polymer molecules at some finite rate. Furthermore, this relaxation time decreases as temperature or solvent concentration is increased and the polymer molecules become more mobile. The change from a polymer glass to a rubber is therefore associated with a decrease in the polymer relaxation time due to either an increase in temperature or an increase in solvent concentration. These differences have been classified further (ALFREY 1966) according to the relative rates of the solvent ingress and polymer relaxation. For Case I diffusion the rate of solvent ingress is much less than the rate of polymer relaxation, whilst for Case II diffusion the rate of solvent ingress is very rapid compared to the relaxation of the polymer molecules. In general then, the diffusion of solvent molecules into a polymer depends on two processes, the rate of solvent ingress and the rate of polymer relaxation, which are coupled together.

It is now necessary to examine whether the Monte Carlo method is able to reproduce the finite relaxation rate of the polymer described above. In Chapter 3,

section (3.2.2), the criteria for the Monte Carlo method were described in terms of the polymer chain transition probabilities $p(\omega_n \rightarrow \omega_{n+1})$ for a change of conformation from configuration ω_n to ω_{n+1}. It was stated that these transition probabilities must satisfy the detailed balance principle, where the equilibrium probability density function of state ω_n is $P_{eq}(\omega_n)$ (MULLER-KRUMBHAAR 1973);

$$P_{eq}(\omega_n)p(\omega_n \rightarrow \omega_{n+1}) = P_{eq}(\omega_{n+1})\, p(\omega_{n+1} \rightarrow \omega_n) \qquad (5.1)$$

The dynamic interpretation of the Monte Carlo algorithm involves associating a time with the successive chain configurations so that the probability density function is interpreted as $P(\omega_n,t)$ for a system evolving with time. Furthermore, if the transition probability is taken as the probability per unit time, the Markov chain process can be considered as the numerical realisation of the following master equation (BINDER 1997);

$$dP(\omega_n,t)/dt = -\sum_{\omega_{n+1}} P(\omega_n,t)p(\omega_n \rightarrow \omega_{n+1}) + \sum_{\omega_n} P(\omega_{n+1},t)\, p(\omega_{n+1} \rightarrow \omega_n) \qquad (5.2)$$

This equation states that the probability of state ω_n decreases by all processes that lead away from this state to other states ω_{n+1}. This loss in probability is counteracted by the inverse process from ω_{n+1} to ω_n, leading to a gain in probability. In thermal equilibrium, gain and loss processes compensate each other because of the detailed balance principle and hence $dP(\omega_n,t)/dt=0$. This master equation describes the time evolution of a system simulated by dynamic Monte Carlo methods and it is necessary to know how this is related to the physical dynamics of the polymer. To what extent can the Monte Carlo method model the configurational relaxation of the polymer chain? Equation (5.2) describes a change of probability that depends only on the present state ω_n of the system. There is no memory of the past history of the system. Dynamic moves in the Monte Carlo method therefore depend only on the

current state of the system and have no dependence on slow relaxation dynamics arising from some previous state of the system. The Monte Carlo method simulates the random motions of polymer segments very well where the movement between configurations is instantaneous, but this motion contains no component that relaxes with some finite rate.

An obvious example of this type of problem can be seen for polymer solutions. The hydrodynamic backflow interaction (ZIMM 1956) mediated by the flow of solvent is completely missing. A disturbance in the solvent should create a hydrodynamic flow in the surrounding media, but this type of response is not modelled by the Monte Carlo method. Thus, dynamic Monte Carlo simulations of polymer chains in the dilute solution limit produce Rouse (ROUSE 1953) dynamics rather than the correct dynamics of the Zimm model. This is because the dynamic algorithms used in this work conserve only the particle number and not the momentum. This lack of momentum conservation removes any hydrodynamic effects, but it is not currently known how this could be introduced into the Monte Carlo method (BINDER 1997). In dense polymer solutions this fact remains, but since the viscosity of the solution is high, the hydrodynamic interaction is small and can normally be neglected (BINDER 1995).

5.2.1 Limitations of the "Simple" Model

The "Simple" Monte Carlo model described in Chapter 3 also has inherent limitations as well as the general limitations described above. These will now be discussed in relation to the desire to model Case II diffusion dynamics and the discussion given above. The first limitation of the model is that the volume fraction of polymer placed in the lattice reaches a maximum at $\phi_p \sim 0.7$ for polymer chain lengths of *200* segments. This can be seen in figure (3.7d). Using the current methods, it is not possible to place polymer chains in the lattice at a volume fraction greater than this. This is due to the static Monte Carlo algorithm used to place the polymer chains and the need for sufficient vacancies in the lattice to extend the polymer chain up to the required length. If there are insufficient vacancies, and attempts to place new chain segments are blocked by existing segments, then the

algorithm dismisses the current polymer chain configuration and attempts to place a different one. However, at high polymer volume fractions ($\phi_p > 0.7$), attrition is high and it is almost impossible to find a continuous chain configuration that extends to the desired maximum chain length. This limitation must be considered in future work as there will always be a vacancy volume fraction of at least $\phi_v \sim 0.3$.

It is also necessary to consider the solvent volume fraction dependence of the chemical diffusion coefficient given by equation (3.12). This equation shows an exponential decrease in the diffusion coefficient with increasing solvent volume fraction. This is correct in this simple Monte Carlo model and shows a decrease in the diffusion of the solvent molecules as the vacancies in the lattice fill with solvent molecules and impede the further movement of solvent molecules between the polymer chains. As time increases towards infinity and the lattice becomes saturated with solvent molecules a limit would be reached where all the lattice sites are occupied and no motions would be possible by either the solvent molecules or the polymer chain segments due to the absence of any empty lattice sites. This type of behaviour has been observed in some polymer systems (BARRIE 1966), and Rouse proposed that this was due to the clustering of the solvent molecules within the free volume of the polymer (ROUSE 1947).

However, experimental studies of systems displaying Case I diffusion have generally shown strong evidence for the chemical diffusion coefficient of the solvent actually increasing exponentially with increasing solvent volume fraction (MANSFIELD 1991, 1992, HALSE 1994). This highlights an important difference between the current Monte Carlo model and most real polymer systems. In real polymer solutions, the ingressing solvent causes a change in the dynamics of the polymer. The polymer chains become more mobile and swell in response to the increasing solvent volume fraction. Thus, larger vacancies develop in the polymer, which become available to the ingressing solvent molecules more quickly as the mobile chains move to accommodate the solvent molecules. Hence, the rate of diffusion increases. However, in the Monte Carlo model, there is no change in the polymer dynamics with ingressing solvent. The mobility of the polymer chains remains constant with an increasing solvent volume fraction and the number of free

lattice sites, or vacancies, actually decreases. Hence, the rate of solvent diffusion decreases in this case.

Two other limitations of the Monte Carlo model must be mentioned here, but will not be examined further. Firstly, the random numbers used in the computer simulation are generated by a standard FORTRAN algorithm. However, any random number generator of this type can only produce a sequence of numbers that is pseudorandom. The sequence of random numbers is exactly reproducible and after a long, but finite, period the sequence will be repeated again. Secondly, the use of periodic boundary conditions can produce limitations due to finite size effects. A diffusing solvent molecule will, after a long period of time, move through the same lattice a number of times. Neither of these effects pose serious limitations to the current work but must be considered in the development of such simulations and are themselves independent fields of research.

It is clear that in real polymer systems the ingressing solvent produces changes in the structure and dynamics of the polymer. However, the "Simple" Monte Carlo model currently used in this work is not capable of reproducing such changes. In this simulation the rate of polymer motion is a predetermined parameter that remains constant with increasing solvent volume fraction. The actual probability that a particular attempted move will be successful decreases with increasing solvent volume fraction as the number of vacant lattice sites decreases. This is evident in figure (3.12) where frozen polymer chains, with a process rate of zero, were used to simulate a polymer glass. In this case, the solvent molecules diffused through the free volume between the static polymer chains, since the polymer chains remained frozen and were not activated by the increasing solvent volume fraction. In general, the processes of solvent ingress and polymer relaxation are decoupled in this model. Attempts must be made to modify the Monte Carlo model so that the polymer chain dynamics change in response to the ingressing solvent. Such attempts have been made in the course of this work and are outlined in the next section.

5.2.2 Attempts to Model Case II Diffusion

It is clear that the current Monte Carlo model lacks the coupling between the diffusion of the solvent molecules and the relaxation of the polymer chains necessary to produce Case II diffusion dynamics. In this work, attempts have been made to introduce an effective coupling between these two processes. Initially, it was proposed that the rate of the solvent ingress could be coupled to the rate of the polymer relaxation by introducing an entirely new motion into the dynamic Monte Carlo algorithm. This novel move would involve the direct exchange of a solvent molecule and a polymer chain segment in one instantaneous move as illustrated in figure (5.1).

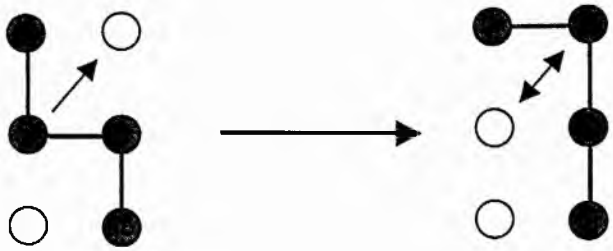

Figure (5.1): A polymer - solvent exchange move showing the exchange of a polymer segment (grey) performing a bend move with a solvent molecule (white) in one instantaneous motion.

However, due to programming considerations and the need to maintain a relatively fast and efficient algorithm, it was only possible to allow this motion to occur if the particle chosen to make an attempted move was a polymer segment. If a solvent molecule were chosen to make the attempted move then it would be quite difficult to determine which type of motion the corresponding polymer segment would be able to perform. Therefore, a polymer - solvent exchange is allowed, but a solvent - polymer exchange is not included.

With this new motion implemented within the "Simple" Monte Carlo model it was necessary to consider ways of increasing the effective density of polymer chains within the lattice above the maximum polymer volume fraction described

above. This was necessary otherwise the solvent molecules could diffuse freely into the free volume of the lattice without the polymer - solvent exchange motion ever being used. As stated previously, it is not possible to use the static Monte Carlo algorithm to place polymer chains at high densities due to the high rate of attrition. Therefore, an entirely new approach was required. This approach was to place polymer chains in the lattice to a volume fraction of $\phi_p=0.5$ and then to restrict the maximum volume fraction of the lattice to this value. Therefore, the lattice is filled to an effective maximum volume fraction, but the number of lattice sites has effectively doubled to produce a finer array of points to which particles can move. Furthermore, the Monte Carlo algorithm had to be modified to consider the probability of a particle making a successful move into a lattice plane at, or near to, the maximum volume fraction. This was accomplished by using a Gaussian probability distribution to determine the probability of a particle making a successful move to another plane in the lattice. This probability distribution is illustrated below.

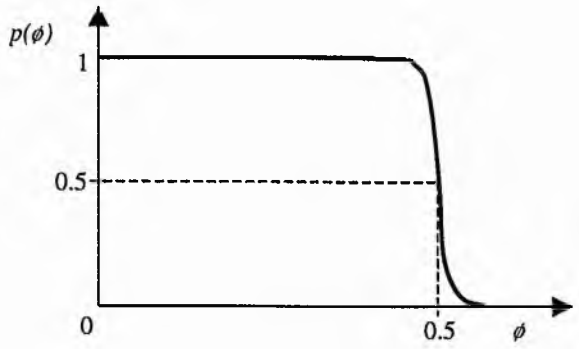

Figure (5.2): The probability distribution function used to determine the success of an attempted move between lattice planes for an effective maximum volume fraction of $\phi=0.5$.

Thus, a particle attempting to move to a lattice plane of low volume fraction will do so with a probability of unity. However, a move to a plane close to the maximum volume fraction will occur with a probability determined by a Gaussian function. This is centred about the effective maximum volume fraction of occupied lattice sites of $\phi=0.5$.

These novel modifications were made to the "Simple" Monte Carlo model, tested extensively, and shown to successfully produce a new motion in the dynamic Monte Carlo algorithm that allows the solvent to move in response to the polymer motion. The probability distribution function described here to increase the effective maximum volume fraction of polymer chains is also a useful method. It avoids the problems of attrition normally associated with the placement of polymer chains by the static Monte Carlo method. However, after being studied under a range of conditions, the only diffusion dynamics measured as a result of these modifications were Case I, or Fickian, dynamics. It seems that these modifications were unsuccessful at producing any dynamics other than those already demonstrated in this work. The new polymer - solvent exchange motion introduced here is an important development, but is incomplete without the opposite process of solvent - polymer exchange. It is this latter motion that would cause the polymer chains to move in response to the solvent ingress, whereas the polymer - solvent move effectively causes the solvent to move in response to the polymer motion. Furthermore, the effective volume fraction of occupied sites within the lattice has been increased, but without the solvent - polymer exchange the solvent molecules will be more likely to diffuse though the unoccupied volume of the lattice. A solvent molecule entering the lattice will see the polymer chain as an obstacle, whereas the polymer chain can move regardless of whether solvent molecules occupy the surrounding sites. However, both of these motions are still relatively simple instantaneous motions that have no time dependent part. Therefore, the introduction of the solvent - polymer exchange into this work has not been attempted considering the complexity of the algorithm that would be required and because it is unclear whether introducing this additional motion would even improve the situation. In the next section, a theory is proposed to suggest that a Monte Carlo model of this type will always produce Case I dynamics where the dynamic algorithm is based on a simple hopping process between lattice sites.

5.3 The Case I Limit

Most, if not all, dynamic Monte Carlo models of polymer solutions use simple hopping algorithms to model the dynamic processes. Simple hopping algorithms refer to the type of dynamic algorithms used in this work where a simple movement between neighbouring lattice sites occurs instantaneously with a certain transition probability or transition rate. A theory is now proposed that relates this type of simple hopping to the diffusional flux of the solvent molecules where a concentration gradient exists.

For simplicity, consider a system of three consecutive lattice planes $i\text{-}1$, i, $i+1$, containing ϕ_{i-1}, ϕ_i, ϕ_{i+1}, volume fractions of solvent molecules respectively. It is assumed that a concentration gradient exists through the x direction of the lattice such that $\phi_{i-1}>\phi_i>\phi_{i+1}$. Now consider the transition probabilities of all possible motions into, or out of, plane i. These probabilities $p(i\rightarrow i')$ are stated in the illustration of this system below for transitions between planes i and i'. Each probability consists of the product of the probability of finding a particle able to move in plane i and the probability of finding a vacant lattice site to which it is able to move in plane i'. In this case the system is athermal with no interaction energies included and the probability of finding an occupied lattice site is equal to the volume fraction of occupied sites.

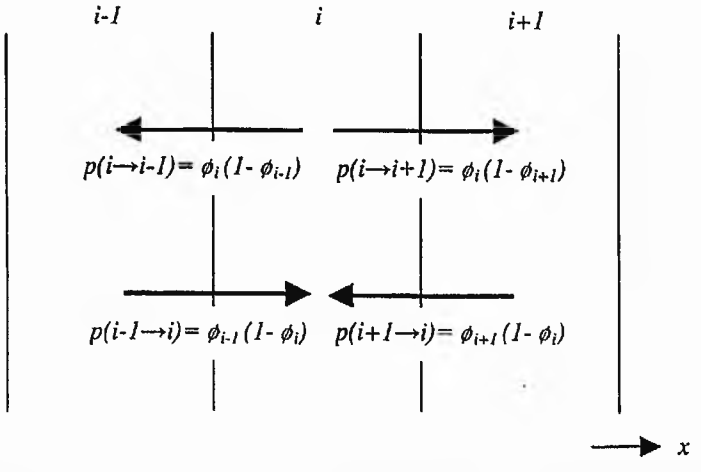

Figure (5.3): Schematic illustration of a system consisting of three lattice planes giving the transition probabilities for particle motions into, and out of, plane i.

Now, the change in volume fraction of plane i in a time increment dt is equal to the sum of these four probabilities;

$$d\phi_i/dt = p(i\text{-}1 \rightarrow i) + p(i+1 \rightarrow i) - p(i \rightarrow i\text{-}1) - p(i \rightarrow i+1) \qquad (5.3)$$

$$d\phi_i/dt = \phi_{i-1}(1-\phi_i) + \phi_{i+1}(1-\phi_i) - \phi_i(1-\phi_{i-1}) - \phi_i(1-\phi_{i+1}) \qquad (5.4)$$

By suitable rearrangement of equation (5.4) it can be shown that;

$$d\phi_i/dt = (\phi_{i+1} - \phi_i) - (\phi_i - \phi_{i-1}) \qquad (5.5)$$

and since the three lattice planes are arranged spatially in the x direction, this is also equal to;

$$d\phi_i/dt = d^2\phi_i/dx^2 \qquad (5.6)$$

This is Fick's differential equation of diffusion for a chemical diffusion coefficient equal to unity and has been derived from a simple consideration of the transition probabilities used in the Monte Carlo method.

If interaction energies are introduced into this analysis, each lattice plane will have a mean energy $E_i=a\phi_i$ where a is the activity of the solvent. Transitions down the concentration gradient will therefore occur with a probability independent of this energy, whereas transitions against the concentration gradient will occur with an additional probability based on Boltzmann statistics and the energy difference between the two planes, $p(i \rightarrow i') \sim \exp[-(E_{i'} - E_i)]$. In addition to this, transitions in the dynamic Monte Carlo method occur with a probability proportional to the energy in each lattice plane, $p(i \rightarrow i') \sim \exp[-E_i]$, which previously was assumed to be equal to unity in all planes. This situation is illustrated in figure (5.4).

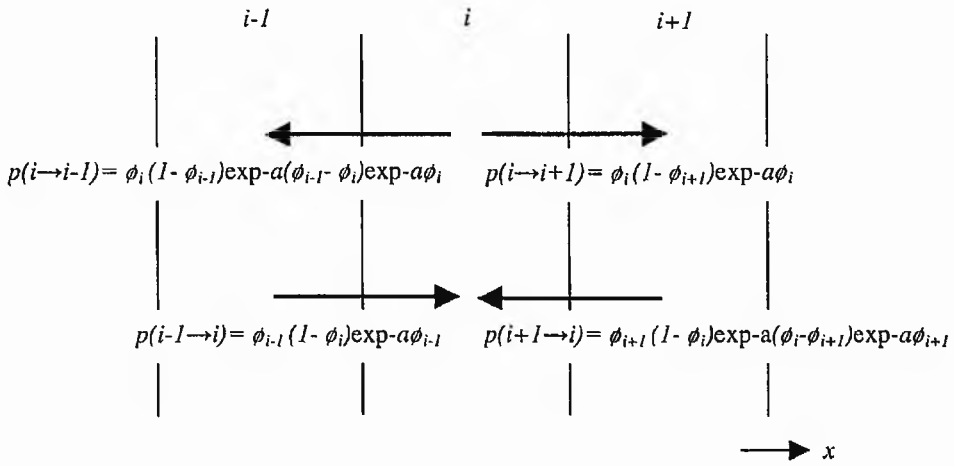

Figure (5.4): Schematic illustration of a system consisting of three lattice planes giving the transition probabilities for particle motions into, and out of, plane *I* with additional probabilities depending on the interaction energies of the system.

Therefore, in this case the rate of change of solvent volume fraction is given by;

$$\begin{aligned} d\phi_i/dt = {} & \phi_{i-1}(1-\phi_i)\exp\text{-}a\phi_{i-1} \\ & + \phi_{i+1}(1-\phi_i)\exp\text{-}a(\phi_i-\phi_{i+1})\exp\text{-}a\phi_{i+1} \\ & - \phi_i(1-\phi_{i-1})\exp\text{-}a(\phi_{i-1}-\phi_i)\exp\text{-}a\phi_i \\ & - \phi_i(1-\phi_{i+1})\exp\text{-}a\phi_i \end{aligned} \qquad (5.7)$$

Again, this can be reduced, by suitable rearrangement, to give Fick's law of diffusion exactly;

$$d\phi_i/dt = d^2\phi_i/dx^2 \qquad (5.8)$$

Therefore, it is possible that for any dynamic Monte Carlo algorithm where the motion of the solvent is modelled by a simple, instantaneous, hopping process, the diffusion dynamics of the solvent will always be Case I, or Fickian. This provides a suitable explanation of the limited dynamics observed so far in this study and also illustrates that an entirely different approach is required if a Monte Carlo model is to be used to simulate Case II diffusion.

5.4 Case II Theories of Diffusion

Many efforts have been made to develop mathematical models of Case II diffusion over recent years. Possibly the earliest theory was proposed by Crank (CRANK 1953), where the diffusion coefficient was considered as a time dependent function of local penetrant concentration. In 1969, Frisch (FRISCH 1969) produced a penetration distance that varied linearly with time by introducing into Fick's equations a corrective term, which itself was linear with time. Peterlin (PETERLIN 1979) proposed that the steep solvent profile was a consequence of a strong dependence of diffusion coefficient on solvent concentration. However, he also noted that the penetration distance of the front must be controlled by a material property of the polymer, possibly the disentanglement of the polymer chains. Astarita and Sarti (ASTARITA 1978) assumed that the velocity of the solvent front was a function of penetrant concentration after some critical concentration had been reached. This arbitrary assumption produced a successful model. Increasingly, it is accepted that the velocity of the solvent front is a consequence of some process of molecular relaxation in the polymer chains (SARTI 1979). Thomas and Windle (THOMAS 1980, 1981, 1982) developed an important model of Case II diffusion where the rate of penetration of the solvent front was due to the time dependent mechanical deformation of the polymer chains in response to thermodynamic swelling. Hui and Wu (HUI 1987a/b) gave analytic solutions of this model in the strong Case II limit and more recent advances were proposed by Wu et al. in 1993 (WU 1993a/b).

5.4.1 The Crank Model

In 1953, Crank (CRANK 1953) wrote a paper on the influence of molecular relaxation on diffusion in polymers. This was possibly the first theory of Case II diffusion based on the idea of polymer relaxation as a rate controlling process. In fact, at the time this paper was written Case II diffusion was yet to be defined, but experimental evidence for anomalous diffusion did exist. Crank proposed a model to relate the solvent diffusion coefficient to slow structural changes in the polymer.

When a penetrant diffuses into a polymer, the polymer chains must take up a new configuration in order to accommodate the solvent molecules. Crank suggested that the polymer motion consisted of an instantaneous component and a relatively slow component compared with the diffusion of the solvent. Therefore, the diffusion coefficient of the solvent will also change with an instantaneous part and a slow part. The instantaneous component of the diffusion coefficient will accompany a change in solvent concentration. The slowly changing component of the diffusion coefficient represents a drift towards an equilibrium value that takes place even when the solvent concentration is not changing. It is this slow drift towards an equilibrium value of the solvent diffusion coefficient that depends on the finite relaxation rate of the polymer chains.

Crank assumed that these two components proceed independently of each other, so that the total change in the diffusion coefficient of the solvent can be written as the sum of these two parts;

$$\partial D/\partial t = (\partial D_i/\partial C)\,(\partial C/\partial t) + \alpha(D_e - D) \qquad (5.9)$$

In this equation, D_i is the instantaneous component of the diffusion coefficient, which is a function of solvent concentration only. The equilibrium diffusion coefficient is denoted by D_e and α is the rate parameter controlling the approach to equilibrium. These three parameters are also assumed to be exponentially increasing functions of solvent concentration. The essential part of this theory is that there is an equilibrium configuration of polymer chains to which there is a corresponding equilibrium value of the diffusion coefficient. In general, this equilibrium value will depend on the solvent concentration, and the diffusion coefficient in any element of the polymer will never attain its equilibrium value for a particular concentration but will get closer to it the longer the concentration remains at a given value. Therefore, the diffusion coefficient in a given element of the polymer depends not only on the concentration there, but also on the time taken by the element to reach that concentration. This implies a diffusion coefficient that depends on the previous history of the diffusion process.

Crank coupled equation (5.9) with Fick's differential equation of diffusion to define a set of equations that describe the solvent diffusion into the polymer and the finite relaxation rate of the polymer molecules. It is not possible to derive exact mathematical solutions for a variable diffusion coefficient of this kind, so Crank employed finite difference methods to obtain numerical solutions. However, general features of this model can be deduced without detailed calculation. At low solvent concentrations where α is very small, $D=D_i$ and the diffusion coefficient is purely concentration dependent. At high concentrations where α is very large, D effectively always has its equilibrium value, $D=D_e$, and the diffusion process is again concentration dependent. Intermediate values of α show time dependent effects. Although Crank was unable to calculate the form of the ingressing solvent profile, he does relate these diffusion coefficients to a sharp discontinuity in the diffusion process suggesting the development of the steep solvent profiles characteristic of Case II diffusion. If α increases very rapidly above some critical concentration, the change from D_i to D_e may occur over a relatively small concentration range. This produces a discontinuous change in the diffusion coefficient and a moving boundary between the dry and swollen polymer.

In 1983, Cohen (COHEN 1983, 1984) developed Crank's theory further to produce a more general mathematical formalism. In this theory the diffusion coefficient is written as an integral equation;

$$D(C,t) = \int_0^t K(t,s,C(x,s))\, f(C(x,s),\partial C(x,s)/\partial t)\, dt \qquad (5.10)$$

The integration of this equation means that the diffusion coefficient at a time t depends on the history of the process prior to this time where the kernel $K(t,s,C)$ represents the history dependence inherent in the polymer relaxation process and $f(C,\partial C/\partial t)$ is a concentration dependent function. The instantaneous response of a rubbery polymer can also be modelled by this equation if the integration kernel is taken as a Dirac delta function. Cohen also showed that Crank's equation was a special case of this more general formalism. With both this model and Crank's

model, numerical solutions can be obtained using finite difference methods. However, problems arise when using this method to solve a discontinuous function. In order to produce an accurate solution the spatial and temporal increments must be made quite small, and this limits the range of dimensions over which a solution can be obtained by a computer simulation.

5.4.2 The Thomas and Windle Model

Thomas and Windle (THOMAS 1980, 1981, 1982) proposed a theory for Case II diffusion where the rate controlling process is the mechanical viscous resistance of the polymer to increase in volume and change shape. The thermodynamic relationship between the solvent concentration ϕ, pressure P and activity a in the swollen polymer is considered in terms of the chemical potential μ, based on the previous work of Flory (FLORY 1953). As the solvent molecules diffuse into the polymer the chemical potential changes due to the thermodynamic interactions between the polymer and solvent molecules. However, the low mobility of chains in a polymer glass creates a resistance to swelling due to the solvent ingress. Thus, the solvent molecules experience an additional osmotic pressure P that also affects the chemical potential. The swelling kinetics depend on the viscous response of the polymer chains to this internal pressure. It is assumed that the increase in volume of the polymer due to swelling is proportional to the volume of solvent absorbed. Furthermore, it is assumed that the viscosity η of the polymer decreases exponentially with increasing solvent concentration as the polymer chains become more mobile. From this an equation is derived for the rate of swelling of the polymer, based on a linear viscous relationship for the viscoelastic response of the polymer;

$$\partial\phi/\partial t = P/\eta \qquad (5.11)$$

The flux of penetrant $F(x,t)$ is obtained from the restatement of Fick's First Law where ϕ_e is the local equilibrium value of the solvent volume fraction;

$$F(x,t) = - D(\phi)\,(\phi/\phi_e)\,\partial\phi_e / \partial x \qquad (5.12)$$

Furthermore, conservation of penetrant implies that;

$$\partial\phi/\partial t + \partial F(x,t)/\partial x = 0 \qquad (5.13)$$

Combining equations (5.12) and (5.13) gives;

$$\partial\phi/\partial t = \partial/\partial x[D(\phi)\ (\phi/\phi_e)\ \partial\phi_e/\partial x] \qquad (5.14)$$

Thus, equations (5.11) and (5.14) define two coupled differential that may be solved for the solvent concentration by finite difference methods assuming that ϕ_e is a state function of ϕ (HUI 1987b). The two equations given by Thomas and Windle represent the increase in solvent concentration due to concentration dependent diffusion, and the swelling of the polymer. They consider these to be the two main processes occurring during the ingress of solvent molecules into a polymer glass. Numerical solutions of these equations produced steep solvent profiles with linear kinetics as expected for Case II diffusion dynamics and this model is still regarded as one of the foremost descriptions of Case II diffusion.

However, this model is far from ideal. Numerical solutions of the coupled, non - linear equations can be highly unstable, with exponential terms diverging rapidly under particular conditions. More importantly, the solvent front progression has been found to scale with the spatial step size used in the model (LANE 1998). For a doubling of the spatial step size, the solvent front scaled by a factor of $1/\sqrt{2}$. These problems again relate to the integration of discontinuous functions and are therefore only serious in the true Case II limit where the solvent profiles are very steep. Fu and Durning (FU 1993) have studied these problems extensively and suggest methods to avoid these problems in the Thomas and Windle model. Further extensions of this model have been considered by Hui et al. in terms of swelling (HUI 1987a) and solvent front formation (HUI 1987b), where the Thomas and Windle model was reduced to a single non - linear differential equation.

5.4.3 The Wu and Peppas Model

Wu and Peppas proposed a model of Case II diffusion (WU 1993a/b, PEPPAS 1994) based on polymer dissolution through the process of polymer chain disentanglement. They began by solving Fick's differential equation of diffusion for a concentration dependent diffusion coefficient, but included a second differential term based on the thermodynamic swelling of the polymer in response to the ingressing solvent. As the increasing solvent concentration in the polymer reaches some critical value ϕ_g, at a time t_1, the polymer undergoes a transition from a glass to a rubber. In this latter state the polymer chains begin to disentangle and diffuse according to the reptation model (DE GENNES 1971). The polymer chains diffuse out of the effective tubes that confine them and become more mobile. Wu and Peppas assume that the characteristic dissolution time of this process is equal to the renewal time τ_t described in section (2.2.4). Thus, after this renewal time the polymer chains have disengaged from the tubes confining them and, at a time t_2, the polymer has dissolved. This renewal time is effectively the delay in the response of the polymer chains to the solvent concentration reaching the critical concentration ϕ_g for the polymer glass to become a rubber. The solvent volume fraction reaches ϕ_g at a time t_1, whereas the polymer has dissolved after a time t_2. Thus this model again introduces a relaxation process that depends on the previous history of the system. As different elements in the polymer reach the critical solvent concentration at different times, the dissolution process begins at different times with distance through the polymer. Therefore, a moving boundary is generated between the entangled chains of the polymer glass and the unentangled chains of the polymer rubber. However, a large number of assumptions are made to relate these characteristic times to the diffusion coefficient of the solvent. Furthermore, finite difference methods are used to solve the equations proposed by Wu and Peppas, which suffer from the same problems previously encountered. Devotta used similar ideas to Wu and Peppas to model the dissolution of the polymer chains in a rubbery polymer (DEVOTTA 1994) and in the presence of a mixed solvent (DEVOTTA 1996) consisting of two different components.

5.5 Conclusions

The ingress of solvent into a polymer relies on the coupled processes of solvent diffusion and polymer relaxation. In a rubbery polymer the polymer relaxation process is very rapid compared to the solvent diffusion and Case I, or Fickian, dynamics are seen. In a polymer glass the polymer chains are relatively immobile and the relaxation process is very slow compared to the solvent diffusion. Under these conditions Case II diffusion is observed. It is clear that these two processes are decoupled in the current "Simple" Monte Carlo model and that the solvent diffusion produces no significant change in the dynamics of the polymer. Efforts to change this situation produced no significant differences and it is proposed that this is due to a fundamental limitation of Monte Carlo models based on simple, instantaneous, hopping motions. Current theoretical models have successfully coupled the solvent and polymer dynamics, but all result in non - linear differential equations that must be solved numerically by finite difference methods. However, the application of this method to a discontinuous function, such as a steep and sudden change in the solvent profile, can produce an unstable solution. Therefore, it would be desirable to construct a numerical method that could model the coupled processes of solvent diffusion and polymer relaxation, whilst avoiding the computational problems faced by current models of Case II diffusion.

Chapter 6

Monte Carlo Modelling of History Dependent Diffusion

6.1 Introduction

The history dependent diffusion of solvent into polymer was first proposed by Crank (CRANK 1953, 1975) and has been introduced in the previous chapter. In this model the diffusion process consists of two components, one that varies instantaneously due to the ingressing solvent, and one that continues to vary slowly due to the finite relaxation time of the polymer chains. Thus, the diffusion of the solvent molecules depends on some previous state of the system and is history dependent. Since then, many successful models of Case II diffusion have relied on the coupled processes of solvent diffusion and polymer relaxation (e.g. THOMAS 1981, PEPPAS 1994). In all of these models, the rate limiting process is the viscoelastic response of the polymer (CODY 1994). However, solutions of these models have encountered many problems due to the methods employed.

The "Simple" Monte Carlo model of solvent diffusion presented in Chapter 3 is now reconsidered. This model of solvent ingress into polymer was successful only at modelling Case I diffusion due to the processes of solvent diffusion and polymer relaxation being decoupled and entirely independent. Furthermore, the simple hopping mechanisms used to model the solvent and polymer motions depend only upon the current state of the system and show no history dependence. Therefore, the aim of this chapter is to demonstrate an entirely new Monte Carlo

method that incorporates the concept of history dependent diffusion and couples together the processes of solvent diffusion and polymer relaxation. It is hoped that this will establish a new method for the modelling of Case II diffusion that will avoid many of the problems encountered previously. In this chapter, the principles of history dependent diffusion are described before explaining the adaptations that are necessary to include them in the Monte Carlo method. The results of this "History Dependent" Monte Carlo model are then studied in a number of important areas.

6.2 Theory of History Dependent Diffusion

The model of history dependent diffusion described here is a development of the Crank model (CRANK 1953). Crank's model used two coupled differential equations, describing the ingress of the solvent and the rate of change of the solvent diffusion coefficient due to the relaxation of the polymer respectively;

$$\partial\phi/\partial t = \partial/\partial x \, (D(\phi) \, \partial\phi/\partial x) \qquad (6.1)$$

$$\partial D/\partial t = (\partial D_i/\partial \phi) \, (\partial\phi/\partial t) + \alpha(D_e - D) \qquad (6.2)$$

where,

$$D_i = D_0 \exp(a\phi) \qquad (6.3)$$

$$D_e = D_0 \exp(b\phi) \qquad (6.4)$$

$$\alpha = \alpha_0 \exp(c\phi) \qquad (6.5)$$

Equation (6.1) is Fick's Second Law for the diffusion of the solvent molecules. Equation (6.2) describes the rate of change of the solvent diffusion coefficient, which varies with an instantaneous part D_i and a part that drifts continuously towards an equilibrium value of the diffusion coefficient D_e. The slowly changing part of the diffusion coefficient is controlled by a relaxation rate α. Crank assumed that these three quantities increased exponentially with solvent volume fraction, given by equations (6.3), (6.4), (6.5), where D_0, α_0, a, b, and c are constants.

In the "Simple" Monte Carlo model of solvent diffusion described in Chapter 3, only the instantaneous part of this theory has been modelled and the second term on the right hand side of equation (6.2) has effectively been neglected. In this case, with a constant value of $\alpha=0$, Crank's coupled equations reduce to Fick's law and hence only Case I, or Fickian, dynamics are observed. This is confirmed by previous simulations. Thus, it is necessary to modify the Monte Carlo method by introducing a component that changes slowly with time toward some equilibrium state of the system.

Crank has used the solvent diffusion coefficient in this theory to describe the rate of ingress of the solvent molecules. In the Monte Carlo model the analogous quantity is the process rate of solvent diffusion r_s described in chapter (3). Thus, it is assumed that r_s approaches some equilibrium rate r_e by a first order process governed by a relaxation time τ;

$$\partial r_s/\partial t = -(r_s - r_e)/\tau \qquad (6.6)$$

Furthermore, it is also assumed that r_e and τ are both functions of the solvent volume fraction. To produce Case II dynamics it is assumed that the polymer is initially in a glassy state (CODY 1994), where r_e is low and the polymer chains are relatively immobile. The equilibrium solvent rate is expected to increase with increasing solvent volume fraction due to the greater mobility of the polymer chains as the polymer undergoes a transition to a rubbery state. Similarly, the relaxation time is expected to decrease as the solvent volume fraction increases (COHEN 1993/1994). The exact form of these functions will be considered later in this chapter, but for now, exponential functions are assumed for r_e and τ similar to those defined by Crank, where A and B are constants;

$$r_e = r_0 \exp(A\phi) \qquad (6.7)$$

$$\tau = \tau_0 \exp(-B\phi) \qquad (6.8)$$

In its initial state, the given system will have a process rate r_s equal to the equilibrium process rate for the solvent defined by equation (6.7) and a relaxation time defined by equation (6.8). As time progresses and solvent molecules diffuse into the system, the equilibrium process rate will increase and the relaxation time will decrease. However, the solvent process rate will no longer vary instantaneously in response to this new state of the system. Instead, the actual solvent process rate r_s will attempt to attain the new equilibrium process rate according to equation (6.6). This is realised according to the solution of equation (6.6);

$$\int_{r_{s1}}^{r_{s2}} \partial r_s'/(r_s - r_e) = \int_0^{\Delta t} - \partial t'/\tau \qquad (6.9)$$

$$r_{s2} = r_e + (r_{s1} - r_e)\exp(-\Delta t / \tau) \qquad (6.10)$$

Thus, an initial value of the solvent process rate r_{s1} will attain a new value r_{s2} in a time Δt following a change of the equilibrium solvent rate in response to the changing solvent volume fraction. This process is illustrated below, where r_s will attain its equilibrium value as time approaches infinity provided the state of the system undergoes no further changes.

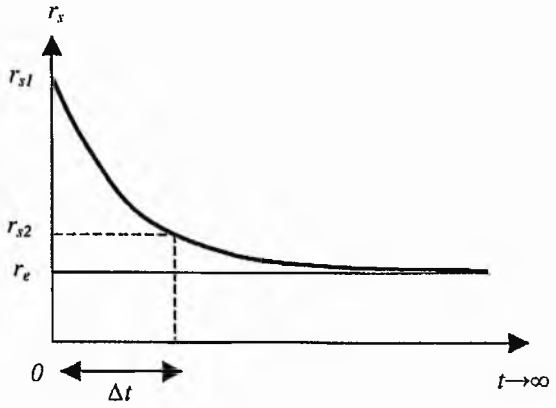

Figure (6.1): A schematic illustration of the relaxation of the solvent process rate r_s toward an equilibrium solvent rate r_e with time t. The solvent process rate attains a value r_{s2} in a time Δt.

Thus, through this process, the solvent rate is continually trying to attain an equilibrium value set by some previous state of the system. This occurs regardless of whether the solvent volume fraction continues to change. The rate at which this process occurs is controlled by the relaxation time τ. It is through this relaxation time that the viscoelastic relaxation of the polymer molecules is modelled. If τ is very long then the solvent process rate will take a long time to attain its equilibrium value, corresponding to a glassy polymer where the polymer chains are slow to relax. If τ is very short then the solvent process rate will rapidly reach its equilibrium value, corresponding to a rubbery polymer where the polymer chains relax quickly in response to the ingressing solvent molecules.

6.3 Adaptation of the Monte Carlo Model

To implement this history dependent diffusion process in the Monte Carlo method requires an important development of the dynamic Monte Carlo method described in Chapter 3. In that chapter the dynamic Monte Carlo method was described in terms of a rate line comprising the sum of the transition rates for the individual processes occurring within the system. In that case the transition rates were global rates for the whole system. The transition rate of a solvent molecule occupying a lattice site in a plane at $x=0$ was the same as a solvent molecule in a plane at $x=\infty$.

In this new dynamic Monte Carlo method it is now necessary to define the transition rates of the individual processes within each plane of the system. Thus, the transition rate of a particular process will vary with distance in the x direction through the lattice. The four process rates r_s, r_e, r_b, r_c, previously defined are now defined as $r_{s,x}$, $r_{e,x}$, $r_{b,x}$, $r_{c,x}$ where x refers to a particular plane of the lattice. The transition rate $R_{p,x}$ for a particular process p is then this process rate $r_{p,x}$ multiplied by the number of particles $N_{p,x}$ corresponding to that process in a plane x. The revised total rate line R, used to select an attempted move in the dynamic Monte Carlo algorithm, is illustrated below.

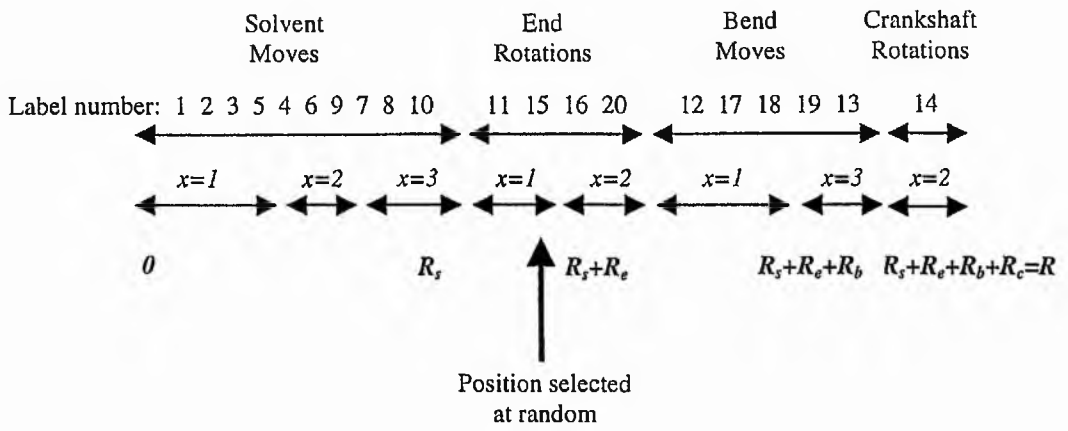

Figure (6.2): An illustration of the new selection method for an attempted move from a transition rate line where the process rate is defined for each individual process in each plane of the system.

Following the random selection of a particle along this rate line, a revised search algorithm is used to determine the type of process that may occur and the plane that it occurs in. From this, the corresponding process rate $r_{p,x}$ can be read for that particular particle in plane x. Once a particle move has successfully been completed, the equilibrium rates and relaxation times corresponding to the lattice planes involved in that process are updated. Equations (6.7) and (6.8) are used to calculate the new values of r and τ corresponding to the new state of the system. After every time increment of the system, equation (6.10) is used to calculate the new values of the actual process rates for every plane in the system, regardless of whether the system has undergone a change of configuration. The operation of the computer program for this "History Dependent" Monte Carlo model is illustrated in the appendix, figure (A.2).

6.4 Results of the "History Dependent" Monte Carlo Model

The Monte Carlo model has been adapted to incorporate this method of history dependent diffusion. However, it is now necessary to examine the operation of this model under a range of conditions to determine the extent to which the "History Dependent" Monte Carlo model is successful. It is particularly important to

discover which parameters produce Case II diffusion and whether Case I diffusion can still be simulated as a limiting case of this new method.

6.4.1 Solvent Front Dependence

The most important parameters in this model are those that determine the equilibrium process rate r_e and the relaxation time τ corresponding to the solvent volume fraction ϕ_s in each plane of the system. In the description of this method given previously, it was assumed that the functions describing r_e and τ were continuous exponential functions of ϕ_s similar to those described by Crank (CRANK 1953); equations (6.7) and (6.8). The form of these functions is now examined in more detail to determine their effects on the system and the conditions necessary to produce Case II diffusion. In the results that follow, no polymer chains are present in the system. The effect of the finite relaxation time of the polymer on the solvent diffusion is modelled entirely through the parameter τ.

If the functions for r_e and τ were constant with ϕ_s, then with increasing solvent volume fraction there would be no change in r_e and the actual process rates would remain unchanged with increasing solvent volume fraction and time. This is the situation that occurred in the previous Monte Carlo model and hence only Case I, or Fickian, diffusion is observed. To model Case II diffusion it is first assumed that both r_e and τ change discontinuously at a critical value of the solvent volume fraction ϕ_g corresponding to the solvent volume fraction at which the polymer glass begins its transition to a rubbery polymer. Therefore, four parameters are defined for the equilibrium process rates and the relaxation times in both the polymer glass and the rubbery polymer: r_g, τ_g, r_r, τ_r respectively. As the solvent volume fraction increases beyond ϕ_g the equilibrium process rate is assumed to increase suddenly as the process rate in a rubbery polymer will be greater with increased mobility. Similarly, the relaxation time will decrease suddenly as the relaxation time becomes shorter. This situation is illustrated in figure (6.3a) where ϕ_g=*0.1*. The resulting solvent volume fraction profiles are shown in figure (6.3b) for ten equal time increments. Whilst these solvent profiles do not display the sharp fronts characteristic of Case II diffusion, their progression with time has become anomalous with a t^n exponent of

$n=0.85 \pm 0.04$. The position of the solvent front is measured at a point of constant volume fraction close to the leading edge of the profile.

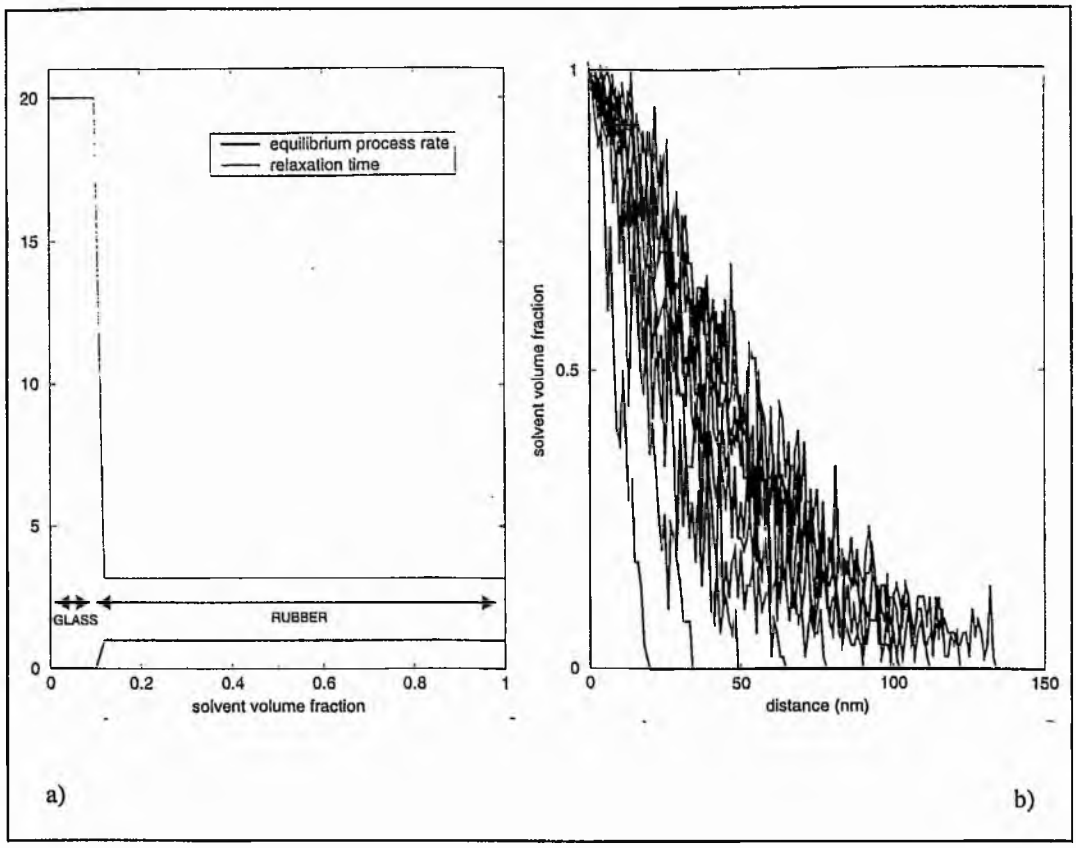

Figure (6.3): a) Illustration of discontinuous functions for the equilibrium process rate and relaxation time showing the glassy and rubbery regions where the discontinuity occurs at the critical solvent volume fraction $\phi_g=0.1$, b) The resulting solvent profiles shown at ten equal time intervals obtained from the "History Dependent" Monte Carlo simulation.

It is then assumed that the equilibrium process rate continues to increase exponentially above the critical solvent volume fraction whilst the function for the relaxation time remains unchanged. This is illustrated in figure (6.4a). The effect of this change is shown in figure (6.4b). Once the solvent volume fraction reaches ϕ_g the equilibrium process rate increases exponentially with solvent volume fraction and the actual process rate quickly attains this value due to the short relaxation time. Therefore, the ingress of solvent into planes that have reached ϕ_g increases with ϕ_s and is much greater than the diffusion of solvent into planes ahead of the solvent front. Thus, the solvent volume fraction increases behind the solvent front and the

profiles become sharper and more characteristic of Case II diffusion. In this case the value of the exponent n is $n=0.87 \pm 0.05$.

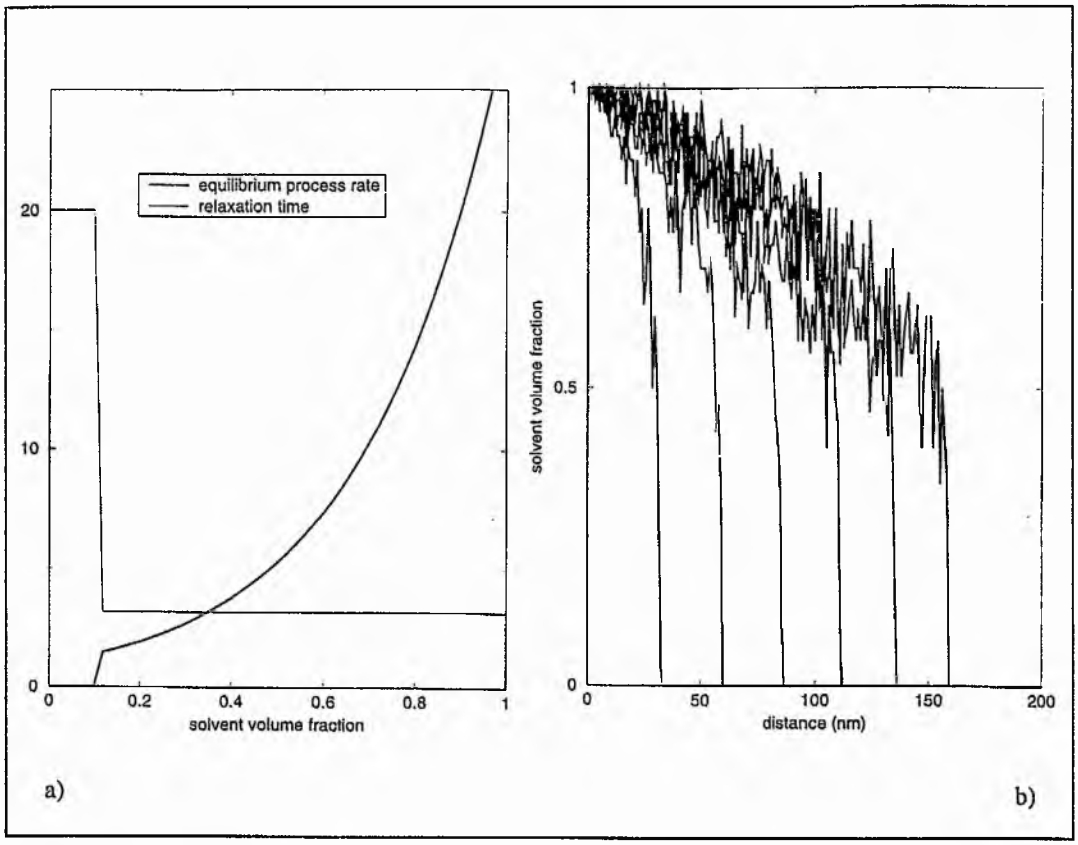

Figure (6.4): a) Illustration of discontinuous functions for the equilibrium process rate and relaxation time where the equilibrium process rate increases exponentially above $\phi_g=0.1$, b) The resulting solvent profiles shown at six equal time intervals.

It was found that the equilibrium process rate must increase quite substantially above ϕ_g to produce solvent profiles that approach those of Case II diffusion dynamics. Then the discontinuous step function at $\phi_s=\phi_g$ becomes insignificant compared to the exponential function above ϕ_g. Therefore, the step function is neglected and the equilibrium rate can be defined by a single continuous exponential function;

$$r_e = r_g \exp\left[(\phi_s - \phi_g)/A\right] \qquad (6.11)$$

In this equation, r_g is the initial process rate in the glass where $\phi_s=0$, and A is a constant. This is illustrated in figure (6.5a), with the results shown in figure (6.5b). Here, the solvent front proceeds still with an exponent of $n=0.87 \pm 0.04$, but the solvent profiles are now very steep and characteristic of Case II diffusion.

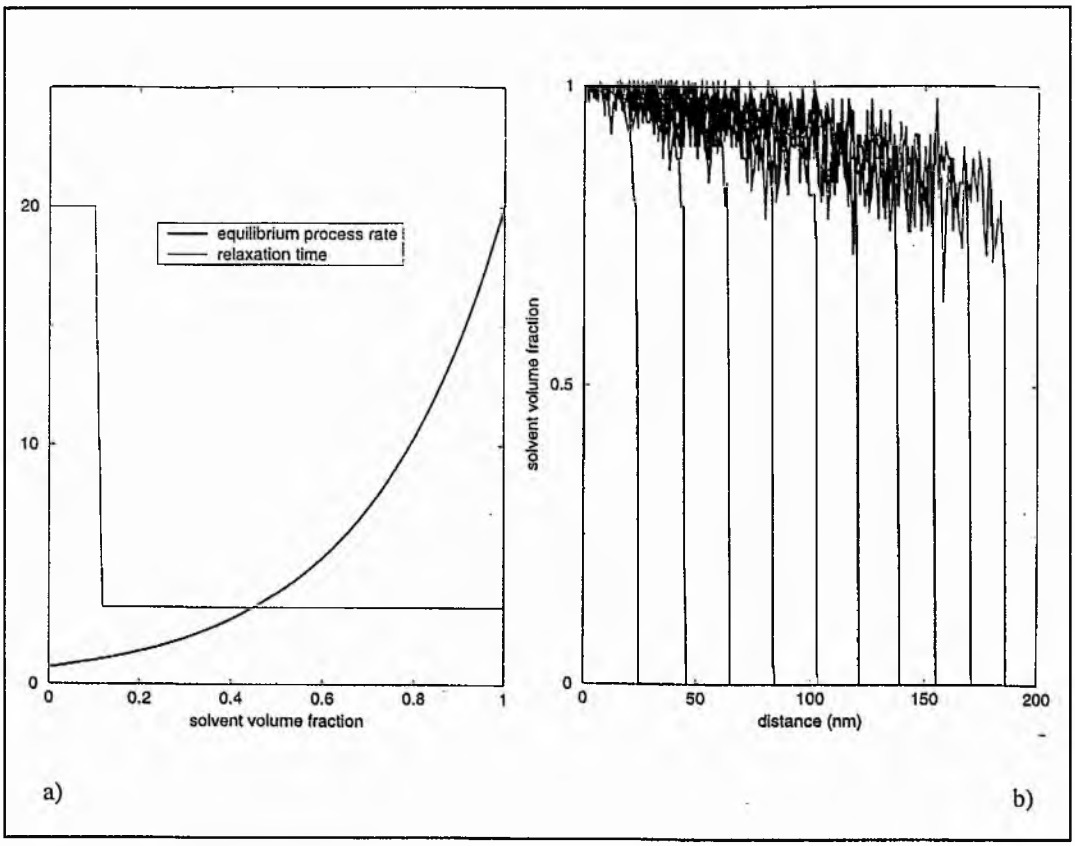

Figure (6.5): a) Illustration of the functions for the equilibrium process rate and relaxation time where the equilibrium process rate is now a continuous exponential function, b) The resulting solvent profiles shown at ten equal time intervals.

Finally, the form of the function for the relaxation time is considered. This must be a decreasing function of the solvent volume fraction. Since the value of the relaxation time τ_g is very long in the polymer glass, $\phi_s < \phi_g$, the system is insensitive to this value providing the polymer chains are essentially frozen at this solvent volume fraction. Therefore, this value of τ_g is set equal to infinity. Above the critical volume fraction ϕ_g the Williams, Landel, Ferry (WLF) equation (WILLIAMS 1955) is used to model the discontinuity in the relaxation time;

$$\tau = \tau_r \exp\,[B/(\phi_s - \phi_g)] \qquad (6.12)$$

Here, τ_r is the relaxation rate in the polymer rubber where $\phi_s=1.0$, and B is a constant. This function is illustrated in figure (6.6a) and the results of this simulation are shown in figure (6.6b). In this final figure of this series the solvent profiles are characteristic of Case II diffusion and progress with an exponent of $n=0.88 \pm 0.05$. Whilst this progression is still not linear, $n=1.0$, this model has clearly produced diffusion dynamics that are non-Fickian and are a definite departure from the Fickian dynamics produced by the previous Monte Carlo model.

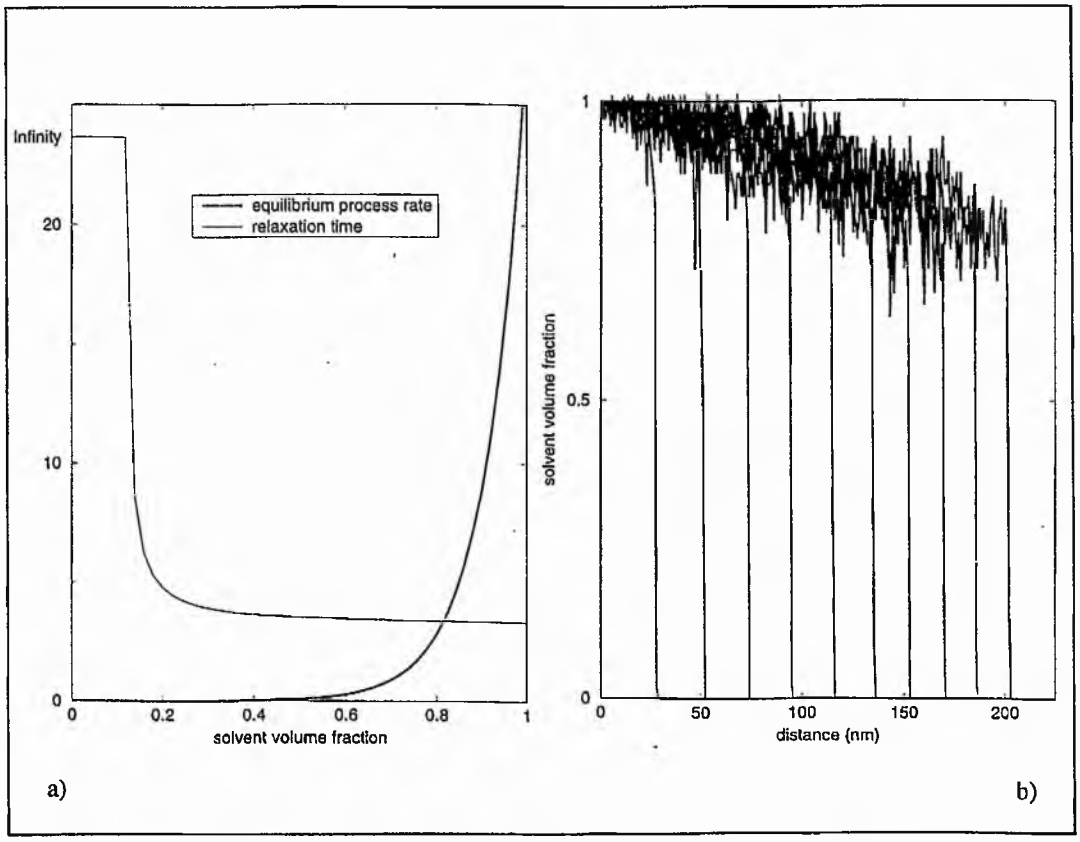

Figure (6.6): a) Illustration of the functions for the equilibrium process rate and relaxation time where the relaxation time is now equal to infinity below $\phi_g=0.1$ and is modelled by the WLF equation above this critical solvent volume fraction, b) The resulting solvent profiles shown at ten equal time intervals.

This model of history dependent diffusion is based on an equation for the equilibrium solvent process rate, equation (6.11), and an equation for the relaxation time of the polymer, equation (6.12). These two equations are coupled through equation (6.6), which defines the rate of change of the actual process rate. Finally in this section, these two equations are used to study the different types of behaviour that this model can simulate. Primarily, the value of the exponent n is given for a range of parameters to show the conditions under which both limiting cases of solvent diffusion can be observed.

Figure (6.7) shows the dependency of this Monte Carlo model on the solvent process equilibrium rate r_e given by equation (6.11), and on the value of the constant A. In this simulation the initial solvent volume fraction is maintained at a constant $\phi_s=1.0$, with no polymer present in the system. The critical solvent volume fraction remains fixed at $\phi_g=0.05$ with a relaxation time of $\tau=320\ ms$. The equilibrium process rate in the polymer glass r_g was then varied between $10^{-6}\ s^{-1}$ and $10^{-2}\ s^{-1}$ for three different values of the constant A. The exponent n is recorded for each of these values and the results of this are shown as a linear – logarithmic plot in figure (6.7b). This graph shows the dynamics of the diffusion process changing from $n=0.5$ (Case I) to $n=1.0$ (Case II) with increasing r_g. This shows a linear trend on this plot. At small values of r_g, the equilibrium process rate is relatively slow compared to the relaxation rate of the polymer. In this case, the time between actual solvent moves is quite long and it is possible that the actual process rate is able to quickly approach this equilibrium value and Case I diffusion dynamics are observed. If r_g is high, the equilibrium process rate is fast and the time between actual solvent moves is relatively short. In this case it would be more difficult for the actual process rate to ever attain its equilibrium value and Case II diffusion dynamics are observed. Figure (6.7b) also shows this trend for two other values of the constant A. As A decreases, this trend approaches $n=1.0$ more quickly. This corresponds to the exponential function for r_e, equation (6.11), increasing more rapidly and the equilibrium process rate increasing at lower solvent volume fractions. The three trends appear to converge towards $n=1.0$ at large values of r_g and towards $n=0.5$ at small values of r_g. This is reasonable, as these are the limiting values of the exponent n. Also included in figure (6.7) are two sets of solvent profiles demonstrating typical results for the

two limiting cases of solvent diffusion. Figure (6.7a) demonstrates Case I diffusion for an equilibrium process rate of $r_g=10^{-6}\ s^{-1}$ where $n=0.5 \pm 0.05$, and figure (6.7c) demonstrates Case II diffusion for $r_g=10^{-2}\ s^{-1}$ where $n=1.0 \pm 0.06$.

Figure (6.8) shows the dependency of this Monte Carlo model on polymer relaxation time τ given by equation (6.12), and on the value of the constant B. The critical solvent volume fraction remains fixed at $\phi_g=0.05$ with the equilibrium process rate r_g now having a constant value of $10^{-3}\ s^{-1}$. The relaxation time in the polymer rubber τ_r was then varied between *0 ms* and *1500 ms* for three different values of the constant B. The exponent n is recorded for each of these values and the results of this are shown in figure (6.8b). This graph shows the dynamics of the diffusion process changing from $n=0.5$ to $n=1.0$ with increasing τ_r. This displays and exponential trend, with the exponent n approaching unity with increasing τ_r. As the relaxation time in the rubbery polymer becomes longer, the actual solvent process rate takes more time to approach its equilibrium value and Case II dynamics are observed. If the relaxation time is shorter, the actual solvent process rate will approach its equilibrium value more quickly and Case I dynamics are observed. Figure (6.8b) also shows this trend for two other values of the constant B. As B increases, the exponent n approaches unity more quickly, corresponding to the relaxation time decreasing more slowly with increasing solvent volume fraction. Therefore, the relaxation time is greater at lower volume fractions and the equilibrium solvent rate is approached more slowly at lower solvent volume fractions. Figure (6.8) again displays two sets of solvent profiles to show the typical results of this simulation at the two extremes of solvent diffusion. Figure (6.8a) shows the case for $\tau_r=1.0$ *ms* where $n=0.5 \pm 0.04$ and figure (6.8c) shows the case for $\tau_r=1500$ *ms* where $n=0.9 \pm 0.05$. Thus, it is possible to demonstrate a complete range of diffusional behaviour based on the relatively simple set of equations defined in this model of history dependent solvent diffusion.

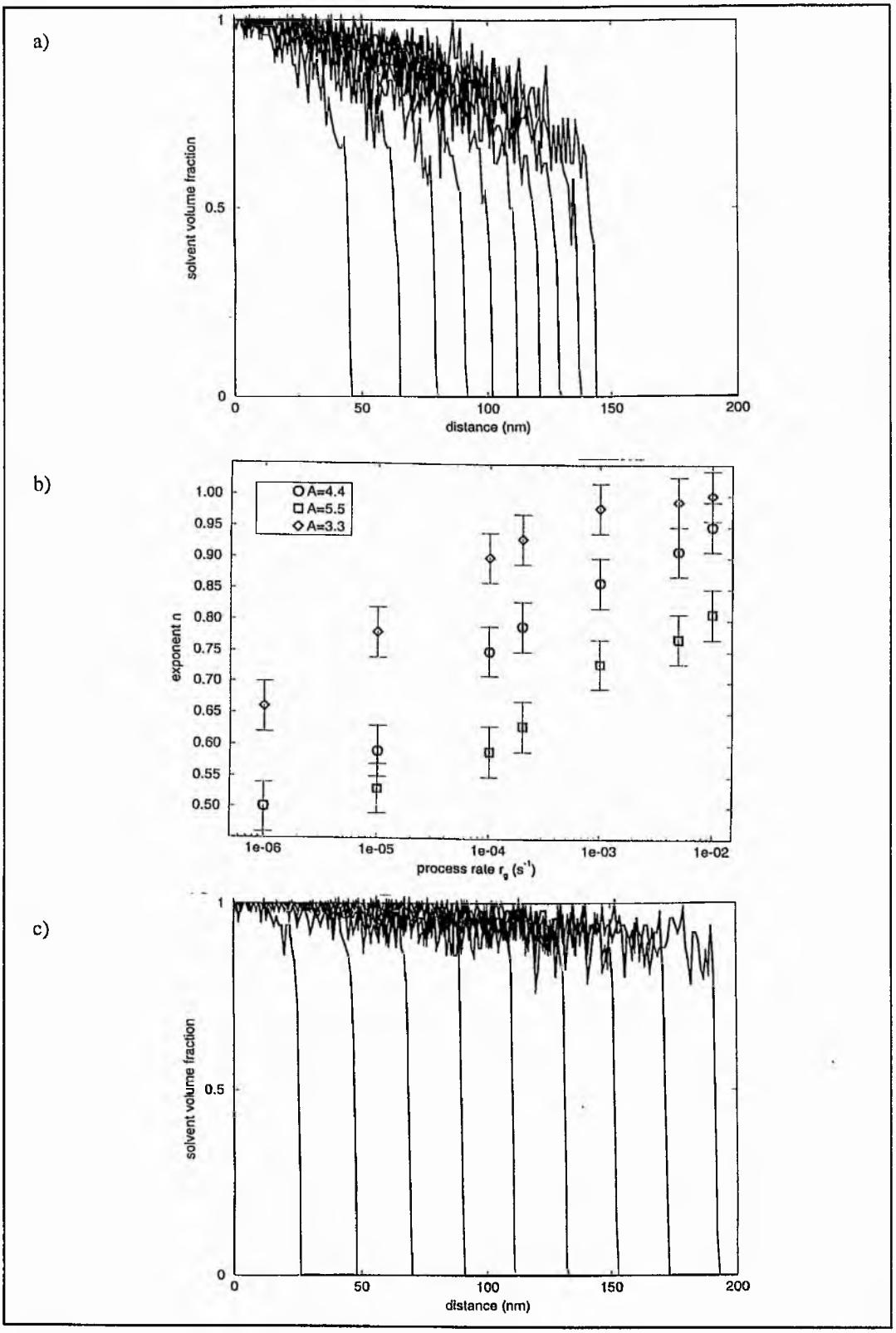

Figure (6.7): a) Case I solvent profiles obtained from the "History Dependent" Monte Carlo model for $r_g=10^{-6}\ s^{-1}$, b) Variation of the exponent n with r_g for three values of the constant A, each exponent obtained from the gradient of a double logarithmic plot of solvent penetration distance against time, c) Case II solvent profiles for $r_g=10^{-2}\ s^{-1}$.

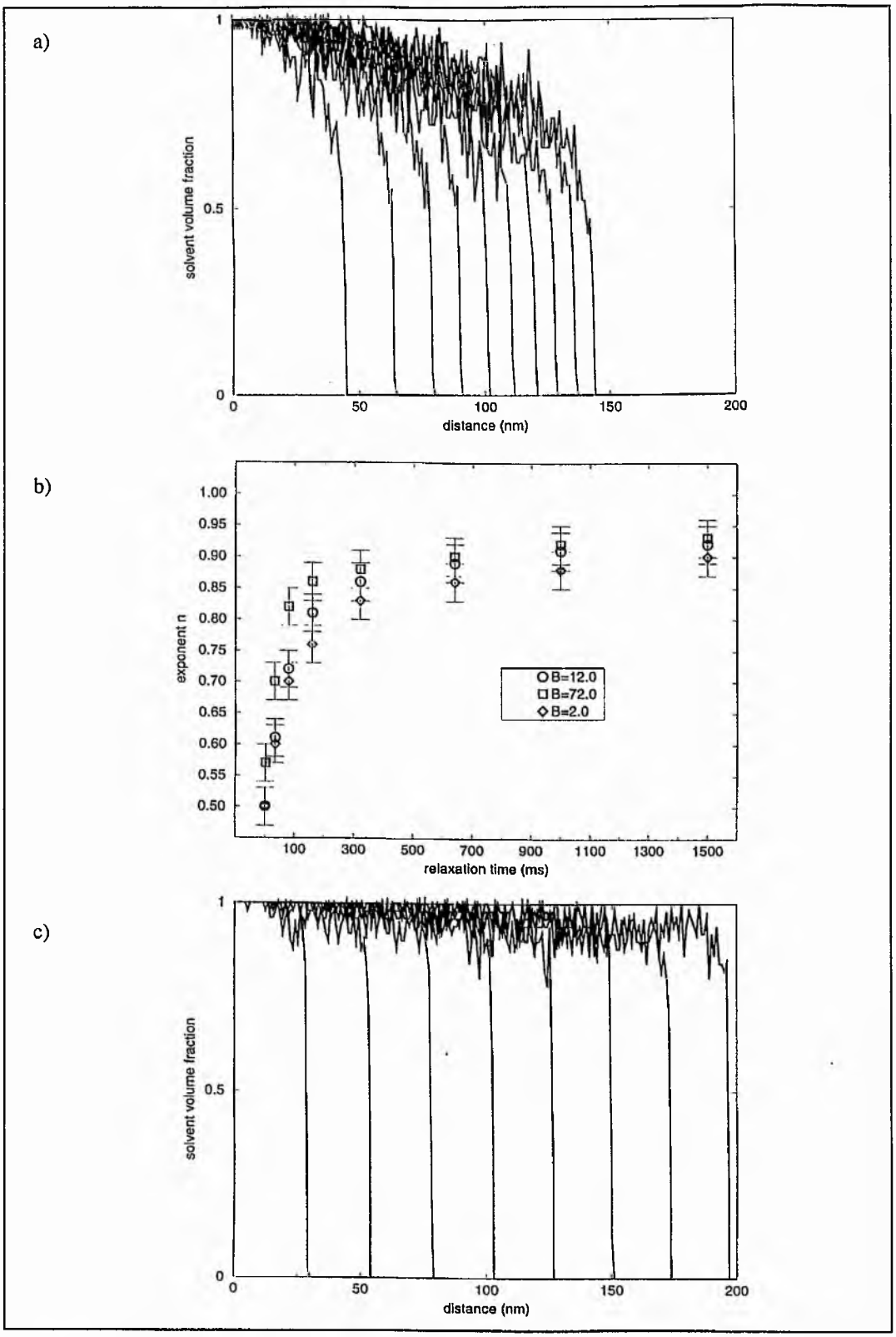

Figure (6.8): a) Case I solvent profiles obtained from the "History Dependent" Monte Carlo model for τ_r=*1.0 ms*, b) Variation of the exponent n with τ_r for three values of the constant B, each exponent obtained from the gradient of a double logarithmic plot of solvent penetration distance against time, c) Case II solvent profiles for τ_r=*1500 ms*.

6.4.2 Velocity Dependence

During the course of the study presented in the previous section, it was noted that the penetration distance of the solvent front varied dramatically with changing parameters, despite a constant simulation time. Therefore, the velocity v of the solvent front must also be a function of the parameters r_g and τ_r discussed in the previous section. The velocity v of the solvent front was deduced from the total penetration distance of the solvent front for a given simulation time assuming that the velocity of the solvent front is constant with time for the strong Case II limit. This velocity was recorded for the parameters r_g and τ_r within the ranges used in the previous section. This is shown in figure (6.9). Figure (6.9a) shows the solvent process rate r_g against v^2 and illustrates that v^2 is proportional to r_g. Figure (6.9b) shows the relaxation time τ_r against v^2 and suggests that v^2 is inversely proportional to τ_r. Thus, it is possible to write;

$$v \propto (r_g/\tau_r)^{1/2} \qquad (6.13)$$

Lasky et al. (LASKY 1988) measured the velocity of an iodohexane Case II solvent front in polystyrene using Rutherford back - scattering spectrometry. They deduced that the velocity dependence of the solvent front could be written as;

$$v \propto (D/\eta_0)^{1/2} \qquad (6.14)$$

where D is the diffusion coefficient of the solvent in the glassy polymer and η_0 is the viscosity of the polymer glass in the absence of penetrant. This relationship can also be deduced from the Thomas and Windle model (LASKY 1988, THOMAS 1982). Therefore, if the parameters used in equation (6.13) can be shown to be analogous to the parameters used by Lasky in equation (6.14), the behaviour of the history dependent Monte Carlo model is consistent with the behaviour of the Thomas and Windle model.

It is straightforward to relate D to r_g. Firstly, both of these quantities are measured where the polymer is in a glassy state and the solvent volume fraction is less than some critical value ϕ_g. Secondly, Bueche (BUECHE 1962) considered a simple three - dimensional model of solvent diffusion and related the diffusion coefficient D of the solvent to the frequency of the solvent "jumps" by;

$$D = rl^2/6 \qquad (6.15)$$

where r is the solvent jump frequency, or rate, and l is the mean jump distance. Therefore, it is reasonable to assume that the diffusion coefficient D is proportional to the solvent process rate r_g.

It is less obvious how to relate η_0 to τ_r, although both are properties of the polymer. Cody and Botto (CODY 1994) discuss solvent diffusion in glassy polymers and state that the diffusion of solvent is governed by the viscoelastic response of the polymer. They write a relaxation rate constant α_r;

$$\alpha_r = K_r/\eta_0 \qquad (6.16)$$

where K_r is the osmotic bulk modulus of the rubbery polymer and η_0 is the viscosity of the bulk polymer. K_r is a quantity proportional to the rate of change of osmotic pressure P with the localised polymer volume fraction ϕ_p in the rubbery polymer. This relaxation rate α_r is the reciprocal of the relaxation time τ_r and thus the relaxation time τ_r is proportional to the polymer viscosity η_0. As the polymer becomes less viscous and polymer mobility is increased, the relaxation time of the polymer will decrease. Therefore, the relaxation time τ_r should be proportional to the polymer viscosity η_0.

Therefore, it is reasonable to conclude that equations (6.13) and (6.14) are consistent and that the Monte Carlo model developed here confirms the behaviour observed by Lasky, predicted by the Thomas and Windle model.

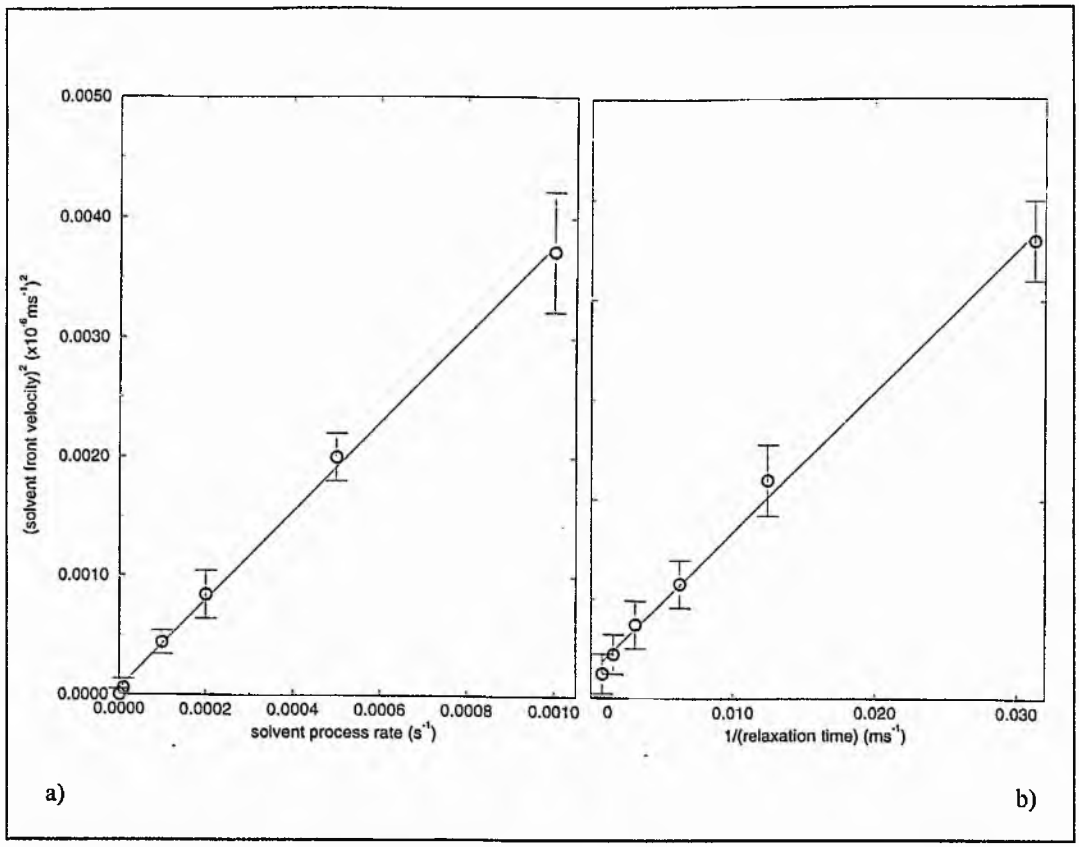

Figure (6.9): The velocity dependence of the solvent front showing the square of the velocity against: a) the solvent process rate r_s and b) the reciprocal of the polymer relaxation time $1/\tau_r$. The solid lines show best fits to the data points.

6.4.3 Comparison With MRI Experiment

It is now useful to compare the results of this Monte Carlo model to experimental data in order to ascertain the reality of the simulation. A system displaying Case II diffusion dynamics that has been extensively studied by MRI methods is the ingress of methanol into polymethylmethacrylate (PMMA). This has been studied by a novel MRI method known as Stray - Field Magnetic Resonance Imaging (STRAFI) by Lane (LANE 1997, 1998) at the University of Surrey. This technique makes use of the large magnetic field gradients that exist in the fringe fields surrounding superconducting magnets. Thin sheets of PMMA were exposed to liquid methanol, and solvent profiles were obtained using the STRAFI technique. Methanol is a poor solvent, and the influence of a good solvent, acetone, on the ingress rate of the methanol was also studied by preparing PMMA samples with

residual amounts of acetone in the polymer. The ingress of the methanol in the PMMA was then monitored as normal in these pre-swollen samples.

Data from these experiments is given in figure (6.10). Figure (6.10a) shows the solvent profiles obtained for methanol ingress into PMMA. Figures (6.10b) and (6.10c) show the methanol profiles for ingress into pre-swollen PMMA samples exposed to *3.3%* and *8%* acetone weight fraction respectively. All data was taken at a temperature of *25°C*. The solid lines shown in figure (6.10) show the fits obtained from the history dependent Monte Carlo model described above. These simulated solvent profiles have been convolved with a Gaussian point spread function as described in section (4.4). In this case, the adjustable parameter used was $\Delta x=24\mu m$ as indicated by Lane (LANE 1998).

The simulated solvent profiles in figure (6.10a) show good agreement with the experimental points and the distance of penetration is reproduced well by the Monte Carlo model. The shape of the experimental solvent profiles is reproduced less well by the Monte Carlo model which fails to show the rounding of the profiles, particularly at long times. In this case the exponent n was found to be $n=0.89 \pm 0.05$ which is close to the linear dependence expected. The parameters used to model this data were as follows: $r_g=1x10^{-4}\ s^{-1}$, $\tau_r=320\ ms$ and $\phi_g=0.05$. The simulated profiles shown in figure (6.10b) were produced with the same parameters but with the time increment between successive profiles increased by a factor of *1.33*. In this case the PMMA was pre-swollen with *3.3%* acetone. No attempt has been made to modify the Monte Carlo model to include the effect of this pre-swelling and the agreement between the simulated solvent profiles and the experimental data is less clear. The situation becomes worse in figure (6.10c) for the case of *8%* acetone pre-swelling. In this case, the best fit was obtained for a reduced relaxation time of $\tau_r=100\ ms$ which produced an exponent of $n=0.61 \pm 0.06$. This perhaps indicates a more mobile polymer with a shorter relaxation time due to the pre-swelling by acetone. Consequently, the diffusion dynamics move toward the Case I limit. However, the simulated solvent profiles fail to reproduce the shape of the experimental solvent profiles.

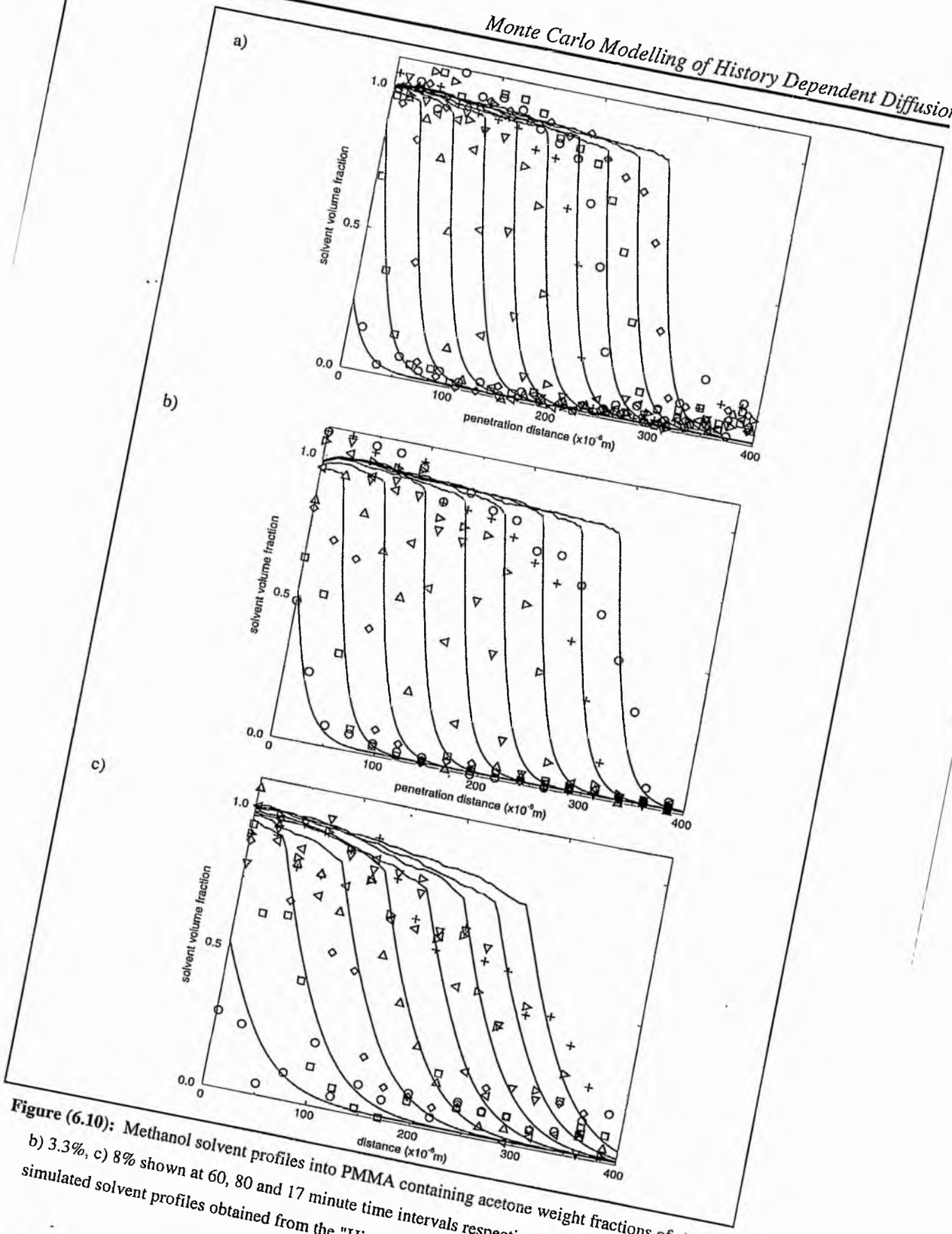

Figure (6.10): Methanol solvent profiles into PMMA containing acetone weight fractions of a) 0%, b) 3.3%, c) 8% shown at 60, 80 and 17 minute time intervals respectively. The solid lines are simulated solvent profiles obtained from the "History Dependent" Monte Carlo model and are described in the text.

6.4.4 Polymer Motion

A particularly novel aspect of the "History Dependent" Monte Carlo model presented here is now introduced. This feature is the model's ability to explicitly simulate both the ingress of the solvent molecules and the motion of the polymer molecules. Previous results presented in this chapter have not explicitly included the polymer component within the lattice. Instead, the effect of the finite polymer relaxation rate on the ingress of the solvent was modelled through the relaxation time τ_r. As a final study of the operation of this new Monte Carlo method, the polymer molecules are explicitly included within the lattice of the model. The method of placement of the polymer chains and their individual motions are unchanged from the original Monte Carlo model presented in Chapter 3. However, the history dependent algorithm described at the start of this chapter now governs the process rates for each type of polymer motion. Therefore, the polymer also has an equilibrium process rate described by equation (6.11), which the polymer chains continually attempt to attain. The approach to this equilibrium is also governed by the relaxation time given by equation (6.12). Therefore, the polymer is initially in a glassy state with the mobility of the polymer chains increasing in response to the increasing solvent volume fraction as the polymer becomes a rubber.

For comparison, figure (6.11) first shows the result of a simulation carried out using this history dependent Monte Carlo model with no polymer present. In this case the simulation has been performed on a larger system than previously to reduce the statistical errors of the result and to yield more detailed information about the solvent profiles. The dimensions of the lattice used were *30x30x30* units with a lattice spacing of $1x10^{-10}$ *m*. The model parameters were chosen from those defined previously with $r_g=0.001\ s^{-1}$, $\tau_r=320\ ms$, $A=0.045$, $B=0.001$, to produce Case II solvent profiles that progress through the lattice linearly with time. This is indeed shown in this simulation, with the sharp solvent fronts that are typical of Case II solvent diffusion and an exponent $n=0.90 \pm 0.05$. Furthermore, in this figure there is now evidence of a Fickian precursor at the leading edge of the solvent front as described by Peterlin (PETERLIN 1965). This is due to Fickian diffusion dynamics

into the glassy polymer ahead of the solvent front, where the solvent volume fraction is less than the critical solvent volume fraction, in this case ϕ_g=*0.1*. Therefore, this appears to be a successful demonstration of Case II dynamics produced by this Monte Carlo model.

In previous numerical simulations of Case II diffusion, problems have arisen through the method of numerical solution as described in Chapter 5. Often finite difference methods have been employed to solve the model equations, but these methods suffer from inaccuracies for discontinuous functions such as the sharp solvent profiles of Case II diffusion. However, these problems are not evident within this Monte Carlo model. Changing the spatial step size, or lattice spacing, of the model simply produces a simulation on a different spatial scale. No changes are seen in the solvent profile shape or its progression with time. This must be a significant advantage of this new method over other simulations of Case II diffusion.

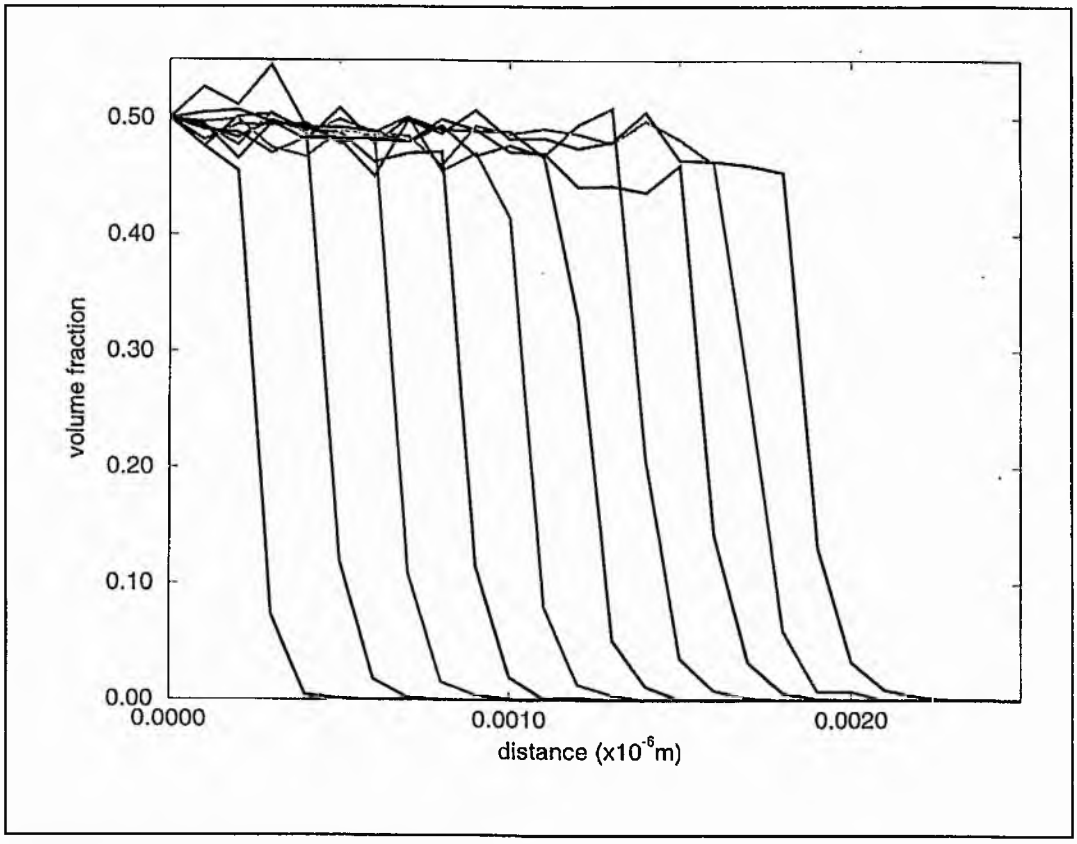

Figure (6.11): Case II diffusion profiles produced by the "History Dependent" Monte Carlo model for ten equal time increments. No polymer chains are present in this case. Fickian precursors are seen at the leading edge of each solvent front.

Figure (6.12) shows the same simulation as figure (6.11) but with an average polymer volume fraction of $\phi_p=0.5$ now placed throughout the lattice, with polymer chains of length $N=20$ lattice units. In figure (6.12a), the solvent profiles show no significant changes due to the effect of the polymer content. A longer simulation time is required to produce the same penetration distances as previously, but this is a computational factor due to the greater numbers of molecules within the system that attempt to move at each time increment. A small decrease is seen in the exponent n, with $n=0.85 \pm 0.05$, which must be due to the presence of the polymer impeding some of the solvent motions. However, it is now possible to observe the microscopic motion of the polymer chains with time as the solvent diffuses through the lattice.

The polymer profile is shown in figure (6.12a) as a thin dark line corresponding to each solvent profile at ten equal time intervals. The polymer chains to the left of each solvent front are in a rubbery state and are highly mobile due to the high volume fraction of solvent in that part of the lattice. With the ingress of solvent molecules polymer motions are, on average, more likely to move away from this ingressing solvent front as the number of free lattice sites in that part of the lattice is reduced. This is illustrated in figure (6.12a), which shows a discontinuity in the polymer volume fraction at the leading edge of the solvent front and an increase in the local polymer volume fraction ahead of the solvent front. To the right of the solvent front the polymer chains are still in their initial glassy state and are relatively immobile. This is also demonstrated by this figure. This local movement of the polymer chains is correct according to the algorithm of this model and demonstrates a discontinuous moving boundary created between the rubbery and the glassy polymer. This movement of the polymer chains may help to explain the formation of the sharp solvent profiles typical of Case II diffusion dynamics, but it is physically unrealistic to expect the polymer volume fraction to increase ahead of the solvent front. However, if this change in polymer volume fraction can be related to the density of the polymer chains, then this model begins to illustrate the swelling of the polymer commonly observed with Case II diffusion.

In Chapter 3, the Monte Carlo model was modified to introduce a localised swelling of the lattice. If the total volume fraction of occupied lattice sites in a particular plane changes from its initial average value then the distance between this lattice plane and the next will change by a distance proportional to that change in volume fraction. Thus, the density in every lattice plane remains constant with changing volume fractions and a swelling of the lattice is simulated. This has been reintroduced in this simulation, the results of which are shown in figure (6.12b) where the only difference from figure (6.12a) is the inclusion of the swelling process. This causes the lattice planes in the region of the rubbery polymer to swell to a greater extent than the planes in the glassy polymer where the total volume fraction of occupied sites is lower. Thus, the rate of diffusion increases in the rubbery polymer as the average lattice spacing increases in the x direction and the molecules jump a greater distance with each successful move. This is evident in figure (6.12b) as the total penetration distance of the solvent front is greater by a factor of *1.8* than in figure (6.12a). At the same time, the exponent n in this case has returned to its original value of $n=0.90 \pm 0.05$. The extent of the swelling can be seen in the polymer profiles. The polymer chains were initially placed in a lattice of length *0.003 μm*, but the final polymer profile in figure (6.12b) extends to a distance of approximately *0.004 μm*. Furthermore, the swelling of the lattice scales approximately linearly with time as expected for Case II diffusion, where $n=0.87 \pm 0.05$ in this example.

Figure (6.12c) shows this same simulation again, but with the total simulation time increased by a factor of 2 to produce a total of twenty solvent profiles. The purpose of this is to examine whether the exponent n changes in any way for long simulation times. It is believed that Case II diffusion will return to Case I diffusion in the limit of long times. This is because the rate of swelling of the polymer depends on the solvent gradient in the swollen polymer. This solvent flux decreases with time so that at long times the polymer may reach at point at which it is unable to swell any further. Thus a transition is possible from the Case II limit to the Case I limit at long times. This Monte Carlo model offers the opportunity to study the progression of the solvent fronts at long simulation times where experimental data may be difficult to obtain. In the case of this simulation a change in the progression

of the solvent fronts with time is clearly seen in figure (6.12c) with the separation between successive solvent fronts becoming increasingly less with time. If the progression of the solvent front is measured over the total simulation time an average value of the exponent n is found to be $n=0.80 \pm 0.05$ compared to the original value of $n=0.90 \pm 0.05$. However, if the double logarithmic plot of penetration distance against time is studied it is evident that its gradient decreases with time. This is shown in figure (6.13a). To quantify this change in the exponent n, the gradient of figure (6.13a) is measured separately for the initial ten profiles and for the final ten profiles. It is found that the gradient initially gives a value of $n=0.87 \pm 0.04$ before falling to a value of $n=0.71 \pm 0.05$. The total simulation time was then increased by a factor of *3* and this procedure repeated for thirty equal time increments. The double logarithmic plot for this case is shown in figure (6.13b). The exponent for the final ten profiles in this case gives a value of $n=0.62 \pm 0.05$. Therefore, the exponent n decreases with time indicating a move towards Case I diffusion. Had the simulation time been continued for much longer times it is believed that the exponent would eventually fall to a value of *0.5* characteristic of Case I diffusion. This is significant and demonstrates that the progression of the solvent fronts is returning towards the Case I limit for long times. In this model the polymer volume fraction increases ahead of the solvent front and the number of free lattice sites remaining in that part of the lattice becomes increasingly smaller with time. Therefore, the number of free lattice sites to which the solvent molecules can move becomes less with time as the increasing polymer volume fraction begins to impede the progression of the solvent molecules further into the lattice. This movement of the polymer chains reduces the diffusion of the solvent further into the lattice resulting in the falling exponent described above. This reduction in the number of vacant lattice sites available to the solvent molecules is because the swelling simulated here does not introduce additional free lattice sites but simply increases the distance between existing lattice sites. Therefore, the return towards Case I dynamics is due to the decreasing number of free sites in the lattice, but the result is the same as that due to the decreasing flux of solvent. The simulation of this transitional behaviour is an important development that has not been demonstrated by other models of Case II diffusion. It confirms that Case II diffusion can return towards the Case I limit for long times.

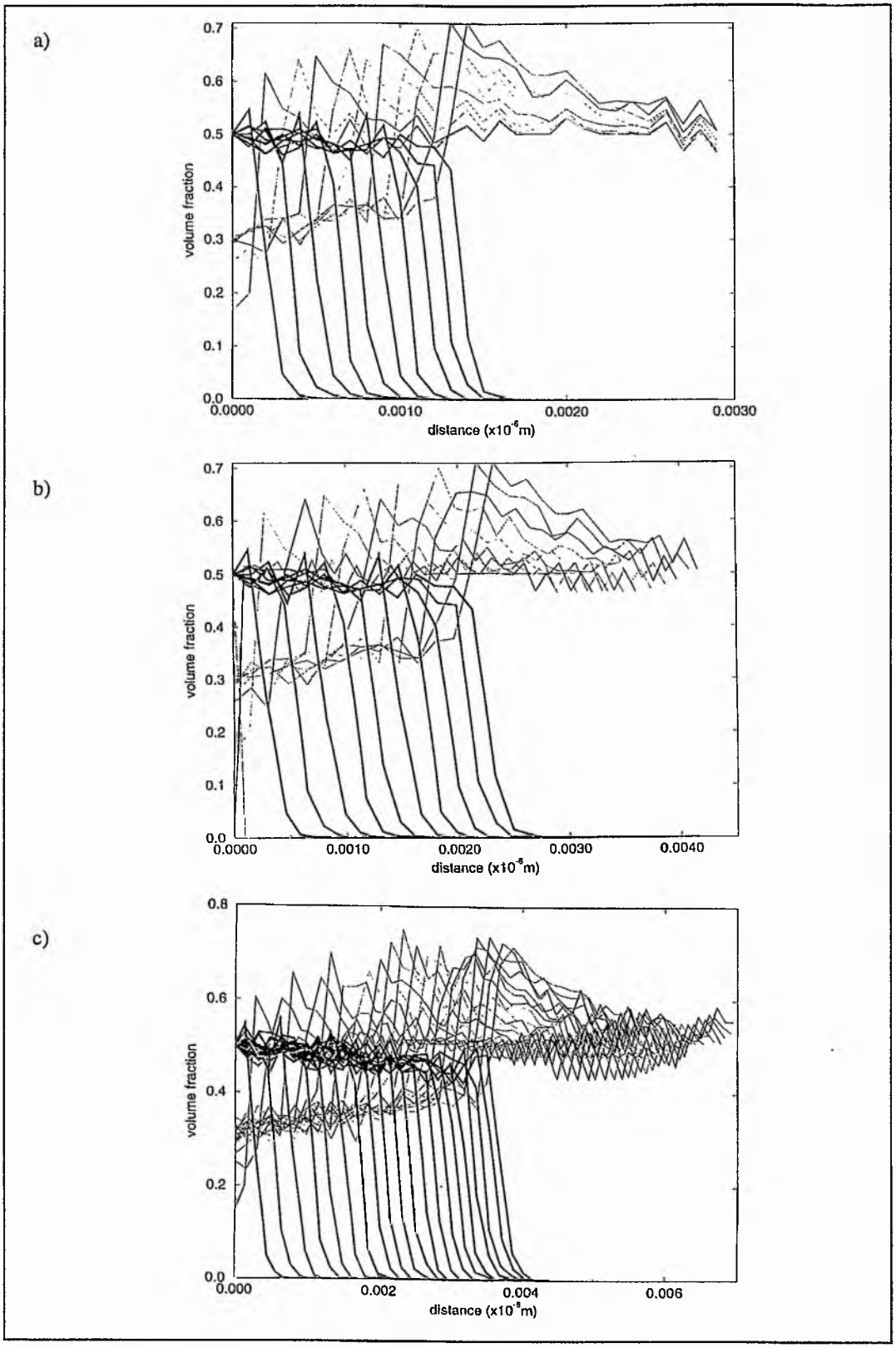

Figure (6.12): a) Case II diffusion in the presence of polymer showing the discontinuous change in the polymer volume fraction with distance moving with time but excluding the swelling process, b) including swelling, c) for long times with the total simulation time increased by a factor of 2.

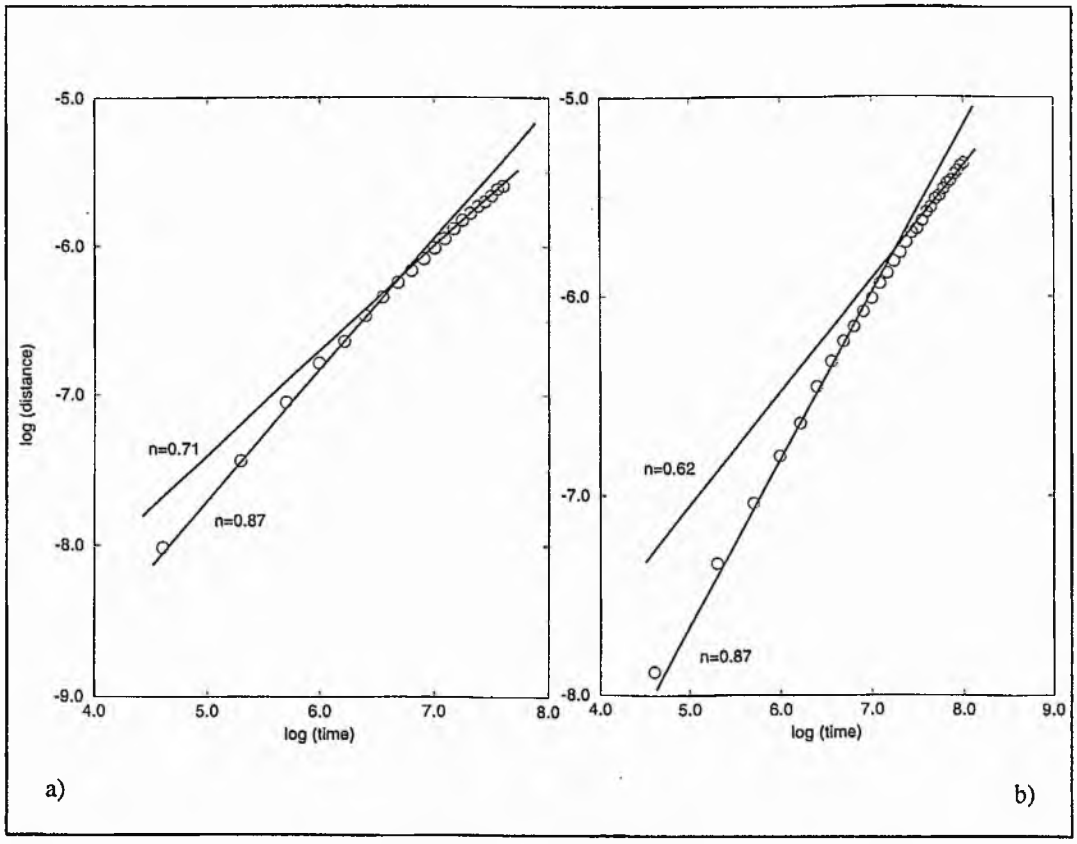

Figure (6.13): Double logarithmic plot of solvent penetration distance against time showing a decreasing gradient with time where the simulation time has been increased by a factor of a) *2*, b) *3*. The solid lines show the average gradient measured over the initial ten profiles and the final ten profiles in each case.

The effect of the polymer motion on the ingress of the solvent can be seen by changing the relative equilibrium rates of the two processes. This is illustrated in figure (6.14), which shows the ingress of the solvent for three different polymer equilibrium process rates respectively. Here the swelling process has been neglected. In figure (6.14a), the polymer process rate is a factor of *10* lower than the solvent process rate for all solvent volume fractions. In this case, the diffusion of the solvent is impeded by the relatively immobile polymer chains, resulting in a reduced penetration distance. The exponent n in this case is also reduced to $n=0.62 \pm 0.05$. However, this example clearly illustrates the activation of the polymer chains by the ingressing solvent molecules. The polymer chains at the furthest extreme from the ingressing solvent molecules are frozen and show no motion, as is expected.

Figure (6.14b) shows the case for equal solvent and polymer process rates, with a total penetration distance of approximately $0.0015\ \mu m$ and an exponent of $n=0.85 \pm 0.05$. The polymer in the glassy region of this example increases as the mobile polymer chains are moved ahead of the solvent front. Figure (6.14c) shows the case where the polymer process rate is now a factor of *5* greater than the solvent process rate. The polymer chains are now highly mobile, allowing the solvent molecules to diffuse into the lattice with little hindrance. This is evident from the greater penetration distance of the solvent fronts and an increased exponent of $n=0.93 \pm 0.05$. The polymer volume fraction ahead of the solvent front is seen to increase significantly due to the mobile chains moving away from the ingressing solvent molecules so that they may be more easily accommodated within the lattice.

The ingress of the solvent molecules in this Monte Carlo model still relies on the co-operative motion of the polymer chains to allow sufficient free volume in the lattice to accommodate the solvent molecules. The motion of the polymer chains creates a discontinuous moving boundary at the leading edge of the solvent front between the rubbery and the glassy regions of the polymer. This is a characteristic feature of Case II diffusion as originally described by Crank (CRANK 1953).

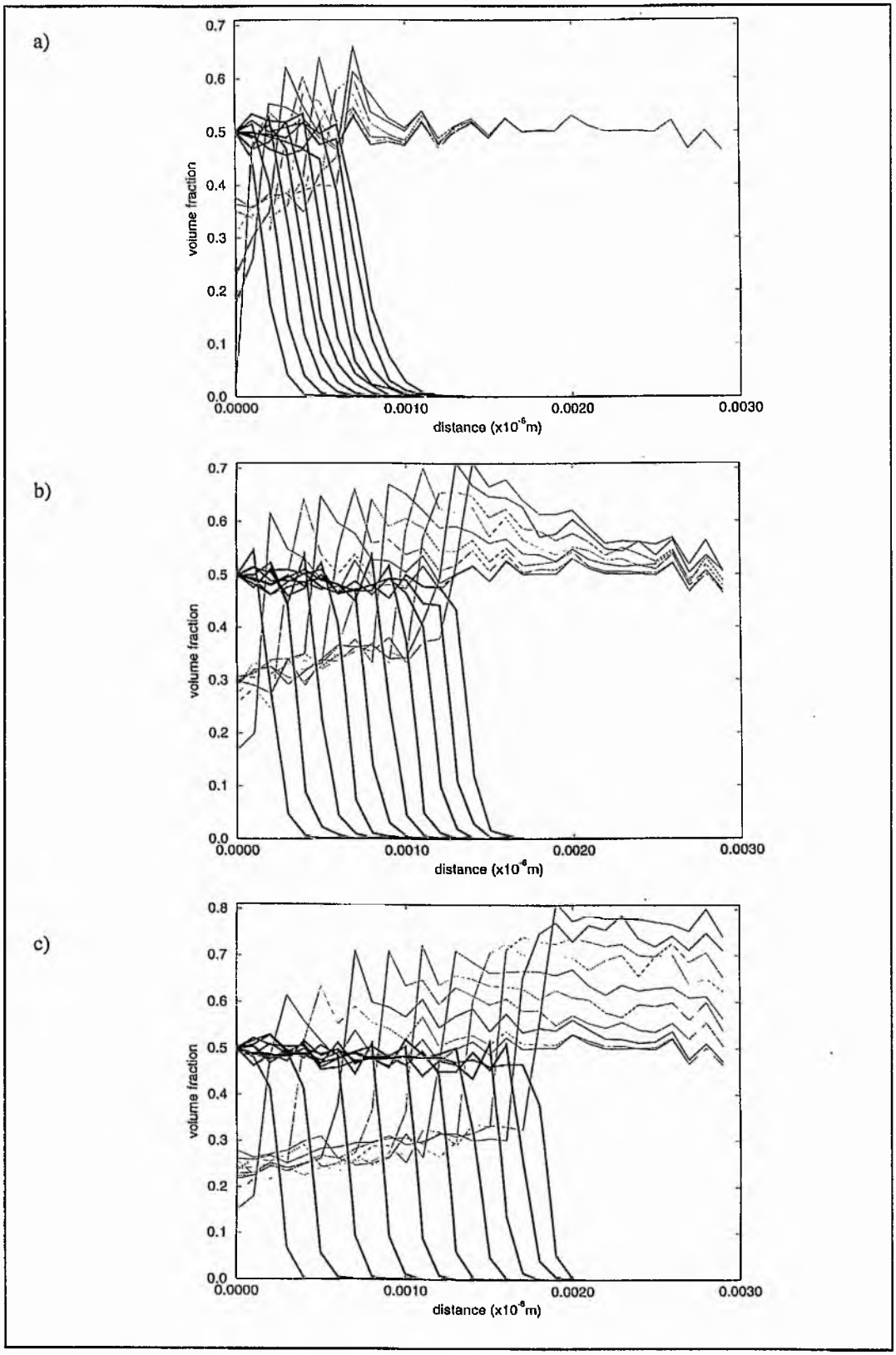

Figure (6.14): The effects of varying the relative solvent r_s and polymer r_p equilibrium process rates where: a) $r_p=r_s/10$, b) $r_p=r_s$, c) $r_p=5r_s$.

6.5 Conclusions

A novel Monte Carlo model of solvent diffusion into a polymer has been developed in this chapter using the concept of history dependent diffusion first proposed by Crank (CRANK 1953). The process rates of both the solvent and the polymer are described by a first order approach to an equilibrium rate, controlled by a relaxation time characteristic of the viscoelastic response of the polymer. By careful selection of suitable functions for both the equilibrium rate and the relaxation time with solvent volume fraction, it has been possible to demonstrate the formation of non-Fickian solvent profiles that approach the Case II limit. It has also been possible to show the change from Case I to Case II diffusion dynamics by variation of the model parameters for these functions. Consequently, this model has been able to successfully simulate Case II diffusion dynamics, showing linear dynamics and characteristic solvent profiles.

The scaling of the velocity of the solvent front has been studied and shown to be consistent with the predictions of the Thomas and Windle model (THOMAS 1982) as described by Lasky (LASKY 1988). Simulated data has also been fitted to experimental data gained in a MRI study of methanol ingress into PMMA (LANE 1998). The simulated data has shown a good fit to the experimental data providing confidence in the results of the model.

Importantly, this model's ability to simultaneously study the microscopic motion of both the solvent and polymer molecules is a novel feature not thought to have previously been achieved in a Monte Carlo model. Through this, the effect of the polymer motion on the ingress of the solvent has been illustrated. Furthermore, the localised movement of polymer within the lattice in response to the ingressing solvent has been shown to create a discontinuous boundary between the swollen rubbery polymer and the unswollen glassy polymer. These features are typical of those observed in studies of Case II diffusion and have been reproduced well by this "History Dependent" Monte Carlo model of solvent diffusion.

The Monte Carlo method is an established numerical method that has been used to study a wide range of problems. Its application here provides a novel way of solving a difficult coupled differential equation as specified by Thomas and Windle (THOMAS 1981) and others. By specifying a set of elementary moves for the solvent and polymer molecules that occur with a time dependent probability, the need to define and solve a difficult non - linear differential equation is avoided. Hence, by specifying a relatively simple set of elementary "rules" the problems associated with solving a non - linear differential equation for the case of a discontinuous function are also avoided, producing a more stable result. The Monte Carlo algorithm can produce a relatively slow computer simulation with computing times of a few hours for most problems studied in this thesis. If polymer chains are absent from the simulation then this time is reduced to approximately an hour. By comparison, the Fickian solvent profiles presented in this thesis that were obtained from a simple finite difference simulation had a typical computing time of only a few minutes. However, this "History Dependent" Monte Carlo model has been successful in demonstrating Case II diffusion and its associated features. It offers the opportunity to systematically change the microscopic parameters of the model to study the effects on the macroscopic properties that are observed.

Chapter 7

Conclusions

7.1 Summary

In this thesis, the development of two original Monte Carlo models of solvent diffusion into polymer has been described. The "Simple" Monte Carlo model uses a coarse grained model of a polymer solution on a regular lattice. The dynamic properties of both the solvent and polymer molecules can be observed where their motions are modelled by simple instantaneous moves between neighbouring lattice sites. This Monte Carlo model has reliably reproduced Case I, or Fickian, dynamics for a solvent ingressing into a semi - infinite lattice. The operation of this model has also been demonstrated under a range of conditions. However, the most important limitation of this model is the fact that no departure from Case I dynamics is seen for any reasonable model parameters. This "Simple" Monte Carlo model is not able to reproduce Case II diffusion dynamics. The reason for this is that in this simple Monte Carlo model the processes of solvent diffusion and polymer relaxation are entirely independent processes. In most successful models of Case II diffusion it is recognised that these two processes are coupled processes and that the diffusion of the solvent is controlled by the viscoelastic relaxation of the polymer molecules. Efforts to modify this Monte Carlo model to couple the solvent diffusion to the polymer motion have been unsuccessful, and only Case I diffusion dynamics have been observed. It is suggested that a simple Monte Carlo model of this type will always produce Case I diffusion dynamics. The dynamic algorithm described in this work relies on simple instantaneous molecular motions between neighbouring lattice sites. It has been shown that a diffusion process based on these motions is purely

concentration dependent, relying only on the current state of the system. The diffusion process shows no time dependent features and has no memory of the past history of the system. Under these circumstances, only Case I diffusion dynamics can be modelled.

To use the Monte Carlo method to simulate Case II diffusion dynamics, the diffusion process is made time dependent by incorporating a history dependent model of diffusion first proposed by Crank in 1953 (CRANK 1953). In this "History Dependent" Monte Carlo model the motions of both the solvent and the polymer are no longer instantaneous, but occur at a rate that approaches an equilibrium value by a first order process governed by a relaxation time characteristic of the viscoelastic relaxation of the polymer. Therefore, the diffusion process is time dependent and depends on the previous history of the state of the system. Instead of a purely concentration dependent process, a diffusion process is now produced that depends explicitly on the solvent concentration and on the time of the system. This novel Monte Carlo model has successfully simulated most of the features of Case II diffusion, including the linear progression of the solvent front with time, the sharp solvent profiles, even showing evidence of a Fickian precursor. Case I dynamics can also be reproduced by suitable choice of the model parameters, where a rapid relaxation of the polymer in response to the ingressing solvent reduces the time dependent effects.

Unlike many models of Case II diffusion, this "History Dependent" Monte Carlo model is able to simultaneously model the microscopic motions of both the solvent and the polymer molecules. This novel feature is not thought to previously have been achieved in a Monte Carlo model of solvent diffusion into polymer. This has demonstrated the formation of a discontinuous moving boundary between the rubbery polymer and the glassy polymer that is typical of this type of diffusion. The model has also been able to demonstrate a transition from Case II diffusion to Case I diffusion in the limit of long simulation times. A swelling process has been incorporated in this model to compensate for the observed changes in the polymer volume fraction, but has had limited success and requires a more detailed examination of the swelling of the polymer. However, using this method to study

Case II diffusion avoids many of the problems previously encountered with the solution of non-linear equations described by other models of Case II diffusion. This Monte Carlo model does not suffer from the same sensitivity to model parameters that has arisen in other Case II models.

This work has studied the fundamental operation of this novel "History Dependent" Monte Carlo model and has shown that the essential features of Case II diffusion can be simulated successfully. The most important feature of this model is the realisation that the solvent diffusion process must be time dependent. In glassy polymers the relaxation of the polymer is slow and time dependent effects are dominant which give rise to Case II diffusion dynamics. In rubbery polymers the relaxation of the polymer is rapid and time dependent effects are less prevalent, eventually producing Case I diffusion dynamics. However, it would now be of considerable interest to apply this model to specific problems of solvent diffusion into polymers and to hopefully gain new insights into the microscopic processes taking place.

7.2 Future Work

This "History Dependent" Monte Carlo model could now be applied to specific problems of solvent diffusion into polymers. One example that could be easily simulated by this model is the ingress of binary mixtures of solvents into polymers. This is of importance in several industrial applications where it is thought that the combined effect of multiple solvent components is very different to the effect of any single component acting alone. This was studied by Lane (LANE 1998) who examined the diffusion of acetone - methanol mixtures in PMMA as described in Chapter 6. It would be straightforward to adapt the Monte Carlo model to simulate this problem, simply by defining a fifth process rate for the additional solvent component. This additional solvent rate could be specified independently of the original solvent process rate, thus allowing two different types of solvent to be modelled. Then the combined effects of good and bad solvents could be examined. The use of process rates in the Monte Carlo model developed here provides great potential for future simulations. It is possible to define any number of process rates

for any number of different polymer or solvent processes, each of which can be defined independently. Therefore, it would also be possible to refine the model at a later date by introducing additional polymer motions to the set of elementary moves used in this model.

Other problems of interest that could be easily studied with simple modifications to this model include such problems as the size of the solvent molecules ingressing into the polymer (ENSCORE 1977, ARNOULD 1992). This was studied by Gall et al. (GALL 1990), who used Rutherford back - scattering to examine the exposure of polystyrene to the vapour of a series of iodo-*n*-alkanes ranging from iodopropane ($n=3$) to iodooctane ($n=8$), where n is the number of carbon atoms on the alkane chain. All solvents used in this study exhibited Case II solvent profiles and it was found that the velocity of the solvent front decreased exponentially with n. Solvent molecules of different sizes could be simulated in this Monte Carlo model by changing the definition of the solvent molecule within the simulation. Currently, each solvent molecule occupies only a single lattice site, but the solvent molecule could be defined as a chain in the same way as the polymer is modelled. Then it would be reasonable to expect the velocity of the solvent front to decrease as the solvent chain length increases, due to the need for a larger number of free lattice sites to be available for each successful solvent move.

Finally, the simulations presented here have been performed on a three - dimensional, semi - infinite lattice only. It would be of interest to observe the diffusion process in systems of different dimensions, particularly for thin polymer films. This is of particular interest where polymer materials are used in industrial coatings to form protective barriers (EDWARDS 1996). It would be straightforward to define a lattice of different dimensions to represent a thin polymer film, but edge effects would then become more important and more work would be required to define more exactly the motions of the polymer chains at the edge of the lattice. However, these examples of areas where this Monte Carlo model could be applied illustrate how simple modifications could make this "History Dependent" Monte Carlo model a useful tool in the study of a range of different problems where the ingress of solvent into a polymer is of primary interest.

References

A

Alder B J, Wainwright T E, J. Chem. Phys, 27, 1208 (1957).

Alder B J, Wainwright T E, J. Chem. Phys, 31, 459 (1959).

Alfrey T, Gurnee E F, Lloyd W G, J. Polym. Sci, C, 12, 249 (1966).

Allen M P, Tildesley D J, Computer Simulation of Liquids, Oxford University Press (1989).

Arnould D, Laurence R L, Ind. Eng. Chem. Res, 31, 219 (1992).

Astarita G, Sarti G C, Polym. Eng. Sci, 18, 388 (1978).

Antonietti M, Coutandin J, Sillescu H, Macromolecules, 19, 793 (1986).

B

Barrie J A, J. Polym. Sci, A1, 4, 3081 (1966).

Bartels C R, Crist B, Graessley W W, Macromolecules, 17, 2702 (1984).

Baschnagel J, Binder K, Macromolecules, 28, 6808 (1995).

Baumgarten A, Heermann D W, Polymer, 27, 1777 (1986).

Binder K, The Monte Carlo Method in Statistical Physics, Springer (1979).

Binder K, Monte Carlo and Molecular Dynamics Simulations in Polymer Science, Oxford University Press (1995).

Binder K, Paul W, J. Polym. Sci, Part B: Polym. Phys, 35, 1 (1997).

Blackband S, Mansfield P, J. Phys. C: Solid State Physics, 19, 49 (1986).

Bloch F, Hansen W W, Packard M, Phys. Rev, 70, 474 (1946).

Bloembergen N, Purcell E M, Pound R V, Phys. Rev, 73, 679 (1948).

Bowtell R, Sharp J C, Peters A, Mansfield P, Rajabi-Siahboomi A R, Davies M C, Melia C D, Magnetic Resonance Imaging, 12, 361 (1994).

Bueche F, Cashin W M, Debye P V, J. Chem. Phys, 20, 1956 (1952).

Bueche F, Physical Properties of Polymers, Interscience Publishers (1962).

C

Callaghan P T, Principles of Nuclear Magnetic Resonance Microscopy, Oxford Scientific Publications (1991).

Carr H Y, Purcell E M, Phys. Rev, 94, 630 (1954).

Chandrasekhar S, Rev. Mod. Phys, 15, 3 (1943).

Cody G D, Botto R E, Macromolecules, 27, 2607 (1994).

Cohen D S, J. Polym. Sci, Polym. Phys, 21, 2057 (1983).

Cohen D S, J. Polym. Sci, Polym. Phys, 22, 1001 (1984).

Colbourn E A, Computer Simulation of Polymers, Longman Scientific and Technical (1994).

Cowie J M G, Polymers: Chemistry and Physics of Modern Materials, International Textbook Co Ltd, 130 (1973).

Crabb C C, Kovac J, Macromolecules, 18, 143 (1985).

Crank J, J. Polym. Sci, 11, 151 (1953).

Crank J, Park G S, Diffusion in Polymers, Academic Press NY (1968).

Crank J, The Mathematics of Diffusion, 2nd ed. Clarendon Press, Oxford (1975).

D

De Gennes P G, J. Chem Phys, 55, 572 (1971).

De Gennes P G, Macromolecules, 9, 587 (1976a).

De Gennes P G, Macromolecules, 9, 594 (1976b).

De Gennes P G, Scaling Concepts in Polymer Physics, Cornell University Press (1979).

De Gennes P G, Introduction to Polymer Dynamics, Cambridge University Press (1990).

Devotta I, Premnath V, Badiger M V, Rajamohanan P R, Ganapathy S, Mashelkar R A, Macromolecules, 27, 532 (1994).

Devotta I, Mashelkar R A, Chem. Eng. Comm, 156, 31 (1996).

Dial M, Crabb K S, Crabb C C, Dahlin D M, Kovac J, Macromolecules, 18, 2215 (1985).

Doi M, Edwards S F, J. C. S, Faraday Trans, II, 74, 1789, 1802, 1818 (1978).

Doi M, Introduction to Polymer Physics, Oxford University Press (1996).

Dunweg B, Kremer K, J. Chem. Phys, 99, 6983 (1993).

E

Edwards D A, J. Polym. Sci, Part B: Polym. Phys, 34, 981 (1996).

Edwards S F, Proc. Phys. Soc, 88, 265 (1966).

Edwards S F, Grant J W, J. Phys, A6, 1169, 1186 (1973).

Enscore D J, Hopfenberg H B, Stannett V T, Polymer, 18, 793 (1977).

Ercken M, Adriaensens P, Reggers G, Carleer R, Vanderzande D, Gelan J, Macromolecules, 29, 5671 (1996).

Ernst R, Bodenhausen G, Wokoun A, Principles of NMR in One and Two Dimensions, Oxford Science Publications, Oxford (1987).

Evans K E, Edwards S F, J. Chem. Soc. Faraday Trans. 2, 77, 1891 (1981).

F

Fatkullin N, Kimmich R, Weber H W, Phys. Rev. E, 47, 4600 (1993).

Fatkullin N, Kimmich R, J. Chem. Phys, 101, 822 (1994).

Ferry J D, Viscoelastic Properties of Polymers, 2nd ed., John Wiley and Sons (1970).

Fick A, Annln. Phys, 59, 170 (1855).

Flory P J, J. Chem. Phys, 9, 660 (1941).

Flory P J, J. Chem. Phys, 10, 51 (1942).

Flory P J, Principles of Polymer Chemistry, Cornell University Press (1971).

Frenkel D, Smit B, Understanding Molecular Simulation, Academic Press (1996).

Frisch H L, Wang T T, Kwei T K, J. Polym. Sci, 7, 879 (1969).

Fu T Z, Durning C J, A.I.Che. Journal, 39, 1030 (1993).

Fujita H, in: Diffusion in Polymers, eds. G S Park, J Crank, Academic Press NY (1968).

Fukumori K, Kurauchi T, Kanigaito O, Polymer, 31, 713 (1990).

G

Gall T P, Lasky R C, Kramer E J, Polymer, 31, 1491 (1990).

Graessley W, Adv. Polym. Sci, 16 (1974).

Gedde U W, Polymer Physics, Chapman and Hall (1995).

Gerroff I, Milchev A, Binder K, Paul W, J. Chem. Phys, 98, 6526 (1993).

Goldman M, Quantum Description of High Resolution NMR in Liquids, Oxford Scientific Publications (1993).

Green M, Tobolsky A, J. Chem. Phys, 14, 80 (1946).

Grosberg A Y, Khoklov A R, Giant Molecules Here There and Everywhere, Academic Press, 114 (1997).

Gurler M T, Crabb C C, Dahlin D M, Kovac J, Macromolecules, 16, 3298 (1983).

H

Hahn E L, Phys. Rev, 80, 580 (1950).

Halse M R, Rahman H J, Starnge J H, Physica B, 203, 169 (1994).

Halse M R, Magnetic Resonance Imaging, 14, 745 (1996).

Hartley G S, Trans. Faraday Soc, 45, 820 (1949).

Hildebrand J H, Wood S E, J. Chem Phys, 1, 817 (1932).

Holroyd L V, Codrington R S, Mrowca B A, Guth E, J. Appl. Phys, 22, 696 (1951).

Huggins M L, J. Chem Phys, 9, 440 (1941).

Huggins M L, J. Chem Phys, 46, 151 (1942).

Hui C Y, Wu K C, J. Appl. Phys, 61, 5129 (1987a).

Hui C Y, Wu K C, J. Appl. Phys, 61, 5137 (1987b).

K

Kimmich R, Weber H W, J. Chem. Phys, 98, 5847 (1993).

Kramer O, Greco R, Neira R, Ferry J D, J. Polm. Sci, Polym. Phys, 12, 2361 (1974).

Kramer O, Greco R, Ferry J D, J. Polm. Sci, Polym. Phys, 13, 1675 (1975).

Kremer K, Grest G S, Phys. Rev. A33, 3628 (1986).

Kremer K, Grest G S, J. Chem. Phys, 92, 5057 (1990).

Kremer K, Dunweg B, J. Chem. Phys, 99, 6983 (1993).

KuhnW, Ber, 63, 1503 (1930).

Kuhn W, Kolloid Z, 68, 2 (1934).

Kuhn W, Kuhn H, Helv. Chim. Acta, 26, 1394 (1943).

L

Lane D M, McDonald P J, Polymer, 38, 2329 (1997).

Lane D M, PhD thesis, University of Surrey (1998).

Lasky R C, Kramer E J, Hui C Y, Polymer, 29, 1131 (1988).

Lauterbur P C, Nature, 242, 190 (1973).

Lodge A, Trans. Faraday Soc, 52, 120 (1956).

Lowry G G, Markov Chains and Monte Carlo Calculations in Polymer Science, Marcel Dekker (1970).

M

Madras N, Sokal A D, J. Stat. Phys, 50, 109 (1988).

Maksym PA, Semicond. Sci. Technol, 3,594 (1988).

Mansfield P, Bowtell R, Blackband S, Cawley M, Magnetic Resonance Imaging, 9, 763 (1991).

Mansfield P, Bowtell R, Blackband S, J. Magn. Reson, 99, 507 (1992).

Meiboom S, Gill D, Rev. Sci. Instr, 29, 688 (1958).

Metanomski W V, Compendium of Macromolecular Nomenclature, Blackwell Scientific, Oxford (1991).

Metropolis N, Ulam S, J. Am. Stat. Ass, 44, 335 (1949).

Metropolis N, Rosenbluth A W, Rosenbluth M N, Teller A N, Teller E, J. Chem. Phys, 21, 1087 (1953).

Milchev A, Paul W, Binder K, J. Chem. Phys, 99, 4786 (1993).

Muller-Krumbhaar H, Binder K, J. Stat. Phys, 8,1 (1973).

Muller-Plathe F, Rogers S C, Van Gunsteren W F, J. Chem. Phys, 98, 9895 (1993).

N

Naghizadeh J, Kovac J, J. Chem. Phys, 84, 3559 (1986).

P

Parker W J, Jenkins R J, Butler C P, Abbott G L, J. Appl. Phys, 32, 1679 (1961).

Peppas N A, Wu J C, Von Meerwall E D, Macromolecules, 27, 5626 (1994).

Peterlin A, J. Polym. Sci, B, 3, 1083 (1965).

Peterlin A, J. Polym. Sci, Polym. Phys, 17, 1741 (1979).

Petropoulos J H, J. Polym. Sci, A2, 8, 1797 (1970).

Pierleoni C, Ryckaert J-P, J. Chem. Phys, 96, 8539 (1992).

Purcell E M, Torrey H C, Pound R V, Phys. Rev, 69, 37 (1946).

R

Richter D, Ewen B, Farago B, Wagner T, Phys. Rev. Lett, 62, 2140 (1989).

Richter D, Willner L, Zirkel A, Farago B, Fetters L J, Huang J S, Phys. Rev. Lett, 71, 4158 (1993).

Rogers C E, Physics and Chemistry of the Organic Solid State,
Vol II, 6, Interscience NY (1965).

Rosenbluth M N, Rosenbluth A W, J. Chem. Phys, 23, 356 (1955).

Rouse P E, J. Am. Chem. Soc, 69, 1068 (1947).

Rouse P E, J. Chem. Phys, 21, 1272 (1953).

S

Sariban A, Binder K, Macromolecules, 21, 711 (1988).

Sarti G C, Polymer, 20, 827 (1979).

Scatchard G, Chem. Rev, 8, 321 (1931).

Sheng Y J, Panagiotopoulos A Z, Kumar S K, J. Chem. Phys, 103, 10315 (1995).

Staudinger H, Ber, 53, 1073 (1920).

Sunderrajan S, Hall C K, Freeman B D, J. Chem. Phys, 105, 1621 (1996).

T

Takeuchi H, J. Chem. Phys, 93, 2062 (1990a).

Takeuchi H, J. Chem. Phys, 93, 4490 (1990b).

Ten Brinke G, Ausserre D, Hadziioannou G, J. Chem. Phys, 89, 4374 (1988).

Thomas N L, Windle A H, Polymer, 21, 613 (1980).

Thomas N L, Windle A H, Polymer, 22, 627 (1981).

Thomas N L, Windle A H, Polymer, 23, 529 (1982).

V

Verdier P H, J. Chem. Phys, 45, 2122 (1966).

Verdier P H, J. Chem. Phys, 52, 5512 (1970).

Verdier P H, J. Chem. Phys, 59, 6119 (1973).

Verdier P H, Stockmayer W H, J. Chem. Phys, 36, 227 (1962).

W

Wall F T, Runin R J, Isaacson L M, J. Chem. Phys, 27, 186 (1957).

Wall F T, Erpenbeck J J, J. Chem. Phys, 23, 356 (1955).

Wall F T, Mandel F, J. Chem. Phys, 63, 4592 (1975).

Walpole R E, Myers R H, Probability and Statistics for Engineers and Scientists, Collier MacMillan International Editions, 98, (1978).

Webb A G, Hall L D, Polym. Comms, 31, 422 (1990a).

Webb A G, Hall L D, Polym. Comms, 31, 425 (1990b).

Webb A G, Hall L D, Polymer, 32, 16, 2926 (1991).

Weber H W, Kimmich R, Macromolecules, 26, 2597 (1993).

Weisenberger L A, Koenig J L, Macromolecules 23, 2445 (1990a).

Weisenberger L A, Koenig J L, Macromolecules 23, 2454 (1990b).

Williams M L, Landel R F, Ferry J D, J. Am. Chem. Soc, 77, 3701 (1955).

Wu J C, Peppas N A, J. Appl. Polym. Sci, 49, 1845 (1993a).

Wu J C, Peppas N A, J. Polym. Sci, B: Polym. Phys, 31, 1503 (1993b).

Y

Yamakawa H, Modern Theory of Polymer Solutions, Harper and Row (1971).

Z

Zimm B H, J. Chem Phys, 24, 269 (1956).

Appendix

A.1 Flow Chart of the "Simple" Monte Carlo Model

A.2 Flow Chart of the "History Dependent" Monte Carlo Model

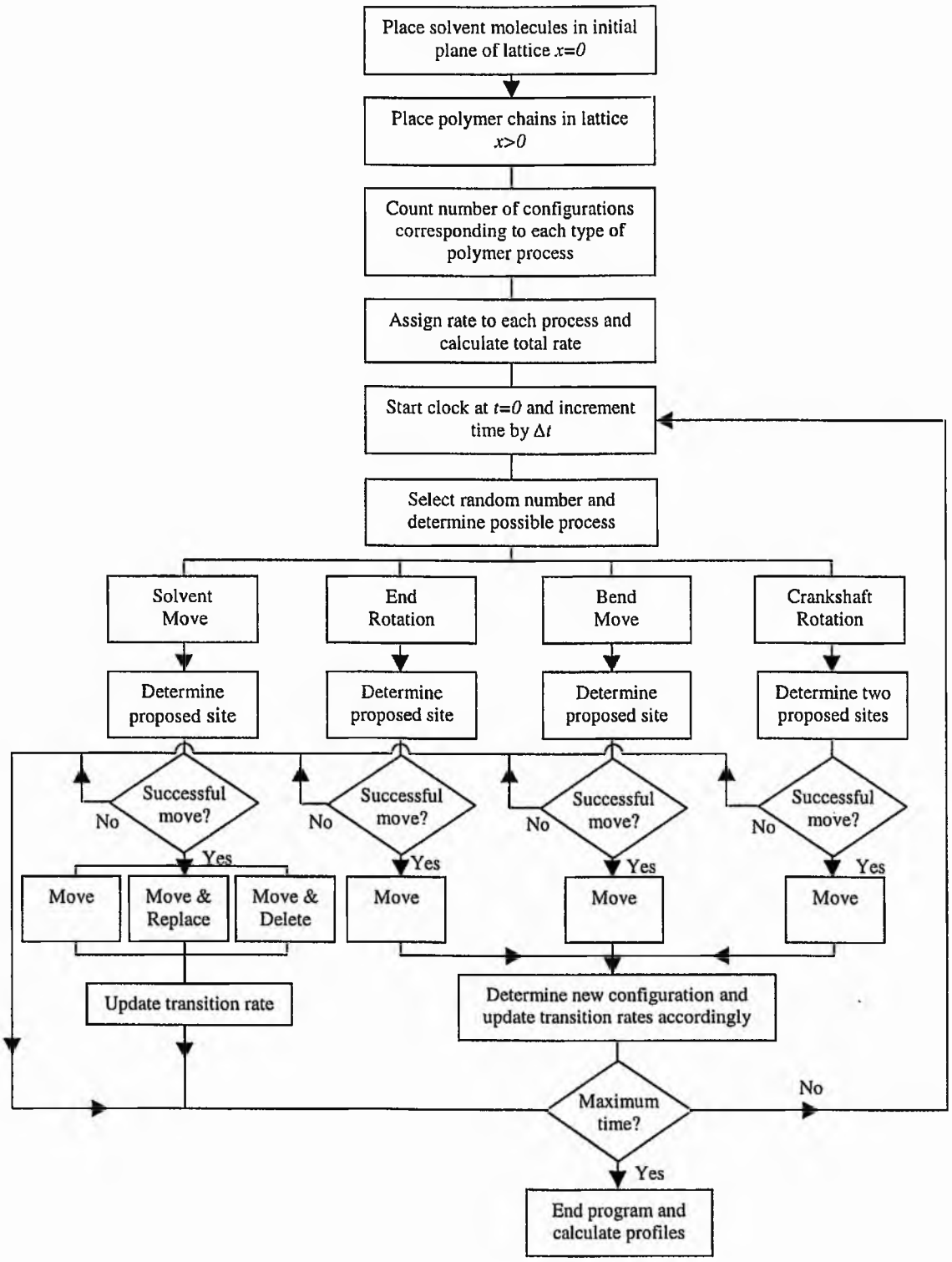

Figure (A.1): Flow chart to illustrate the operation of the "Simple" Monte Carlo model and the main operations that the computer program makes during each cycle. This is explained in full in the text.

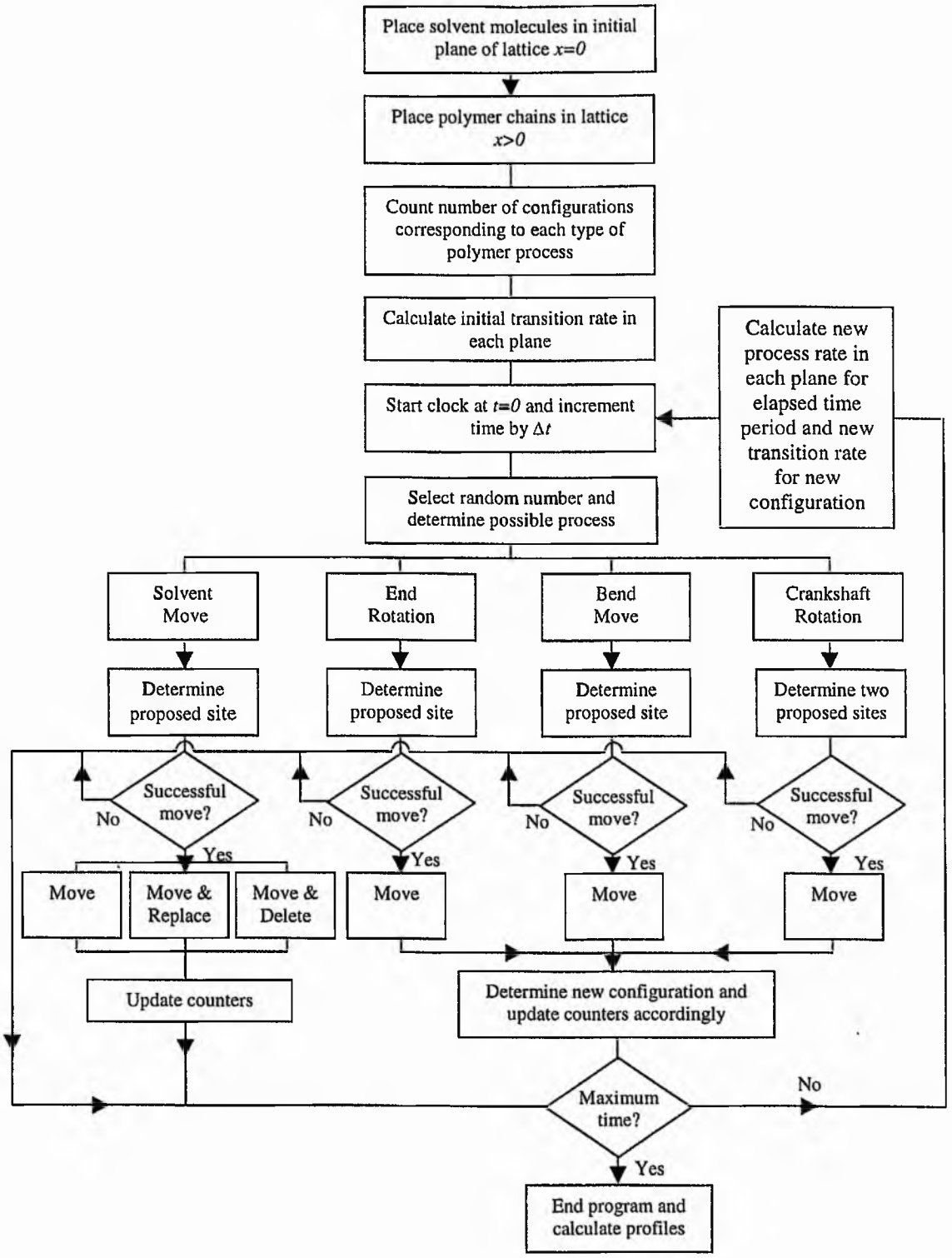

Figure (A.2): Flow chart to illustrate the operation of the "History Dependent" Monte Carlo model and the main operations that the computer program makes during each cycle. This is explained in full in the text.